XXVI INTERNATIONAL SCIENTIFIC AND TECHNICAL CONFERENCE

FOUNDRY 2019

10-12 APRIL 2019, PLEVEN, BULGARIA

PROCEEDINGS

ISSN 2535-017X (PRINT), ISSN 2535-0188 (ONLINE)

SCIENTIFIC-TECHNICAL UNION OF MECHANICAL ENGINEERING
INDUSTRY 4.0
BULGARIA

The FEDERATION OF THE SCIENTIFIC ENGINEERING UNIONS (FSEU)

in Bulgaria is a professional, scientific - educational, non-governmental, non-political non-profit association of legal entities - professional organizations registered under the Law on non-profit legal entities, whose members are engineers, economists and other specialists in the field of science, technology, economy and agriculture.

FSEU performed bilateral cooperation with similar organizations from many countries.

FSEU brings together 19 national associations - Scientific and Technical Unions / STU /, 34 territorial associations, which have more than 15 000 professionals across the country.

FSEU is a co-founder and member of the World Federation of Engineering Organizations (WFEO).

FSEU a member of the European Federation of National Engineering Associations (FEANI), and a member of the Standing Conference of engineering organizations from Southeast Europe / CO.PICEE /, Global Compact, European Young Engineers (EYE). The Federation has the exclusive right to give nominations for the European Engineer (EUR ING) title.

Contacts:

108 Rakovsky Str., Sofia 1000, Bulgaria

web: www.fnts.bg

e-mail: info@fnts.bg

Кондензатори за Индукционно Нагряване

Леярни ■ Загряване преди коване ■ термообработка

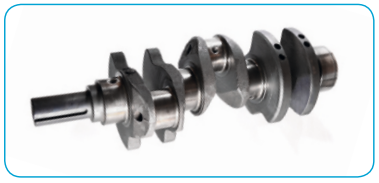

ZEZ SILKO

www.zez-silko.com

SHANDOR

www.kondenzatori.com

esi | ProCAST

Advanced tool of numerical simulation

Complete set of solutions for foundry industry with more than 25 years of tradition

Predictive evaluation of the entire casting process (filling and solidification defects, mechanical properties, part distrortion)

Maximize quality, production & your profit with ProCAST

Learn more at www.esi-group.com/casting

Contact us: Vlastimil Kolda (vko@esi-group.com)

PUBLISHER: SCIENTIFIC TECHNICAL UNION OF MECHANICAL ENGINEERING "INDUSTRY-4.0"

YEAR III **ISSUE 1 (3)**

ISSN 2535-017X (Print), ISSN 2535-0188 (Online)

XXVI INTERNATIONAL SCIENTIFIC AND TECHNICAL CONFERENCE

FOUNDRY

10-12. APRIL 2019, PLEVEN, BULGARIA

TOPIC
„INNOVATIONS FOR THE FOUNDRY ENGINEERING"

ORGANIZER
SCIENTIFIC-TECHNICAL UNION OF MECHANICAL ENGINEERING "INDUSTRY-4.0"
BULGARIA, 1000 Sofia, "G. S. Rakovski"108 str., fl. 4, office 411
e-mail: office@metalcasting.eu; www.metalcasting.eu

INTERNATIONAL EDITORIAL BOARD

C O N T E N T S

RESEARCH INTO THE EFFECT OF CERTAIN CHEMICAL ELEMENTS IN MICROALLOYED STEEL GRADES ON CONCAST SLAB AND ROLLED PLATE SURFACE QUALITY

O. Isayev, O. Hress, S. Yershov, M.Q. Huang, K.L. Zhang

The State Key Laboratory for Refractories and Metallurgy, Hubei Province Key Laboratory of Systems Science in Metallurgical Process, International Research Institute for Steel Technology, Wuhan University of Science and Technology, Wuhan 430081, China
e-mail gunung1961@mail.ru

Abstract: *Investigators has developed a complex technology of manufacture of high quality skelp and shipbuilding grades and nickel-, chromium-, molybdenum-, niobium- and vanadium- microalloyed steels with carbon mass fraction within 0.06% to 0.22% and manganese mass fraction within 1.0% to 1.7%. Over the course of the research, relative occurrence of surface cracks of various morphology – transverse, longitudinal, spider, net-like – on the concast slab surface has been determined. The above research resulted in the development of a number of technological innovations both in preparation of liquid steel for casting and in continuous casting itself, preventing initiation or reducing by 30% – 40% the amount of surface defects on the rolled plates.*
KEY WORDS*: PERITECTICAL STEEL GRADES, CHEMICAL COMPOSITION, CASTING TECHNOLOGY*

Introduction

The experience of prime steel production made it possible to find out that the surface of a concast slab and consequently that of plate steel under certain conditions has a number of defects like cracks of different morphology – cross, longitudinal, net-like and star cracks.

Experimental

A complex procedure of plate steel production of prime steels for large diameter gas line pipes, shipbuilding and steel structures of critical application microalloyed with niobium wherein carbon weight fraction. is in the range of 0.06 to 0.22% and manganese weight fraction – 1.0 to 1.7% was developed and implemented at the Iron and Steel Works. Steel was made in 350 t converters and put to ladle treatment at the metal-refining plants with introduction of silicocalcium wire. Continuous casting was done at curvilinear slab concasters into 220…300 x 1550…2100 mm section slabs as to a worked-out procedure.

Chemical composition of the steel grades studied is shown in Table 1.

Table 1. *Steel chemical composition*

Steel grade	Application	Elements weight fraction, %							
		C	Mn	Si	S	P	Al	Nb	V
08MnNb	Skelp	0.06–0.09	1.00–1.35	0.15–0.35	max 0.006	max 0.020	0.020–0.050	0.020–0.040	0.015–0.035 Ti
09Mn2VNb	Skelp	0.08–0.11	1.50–1.70	0.15–0.35	max 0.006	max 0.020	0.020–0.050	0.020–0.040	0.050–0.070
13Mn1SiNb	Skelp	0.12–0.15	1.30–1.60	0.40–0.60	max 0.007	max 0.025	0.020–0.050	0.020–0.040	0.015–0.035 Ti
ASTMA572	Structure	0.12–0.16	0.80–1.00	0.15–0.35	max 0.015	max 0.020	0.020–0.060	0.005–0.020	–
S355J2G3	Structure	0.16–0.19	1.40–1.60	0.15–0.40	max 0.015	max 0.020	0.020–0.050	0.020–0.040	–

* - other elements are in the range specified by standards for residual content

.

For a more serious study of concast slabs affected with surface defects, determination of factors conducive to crack formation process and elaboration of practices aimed at reducing defect occurrence, surface templates were cut from middle slabs of 5 to 10 heats of the above-mentioned BOF shop current production steel grades. To reveal surface defects the said templates were put to hot etching with 50% aqueous solution of hydrochloric acid. The evaluation of surface quality was done as per the current scales and procedure of researches institutes. Evaluated were the slab wide face surfaces corresponding to the smaller and larger concaster radii (in percentage) and the extent of defect development (severity evaluation system).

In the course of the study relative affection of the concast slab with surface cracks was determined. Each typical concast slab defect, unless revealed and rectified, gets transformed into plate steel surface defects. Slabs with revealed and identified defects were selected for rolling to study concast slab surface defects transformation into plate steel surface defects. Slab rolling was done at 3600 mm Plate Mill as per conventional procedure of slab preheating and rolling.

Results and Discussion

Based on the results of rolling slabs having surface defects transverse cracks 0.5 to 3.0 mm deep as per the folds of the mould oscillation were found to get transformed depending on the gauge of plates, into rolling skin of specific appearance – so called "μ - defects" having the depth of penetration of up to 0.03 mm (vide fig.1). Longitudinal cracks having the depth of 0.5 to 3.5 mm get transformed into skin spread along rolling direction to a considerable length resembling so-called "streaks". Check cracks 0.5 to 3.0 mm deep and star cracks, 3.0 to 10.0 mm deep after rolling plates look like randomly oriented skins and cracks with different depth of penetration (vide fig.2).

Metallographic studies revealed certain regularity between steel product quality indexes and steel chemical composition and, accordingly, between polymorphous transformations of iron-carbon alloy with a number of alloying elements being used.

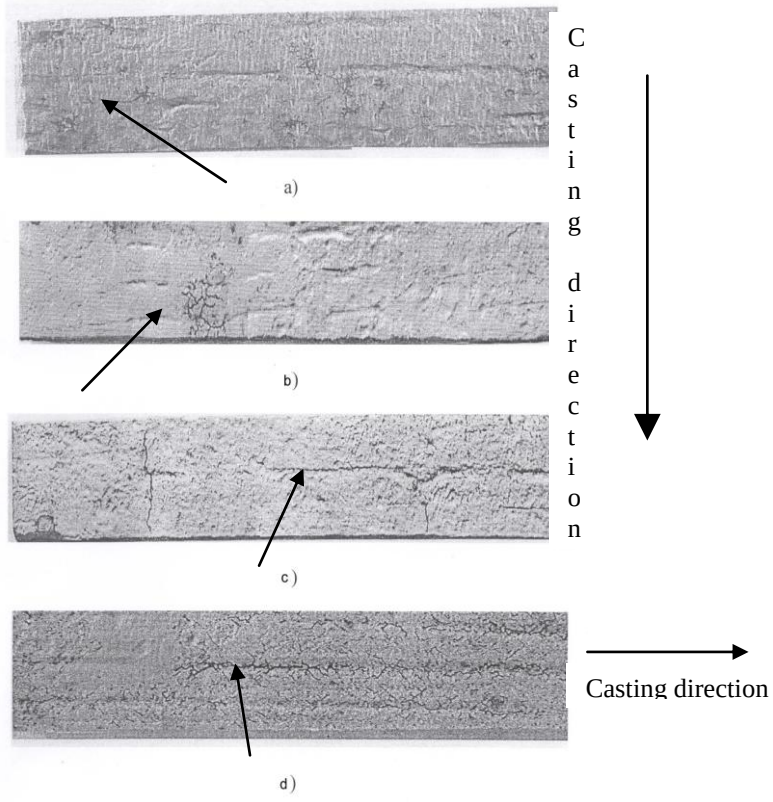

Fig. 1. *Typical slab surface defects.*
a – "star" cracks; ; b – netlike cracks; c – transversal cracks; d – longitudinal cracks

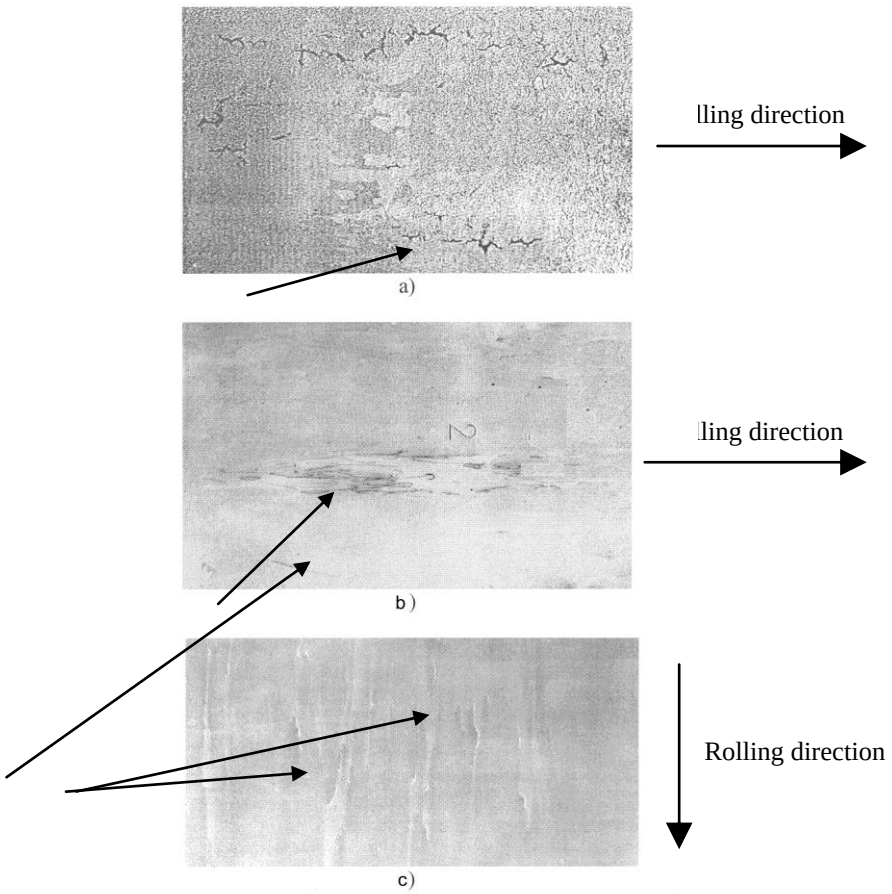

Fig. 2. *Transformation of slab defects to rolling plates.*
a – netlike cracks; b – rough scab; c – shallow scab ("µ"-defect).

Carbon content impact

In the course of study observed was an obvious tendency of crack number increase per unit of area and the degree of their development with an increase of carbon content in the examined range of carbon content changes – from 0.07% to 0.21%. The integral value of the defect-stricken surface of slab of steel grade 08MnNb with carbon content being 0.06 ÷ 0.09% was taken for a unit of crack formation conventional index. The crack formation conventional index takes into account both the value of the slab surface affection with cracks and the crack depth penetration.

Simultaneously it was observed that along with carbon concentration change from 0.09% to 0.21% surface crack morphology undergoes certain changes – at carbon weight fraction being in the range of 0.10 ÷ 0.14% check cracks are prevalent, while at carbon content being 0.15–0.21% there was a considerable amount of transverse and star cracks observed along with check cracks.

Analysis of the Fe-C diagram at carbon weight fraction in steel being within 0.08 to 0.45% shows presence of 3 principally different areas of the melt solidification. Comparing the data of the table and the Fe-C diagram it was noted that steel grades 08MnNb and 09Mn2VNb solidification takes place in the area where there's a transition from δ-iron to γ-iron in the completely solidified metal.

For steel grades 13Mn1SiNb and ASTMA572 having δ-γ transition in accordance with the standard interval of carbon content there's a provision both for a variant of transition into a completely solidified metal and for a variant of peritectic transformation from "δ+liquid" to "δ+γ" at constant temperature. For steel grades S355J2G3 or St52.3 the following variants of solidification are possible: "δ+liquid" into "δ+γ" or "δ+liquid" into "γ+liquid". Under such conditions the factors, which usually play unimportant role, have significant influence on quality indexes of the surface of metal. To these factors should be referred minor fluctuations of hot metal level in the mould while casting steel at a concaster, inessential moisture deviations and deviations of granulometric slag-forming composition (within the limits stated by normative documents), technological deviations of casting rate related to changes of submerged nozzles, tundishes etc.

Based on the results of the study, considering that carbon weight fraction in steel affects consumer qualities of finished metal product to a large extend, the Works' specialists focused their special attention to such steel grades, that were most susceptible to defect formation processes. As a result, a whole series of engineering measures and corrective actions both in the field of preparation of liquid steel for casting and directly at concasting of steel were worked out to avoid or to reduce essentially defect formation processes essentially.

Manganese content impact

It was established that, fraction of surface defects had steady tendency to increase with growth of manganese weight fraction in steel, which was confirmed with essentially greater number of defects on the surface of steel 13Mn1SiNb and 13Mn1Si (manganese content up to 1.6%) in comparison with steel grade ASTM A572 (manganese content up to 1.0%). It was found, that with increase of manganese weight fraction in steel in 0.05% in the range of 1.2% to 1.8% of manganese content defect-stricken surface of the concast billet increased approximately in the same value according to linear dependence. In addition, it was found that most unfavorable conditions of billet skin formation in the mould at casting steel are observed for the grades, whose solidification was possible under various variants so-called peritectic steel grades – 13Mn1SiNb and S355J2G3.

Aluminum and nitrogen content impact

The impact of such elements as aluminum and nitrogen was put to the study too. As a result of these elements emission at grain boundaries in the form of aluminum nitride ALN metal ductility in the temperature interval of embrittlement while casting steel of peritectic type decreased. It promotes the formation of small-sized longitudinal cracks at the temperature of slab surface of 700–900°C, that corresponds to the area of a billet unbending at the concaster secondary cooling zone (curvilinear area), where slab crust is put to considerable fluctuating load. As a result of transformation of this type of defects at rolling, shallow skins were formed, which are situated mostly at side area at a distance of up to 300 mm from the plate edge. Based on the results of the study it was stated, that minimal propagation of longitudinal cracks was formed at nitride content less than 0.006% and aluminum weight fraction in the range of 0.029–0.032%.

Impact of impurities of nonferrous metal

Taking into account, that peritectic steels are susceptible to crack formation initially rather topical question is the issue of rating of impact of impurities of nonferrous metals on quality of concast slab and plate products. It is generally known that residual impurities of nonferrous metals have a harmful effect on the quality of cast and rolled metal. At the analysis of effect of impurities of nonferrous metals on quality indices an essential influence of the increased concentrations of nonferrous metals was marked on: 1) formation of the rough cross cracks in some cases resulting in destruction of slabs; 2) formation of cracks perpendicular to a wide side or narrow and face sides of a slab; 3) increase of a rejecting of plate steel regarding surface defects of steelmaking and the defects revealed with the ultrasonic control (presence of internal cracks in the center line area of a sheet).

A thorough investigation and analysis of the manufacturing method of the slabs, undergone to destruction was carried out: 1) in the slab yard of the BOF shop; 2) during transportation or transfer; 3) at reheating in the furnace before rolling; 4) during rolling.

It is necessary to note, that the fact of slabs destruction at a rough cross crack occurs rather seldom. So, a number of the destroyed slabs at all stages (conversions) in the last years came to 5.5 cases / 100 thousand of slabs. It was noted, that exclusively manganese steel microalloyed with niobium or steel fully alloyed with niobium and vanadium, first of all steel grades: St52.3 under DIN 17100 or S355J2G3 under EN 10025 (about 90%) were susceptible to destruction.

The formed crack in overwhelming number of cases passes all over the dendritic-web areas. In the area of a break small-sized stress cracks depart from the basic crack. Microfractographic study was carried out on a focused-beam electronic microscope REMMA-202M and to show, that destruction of samples basically was characterized by fragile destruction of grain boundaries. It confirmed the statement about embrittlement at grains boundaries due to nonferrous impurities.

According to the carried out studies determined were the maximum permissible impurities concentrations: for lead – 0.0003–0.0004%, for antimony – 0.0003%, for tin – 0.0005–0.0006%, for zinc – 0.0020–0.0030%. It was established, that the degree of effect on increase of crack sensibility decreases in the following order «antimony-lead- tin-zinc». Based on this, the empirical formula determining the given total limiting concentration of impurity of nonferrous metals, not rendering visible deterioration of properties of cast and rolled metal of manganese steels with carbon content 0.17–0.22% is offered: C_M = %Sb + 0,75%Pb + 0,5%Sn + 0,1%Zn ≤ 0,0012, where C is the given total concentration of nonferrous metals in finished steel.

At excess of the given "threshold" value expansive growth of deterioration continuous cast slabs – occurrence of rough transverse cracks on the surface of narrow and wide sides of an billet, face cracks perpendicular to wide sides is observed. In most critical cases (for steels with carbon content in the range of 0.18–0.21% of 78 and manganese more than 0.01%) destruction of slabs or presence of a main cross through-the-thickness transverse crack of plate steel is observed.

"Threshold" value $C_м$ increases with simultaneous decrease of the carbon and manganese content. During studies it is marked, that for steel with the carbon content in the range of 0.17–0.21% at increase by carbon in 0.01% "threshold" value of the given factor

$C_м$ should be decreased by 0.0004%. At excess of "threshold "values" $C_м$ for steels with carbon content in the range of 0.10–0.11% and manganese more than 1.6% or with carbon content 0.14–0.16% and manganese in the range of 1.0–1.2% face cracks perpendicular to wide sides at the worst are observed.

Hydrogen impact

Not less essential effect on quality of a surface of concast slab is rendered by availability of the dissolved hydrogen in steel. Change of a heat sink from a mold wall to a solidified billet skin is the factor resulting in formation of the above-mentioned net-like check and star cracks. This assumption is confirmed by calculation of the amount of hydrogen releasing at steel solidification and its getting into the hit in a liquid layer of slag at the copper wall of a mould.

It's from the known published sources that the data for the equilibrium value of hydrogen solubility in liquid steel was taken to be within the limits of 26 ppm near the liquid point and within 8 ppm near the solidus in solid δ-iron. The thickness and length of a liquid slag interlayer was taken for calculations to be respectively 2–3 mm and 600–700 mm, a reference value of hydrogen concentration in solid steel over equilibrium concentration to be 4 ppm. For case of short periods of time it's possible to assume that up to 2 ppm of hydrogen are released from the solid shell of an billet into the liquid interlayer of slag. Taking into account low sorption ability of slag on the basis of and the initial moisture content in the mix to be within 0.4 – 0.5% it is pertinent to make the assumption that hydrogen released from steel forms bubbles floating up to the surface of slag. The greatest possible amount of the released hydrogen in the way of bubbles is comparable to the volume of the whole liquid interlayer of slag. Simultaneously nonuniform hydrogen allocation along the perimeter of billet can be the additional factor that breaks a uniformity of a heat-conducting path and accordingly results in initiation of concast billet surface defects both on wide and narrow sides of billet.

Development of corrective actions

Taking into consideration that a fracture of total mass of a number of elements contained in steel is defining the consumer properties of finished steel products, particular attention was paid to those steel grades that are to the utmost susceptible to the defect forming process. In the course of work several technological innovations were generated both in the field of liquid steel preparation for casting and directly in the process of continuous casting thus allowing to avoid or essentially minimize negative affect of the unstable processes of crystallization and solidification.
A number of measures were worked out at several Works to significantly improve slab surface quality. In case of possible change in steel chemical analysis, not contradicting the regulatory documents, the content of carbon was changed towards minimization.

Several technological measures were suggested for steels with strict specification of chemical composition (in particular, by carbon content): 1) use of recycled low sulphur scrap only in steel melting and primary aluminum for steel deoxidation; 2) optimization of the granulometric composition of slag-forming mixtures for concasting of steel and in a number of cases use slag-forming mixtures of the molten base for the purpose of improving the slag-forming process on the surface of melt in the mould and conditions of heat abstraction between the mould wall and the slab crust; 3) application of special "mild" secondary cooling mode to melt slab steel grades 13Mn1Si and 13Mn1SiNb to decrease thermal stress in the solidifying rim of the slab; 4) slow cooling slabs of steel grade S355Nb slabs including cooling in boxes to reduce internal macro stresses in cast steel.

Found that changing of the heat sink conditions under unsteady casting conditions has negative effect on solidification of steel undergoing peritectic transformation. In that case unsteady solidification process facilitates extension of lap depth and crack initiation of different morphology – transverse, netlike and spider cracks – on the billet surface. Increasing of mixture viscosity due to mixture temperature reduction at metal mirror and billet surface results in slag pulling into billet subsurface layer. Reduction or full stoppage of metal feeding to the mold during transient process leads to almost complete liquidation of compelled upflows in steel and facilitates nonmetallic inclusions entanglement among growing dendrite axis from the direction of CCP minor radius. Reduction of slag layer temperature and billet temperature is a reason of saturation of liquid slag layer with the bubbles of hydrogen escaping from billet and heat sink abrupt change at local points. Reduction of billet surface temperature in unbending zone towards brittleness temperature interval is a reason of initiation or propagation of surface cracks originated in the crystallization zone both on the narrow and broad billet edges.

Essential increasing of concast slabs rejection due to surface defects and downgrading of rolled plates manufactured from the slabs cast under irregular condition is a confirmation of the above mentioned negative factors effect. Rejection of the slabs cast under transient condition due to surface defects is 1.5 – 2 times more than that during casting under stabilized condition. For example, "pipe" defect is detected only under transient condition. At the same time plate downgrading due to the defects discovered with the help of ultrasonic testing, according to 2^{nd} – 3^{rd} class of SEL 072 standard and similar to it, increases 3 – 5 times more. Rolled metal downgrading due to the skins and slag impurities is increasing 2 – 3 times more.

Casting process under irregular condition increases essentially hazard of off-optimum and emergency situations at the CCP. As example of such negative influence is increasing of billet skin sticking index and bleeding index under the mould. Sticking and bleeding index while casting of the first slab's meter after nozzle exchange is 20 – 30 times more, while casting of the second – third meter is 15 – 20 times more than while casting under stabilized condition. Each case of casting under irregular condition leads to a great amount of technological crops such as teeming arrests, both top and ground scraps, scrap in the form of metal remains in tundish while tundish exchange or the termination of the casting process.

One of the possible solutions of the question of casting speed and temperature stabilization is decreasing of transient conditions quantity. It permits to increase the average casting speed to obtain the reduction of crop and metal quality improvement.

Most of the transient conditions, such as submerged nozzles replacement and tundish replacement, finishing of the casting process are related with limited life time of the casting refractory materials such as stopper rod, no swirl nozzle and submerged nozzle. Increasing of refractory components resistance and, hence, the number of heats a series is one of the important conditions of concast billet quality improvement.

With the purpose to reduce the rate of defects in a concast slab, the usage of rational by chemical composition refractory materials, with more than 1.2% manganese mass fraction, for steel casting was introduced at some Iron and Steel Works. Mullite-graphite submerged nozzles were selected as having higher mechanical wear resistance and low sensitivity to manganese interaction. The usage of stopper rod monoblock units and argon blowing of the no swirl nozzle at the rate 0.1 – 0.2 m^3/hr, which prevents inclusion deposition on work surfaces was suggested for the purpose of steel castability improvement and decrease of non-regular conditions during casting.

More difficult question was a selection of optimal casting refractory materials for casting of ordinary peritectic steels, such as carbon and manganese steel with up to 1.2% Mn content. While casting steel of this type, it is possible to use both quartz submerged nozzles less sensitive to the process of alumina particles deposition on refractory work surfaces and high strength mullite-graphitic submerged nozzles. Three different types of casting refractory complete sets were used for comparative experiments: 1) option 1 – jointed stopper rod, biceramic no swirl nozzle and quartz submerged nozzle with steel silicocalcium treatment of the most important steel grades at argon stirring plant; 2) option 2 – jointed stopper rod rod, periclase-graphite nonswirl nozzle and quartz

submerged nozzle with steel silicocalcium treatment of all grades at argon stirring plant; 3) option 3 – stopper rod monoblock unit, periclase-graphite or corundum-graphite no swirl nozzle and mullite-graphite submerged nozzle with steel silicocalcium treatment for all grades at argon stirring plant;

200–300 heats of ordinary carbon grades or low alloy steel grades with manganese content up to 1.2% were made for each option. The process waste quantity during casting (scrap, crop), casting process stability (stopper rod "no closing", metal penetration into the gap between the no swirl nozzle and the stopper rod, choking of submerged nozzle channel, concast billet and rolled plate quality were evaluated. The main parameters of steel casting process and technological waste quantity are given in Table 2.

Table 2. *Casting technological parameters*

Position	Parameters, conventional index	Production option		
		1	2	3
1	Tundish, heat life time	1	1.06	1.56
2	Nozzles life time	1	1.87	6.40
3	Casts in unstable conditions	1	0.63	0.16
4	Stopper rod pair faults	1	0.70	0.06
5	Crops	1	0.85	0.65
6	Scrap	1	0.76	0.72
7	Slab rejection due "gas blister" defect	1	0.56	0.44

The usage of high strength casting refractories together with steel silicocalcium treatment of all grades is fully reasonable.

As the result of the testing, we recommended to abandon the usage of biceramic no swirl nozzles and to use periclase-graphite or corundum-graphite nonswirl nozzles, which have mechanical erosion resistance and are insensitive to alumina deposition on working surfaces. Additionally, with the purpose of abatement of alumina particles deposition, it is recommended to treat all low-carbon steels with silicocalcium core wire. In this process, complex fusible combinations of calcium and aluminum oxides that do not deposit on refractory surface are formed.

All the measures developed and represented in this paper allowed to reduce essentially the quantity of transient casting conditions and off-optimum situations in slab casting.

Introduction of the above research results in casting of carbon and manganese steels of peritectic grades with manganese content up to 1.2% allowed: 1) to increase tundish life time 1.4 – 1.5 times; 2) to increase submerged nozzle life time 3.5 – 6; 3) to decrease 10 – 15 times the number of stopper rod pairs and submerged nozzle faults; 4) to decrease the technological waste quantity 13 – 15 times; 5) to decrease 1.3 – 2.3 times slab downgrading due to "gas blister" defect; 6) to decrease 2.1 times plates downgrading due to steelmaking defects.

Research results of unsteady steel casting conditions influence

The unsteady casting condition impact on concast billets and rolled plates internal and surface defects initiation and propagation are studied. It is demonstrated that concast slabs rejection due to surface defects and rolled plates downgrading due to steelmaking defects and defects indicated by ultrasonic testing essentially increase under unsteady conditions, the probability of non-regular and emergency situations (specifically, concast billet sticking) occurrence increases substantially.

Technological actions that facilitate stabilization of casting speed and temperature by reduction of solidification transient conditions are recommended: reduction of submerged nozzles replacements and increasing of tundish and number of heats in a series.

Usage of optimal refractories with the aim to reduce the possibility of transient conditions occurrence in continuous casting is suggested. This method implies the usage of mullite-graphite stopper rod monoblock units with stopper rod channel argon blowing, periclase-graphite or corundum-graphite no swirl nozzles and mullite-graphite submerged nozzles. The usage of refractories proposed allows to reduce occurrence of unsteady conditions and their negative impact on the complex indicators of concast slab and rolled plates quality.

References

1. Бережницкий Л.Т., Громяк Р.С., Трущ Н.И. О построении диаграмм локального разрушения хрупких тел с остроконечными жесткими включениями // ФХММ.- 1975. – 11, №5. – С. 40-47.

2. Harkogard G.A. A theoretical study of the influence of inclusions upon the initiation and growth of fatigue cracks in steel // Jernkontorets annaler.- 1991.- 155, N6.- P.209-297.

3. Трефилов В.И., Моисеев В.Ф. Дисперсные частицы в тугоплавких металлах.- Киев: Наук.думка, 2008.- 240 с.

Briant C.L., Banerjee S.K., Ritter A.M. The role of nitrogen in the embrittlement of steel // Met.Trans.- 1982.- A13, N7.- P.1939-1951.

4. Драчинский А.С., Подрезов Ю.М., Трефилов В.И. Влияние элементов структуры на энергию межзеренного разрушения // ФММ.- 1983.- 55.- Вып.1.- С.157-164.

5. Столофф С.Н. Влияние легирования на характеристики разрушения // Разрушение.- М.: Металлургия, 1976.- 6.- С.11-89.

6. Бродецкий И.Л., Белов Б.Ф., Позняк Л.А., Троцан А.И. Влияние адсорбционных процессов в границах зерен на хладостойкость низколегированных сталей // ФХММ.- 2005.- №2.- С.124-128.

7. Бродецкий И.Л., Харчевников В.П., Троцан А.И., Белов Б.Ф. О влиянии кальция на зернограничное охрупчивание сталей с карбонитридным упрочнением // МиТОМ.- 1995.- №5.- С.24-26.

8. Бродецкий И.Л., Харчевников В.П., Троцан А.И. Анализ неметаллических включений на границах зерен стали с карбонитридным упрочнением //МиТОМ.-2004.- №3.-С.12-14

9. Control of Surface Ouality of 0.08%<C<0.12% Steel Slabs in Continuous Casting / Vincent Guyot, J.-F. Martin, A. Ruelle e.a //ISIJ International, Vol. 36. - 1996.- Supplement, P. S227-S230.

10. Mazumdar S., Ray S.K. Solidification control in continuous casting of steel // Sadhana, Vol. 26, Parts 1 & 2, February–April 2001, P. 179–198.

EFFECTS OF BISMUTH ON THE MATRIX STRUCTURE OF DUCTILE IRON CASTINGS

Prof. Glavas Z. PhD.[1], Assoc. Prof. Strkalj A. PhD.[1]
University of Zagreb, Faculty of Metallurgy, Sisak, Croatia [1]

E-mail: glavaszo@simet.hr, strkalj@simet.hr

Abstract: *This paper deals with the effects of the addition of 0.00031, 0.00064, 0.001 and 0.0042 wt.% Bi on the matrix structure of ductile iron castings consisting of 7 sections of different thicknesses (3, 12, 25, 38, 50, 75 and 100 mm) and contain low content of Si (2.11 wt.%) and pearlite promoting element (0.018 wt.% Cu, 0.0055 wt.% Sn, 0.00041 wt.% Sb, 0.098 wt.% Mn). The Bi contents of 0.00031, 0.00064 and 0.001 wt.% were not significantly affected the share of ferrite and pearlite in the section thicknesses of 12, 25, 38, 50, 75 and 100 mm compared to the casting which does not contain Bi. In all these sections the share of pearlite was increased and the share of ferrite was decreased by the addition of 0.0042 wt.% Bi. All of the above-mentioned Bi contents were resulted in the formation of iron carbides in the section thickness of 3 mm. The share of carbides increases with increasing Bi content.*

Keywords: DUCTILE IRON, BISMUTH, MATRIX STRUCTURE

1. Introduction

Ductile iron, as well as gray and compacted graphite iron is a member of the family of graphitic cast irons. Because of the spherical (nodular) shape of graphite particles, ductile iron has significantly better tensile properties and toughness than gray and compacted graphite iron. Its properties enable it to be used in the production of motor vehicles, cast pipes and various construction components.

Microstructural features determine the mechanical properties of ductile iron. Nodule count, the share and shape of non-spherical (non-nodular) graphite particles and especially the share of ferrite and pearlite in the metallic matrix have a key effect [1 – 8].

The chemical composition is one of the most important factors influencing the structure of the metallic matrix [1 - 3]. Other important factors are the cooling rate of the casting after the solidification and nodule count and their distribution [1, 2, 9, 10].

It is well known that Bi can have a detrimental and beneficial effect on the morphology of graphite particles and nodule count in ductile iron, which depends on its content and the presence of other elements. Studies [11, 12] have shown that the Bi content of only 0.006 wt.% can completely prevent the formation of nodular graphite in a 25 mm thick ductile iron casting. However, very small Bi content can increase the nodule count [13 - 17]. In addition, the appropriate amount of Bi can prevent detrimental effect of rare earth (RE) elements on the graphite morphology in the thick-walled ductile iron castings and at the same time increase the nodule count [13, 18 – 22].

On the other hand, very little information exists about the effect of different content of Bi on a metallic matrix of ductile iron. From the pearlitic influence factor (P_x) [20, 23]:

$$P_x = 3.0\ (\text{wt.\% Mn}) - 2.65\ (\text{wt.\% Si} - 2.0) + 7.75\ (\text{wt.\% Cu}) + 90\ (\text{wt.\% Sn}) + 357\ (\text{wt.\% Pb}) + 333\ (\text{wt.\% Bi}) + 20.1\ (\text{wt.\% As}) + 9.60\ (\text{wt.\% Cr}) + 71{,}7\ (\text{wt.\% Sb}) \quad (1)$$

it can be concluded that Bi is a powerful pearlite promoting element. However, the content of the other elements, the nodule count, and the cooling rate of the casting after the solidification should also be taken into account. This paper explored the influence of various additions of Bi on the structure of the metallic matrix in ductile iron casting that contains a low content of ferrite-promoting elements and pearlite-promoting elements and has segments of different thicknesses, from thin to thick.

2. Experimental

In a medium-frequency coreless induction furnace, steel scrap (with a share of 20 wt.%), ductile iron returns (with a share of 30 wt.%) and special low-manganese pig iron (with a share of 50 wt.%) were melted to produce base melt. Preconditioner with the following chemical composition: 0.6 to 1.9 wt.% Ca, 3 to 5 wt.% Al, 3 to 5 wt.% Zr and 63 to 69 wt.% Si was added to base metal in an amount of 0.1 wt.%.

The wire filled with FeSiMg treatment alloy containing 42 wt.% Si, 29 wt.% Mg, 0.5 wt.% Ce, 0.2 wt.% La, 1.4 wt.% Ca and 0.9 wt.% Al was added to the base melt in the ladle in order to perform nodularization. Inoculant containing 67 to 72 wt.% Si, 2.2 wt.% Ba, 1.9 wt.% Al and 1.5 wt.% Ca was also added to the ladle in the amount of 0.6 wt.% to perform the first stage of inoculation.

Five test stepped castings (TSC) was produced by pouring the ductile iron melt into green sand molds. The shape and dimensions of test stepped castings are shown in Figure 1. The second stage of inoculation was performed by addition of 0.2 wt.% of the inoculant containing 0.75 to 1.25 wt.% Ca, 0.75 to 1.25 wt.% Al, 1.5 to 2 wt.% Ce and 70 to 76 wt.% Si in the ductile iron melt stream during pouring into the molds. Bi was not added to the TSC 1. Pure Bi (99.99 wt.% Bi) was added to the ductile iron melt stream during casting of the TSC 2, TSC 3, TSC 4 and TSC 5. Table 1 shows the targeted Bi contents.

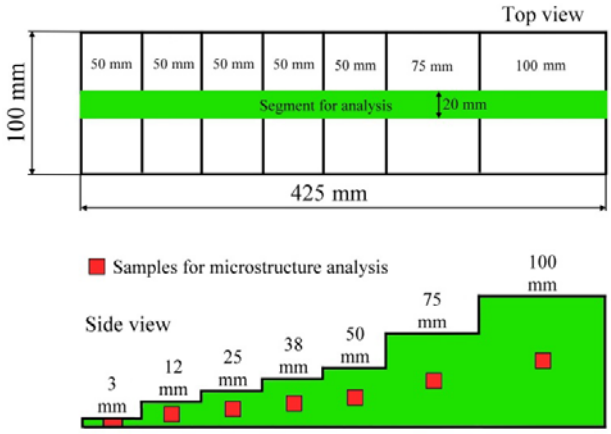

Fig. 1 *The shape and dimensions of test stepped castings.*

Table 1: *Targeted Bi contents in test stepped castings.*

Test stepped castings (TSC)	Targeted Bi contents, wt. %
TSC 1	-
TSC 2	0.00025
TSC 3	0.0005
TSC 4	0.001
TSC 5	0.005

A sample of the ductile iron was taken a few moments before pouring the melt into molds to determine the content of C, Si, Mn, Mg, S, P, Cu, Ni, Cr, Mo, V and W by optical emission spectrometry (OES). Inductively coupled plasma mass spectroscopy (ICP-MS) was used to determine the contents of Bi, Sb, Sn, Nb, Pb, As and Ti in test stepped castings. Samples for this analysis were taken from test stepped castings.

Samples for microstructure analysis on a light metallographic microscope equipped with a digital camera and the image analysis system were taken from each test stepped castings according to Figure 1.

3. Results and discussion

The chemical compositions of the test stepped castings are given in Table 2.

Table 2: *Chemical composition of test stepped castings.*

Test stepped castings (TSC)	Chemical composition		P_x*
	Elements	Bi, wt.%	
TSC 1	3.550 wt.% C, 2.110 wt.% Si, 0.048 wt.% Mg, 0.035 wt.% P, 0.012 wt.% S, 0.098 wt.% Mn, 0.018 wt.% Cu, 0.016 wt.% Ni, 0.029 wt.% Cr, 0.002 wt.% Mo, 0.01 wt.% V, 0.0015 wt.% W, 0.00041 wt.% Sb, 0.0055 wt.% Sn, 0.0169 wt.% Ti, 0.0039 wt.% Nb, 0.00052 wt.% Pb, 0.00015 wt.% As	0.000011	1.14
TSC 2		0.00031	1.24
TSC 3		0.00064	1.35
TSC 4		0.001	1.47
TSC 5		0.0042	2.53

* P_x - pearlitic influence factor (defined by the Eq. [1])

There are no significant differences between the targeted and actual Bi contents. In order to highlight the influence of Bi, the contents of ferrite-promoting elements (Si), pearlite-promoting elements (Cu, Sb, Sn, Mn, Pb, As) and carbide-forming element (Cr, V, Mo, W, Nb) are set to be low to minimize their effects on the microstructure of test stepped castings.

The cooling rate, i.e. wall thickness and Bi content influenced the structure of the metal matrix of the examined test stepped castings (Table 3, Figures 2 and 3).

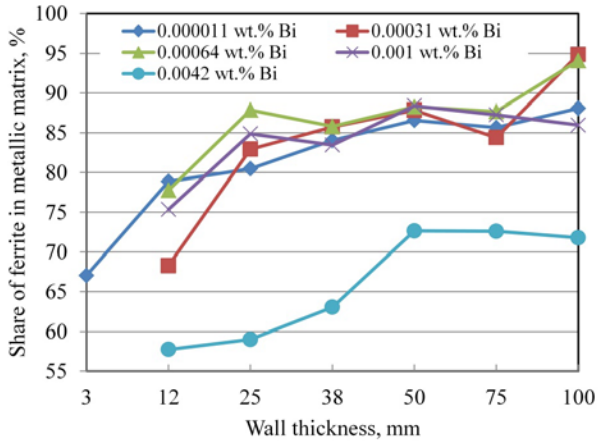

Fig. 2 *Influence of wall thickness and Bi content on share of ferrite in the metallic matrix of test stepped castings.*

In all test stepped castings, decreasing the cooling rate, i.e. increasing the wall thickness from 3 to 100 mm resulted in an increase in the share of ferrite in the metallic matrix. Slower cooling after solidification facilitates the diffusion of the carbon atom from austenite to the graphite nodules. This results in greater removal of carbon from the austenite, which enables transformation of austenite into ferrite.

Table 3: *The share of ferrite and pearlite in the metallic matrix of test stepped castings.*

Test stepped castings (TSC)	Bi, wt.%	Wall thickness, mm	The share of ferrite, %	The share of pearlite, %
TSC 1	0.000011	3	67.05	32.95
		12	78.87	21.13
		25	80.47	19.53
		38	84.04	15.96
		50	86.57	13.43
		75	85.66	14.34
		100	88.08	11.92
TSC 2	0.00031	3	Iron carbides	
		12	68,28	31,72
		25	82,93	17,07
		38	85,75	14,25
		50	87,83	12,17
		75	84,40	15,60
		100	94,87	5,13
TSC 3	0.00064	3	Iron carbides	
		12	77,76	22,24
		25	87,87	12,13
		38	85,81	14,19
		50	88,27	11,73
		75	87,67	12,33
		100	94,10	5,90
TSC 4	0.001	3	Iron carbides	
		12	75,35	24,65
		25	84,88	15,12
		38	83,46	16,54
		50	88,40	11,60
		75	87,26	12,74
		100	85,98	14,02
TSC 5	0.0042	3	Iron carbides	
		12	57,73	42,27
		25	58,99	41,01
		38	63,03	36,97
		50	72,64	27,36
		75	72,59	27,41
		100	71,77	28,23

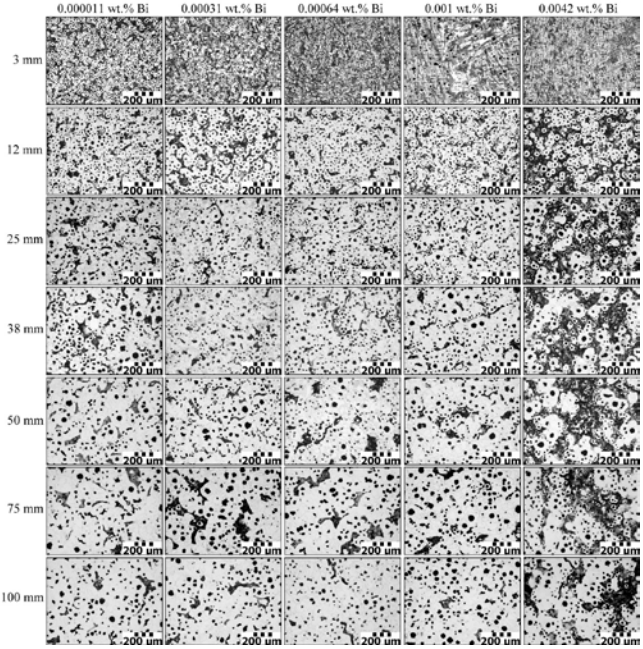

Fig. 3 *Microstructures of the wall thicknesses of 3, 12, 25, 38, 50, 75 and 100 mm in test stepped castings (etched in Nital).*

The data in Table 2 for TSC 1, TSC 2, TSC 3 and TSC 4 show that Bi contents of 0.00031, 0.00064 and 0.001 wt.% were not significantly affect the share of ferrite and pearlite in the walls thicknesses of 12, 25, 38, 50, 75 and 100 mm. However, the addition of 0.0042 wt.% Bi (TSC 5) resulted in a significant decrease of the share of ferrite in these walls compared to TSC 1 where Bi was not added. This clearly shows that Bi promotes the formation of pearlite.

The optical micrographs in Figure 3 show the presence of iron carbides in a 3 mm thick wall in test stepped castings containing 0.00031, 0.00064, 0.001 and 0.0042 wt.% Bi (TSC 2 – TSC 5). The share of carbides increases with increasing Bi content. Since the wall thickness of 3 mm in TSC 1 does not contain carbides, it is obvious that the Bi promotes the formation of carbides in thin walls, especially when the Si content is low.

Figure 3 shows that a proper addition of Bi can improve the morphology of graphite particles and increase the nodule count and nodularity. As the wall thickness increases, these positive effects become more and more pronounced [17].

4. Conclusion

The obtained results show that Bi promotes pearlite formation. In the ductile iron which contains a low content of ferritising elements, the Bi increases the share of pearlite in thin, medium-thick and thick walls. Pearlitic influence factor (P_x) is a good indicator of the effect of Bi on a metal matrix of ductile iron.

From the results of this research it can be concluded that Bi, even in very small contents, promotes the formation of iron carbides in thin sections. The share of iron carbide in microstructure of thin sections increases with increasing Bi content. However, Bi can have a positive effect on graphite morphology, nodule count and nodularity, especially in thicker sections, if added in the proper amount.

5. References

[1] M. Gagné, The Sorelmetal Book of Ductile Iron, Rio Tinto Iron & Titanium, Montreal, Canada, 2004.

[2] …, Ductile Iron Handbook, ed. W. A. Henning, J. Mercer, American Foundry Society, Inc., Illinois, 2010.

[3] …, Ductile Iron Data for Design Engineers, Rio Tinto Iron & Titanium, Montreal, Canada, 1998.

[4] R.A. Gonzaga, Influence of Ferrite and Pearlite Content on Mechanical Properties of Ductile Cast Irons, Materials Science and Engineering A 567(2013), 1 – 8.

[5] R.A. Gonzaga, P. Martínez Landa, A. Perez, P. Villanueva, Mechanical Properties Dependency of the Pearlite Content of Ductile Irons, Journal of Achievements in Materials and Manufacturing Engineering 33(2009) 2, 150 – 158.

[6] P. Ferro, P. Lazzarin, F. Berto, Fatigue Properties of Ductile Iron Containing Chunky Graphite, Materials Science and Engineering A 554(2012), 122 – 128.

[7] I. Riposan, M. Chisamera, A. Stan, Control of Surface Graphite Degeneration in Ductile Iron for Windmill Applications, International Journal of Metalcasting 7(2013) 1, 9 – 20.

[8] C. Labrecque, P.M. Cabanne, Low Temperature Impact Strength of Heavy Section Ductile Iron Castings: Effect of Microstructure and Chemical Composition, China Foundry 8(2011) 1, 66 – 73.

[9] X. Guo, D.M. Stefanescu, Solid Phase Transformation in Ductile Iron – A Benchmark for Computational Simulation of Microstructure, AFS Transactions 105(1997), 533 - 543.

[10] D. Venugopalan, A Kinetic Model of the $\gamma \rightarrow \alpha$ + Gr Eutectoid Transformation in Spheroidal Graphite Cast Irons, Metallurgical Transactions A 21(1990) 4, 913 - 918.

[11] H. Morrogh, Influence of some residual elements and their neutralisation in magnesium treated nodular cast iron, AFS Transactions 60 (1952), 439 – 452.

[12] G.S. Cole, Solidification of Ductile Iron, AFS Transactions 80 (1972), 335 - 348.

[13] P. Ferro, A. Fabrizi, R. Cervo, C. Carollo, Effect of Inoculants Containing Rare Earth Metals and Bismuth on Microstructure and Mechanical Properties of Heavy-Section Near-Eutectic Ductile Iron Castings, Journal of Materials Processing Technology 213(2013) 9, 1601 – 1608.

[14] H. Horie, T. Kowata, A. Chida, Influence of Bismuth on Graphite Nodule Count in Thin-section Spheroidal-graphite Cast Iron, Cast Metals, 2(1990) 4, 197 - 202.

[15] H. Takeda, H. Yoneda, K. Asano Effect of Silicon and Bismuth on Solidification Structure of Thin Wall Spheroidal Graphite Cast Iron, Materials Transactions 51(2010) 1, 176 – 185.

[16] F. Unkić, Z. Glavaš, K. Terzić, Utjecaj broja nodula na žilavost feritnog nodularnog lijeva, Strojarstvo: časopis za teoriju i praksu u strojarstvu 50(2008) 4, 231-238.

[17] Z. Glavas, A. Strkalj, K. Maldini, F. Kozina, Effect of Bismuth and Rare Earth Elements on Graphite Structure in Different Section Thicknesses of Spheroidal Graphite Cast Iron Castings, Archives of Metallurgy and Materials 63(2018) 3, 1547-1553.

[18] I. Riposan, M. Chisamera, A. Stan, Control of Surface Graphite Degeneration in Ductile Iron for Windmill Applications, International Journal of Metalcasting 7(2013) 1, 9 – 20.

[19] I. Riposan, M. Chisamera, V. Uta, S. Stan, The Importance of Rare Earth Contribution From Nodulizing Alloys and Their Subsequent Effect on the Inoculation of Ductile Iron, International Journal of Metalcasting 8(2014) 2, 65 – 80.

[20] I. Riposan, M. Chisamera, S. Stan, Performance of Heavy Ductile Iron Castings for Windmills, China Foundry 7(2010) 2, 163 - 170.

[21] A. Javaid, C. R. Loper, Jr., Production of Heavy-Section Ductile Cast Iron, AFS Transactions 103(1995), 135 – 150.

[22] E.N. Pan, C. Y. Chen, Effects of Bi and Sb on graphite structure of heavy-section ductile cast iron, ASF Transaction 104(1996), 845 – 858.

[23] I. Riposan, M. Chisamera, S. Stan, Influencing Factors on As-cast and Heat Treated 400-18 Ductile Iron Grade Characteristics, China Foundry 4(2007) 4, 300 - 303.

EVALUATION OF MECHANICAL PROPERTIES OF DUCTILE CAST IRON AND INVERSE REGRESSION

ОЦЕНИВАНИЕ МЕХАНИЧЕСКИХ СВОЙСТВ ЧУГУНА С ШАРОВИДНОГО ГРАФИТА И ОБРАТНАЯ РЕГРЕССИЯ

Assoc. Prof, PhD. Alexander Popov [1], PhD. Mr. Eng. Jan Ivanov [2] , Br. Eng. Stefan Georgiev [2]
[1] Institute of Mechanics - BAS, Sofia, Bulgaria, E-mail: alpopov@abv.bg
[2] M+C HYDRAULIC Plc, Kazanlak, Bulgaria, E-mail: jeanivanov@yahoo.de

Abstract: *The evaluation of ductile cast iron is common foundry practice. For the correct non-destructive evaluation (NDE) of mechanical properties (ultimate tensile strength; relative lengthening; Brinell's hardness; elasticity modulus) by means ultrasonic testing and inverse regression analysis are used.*

Kay words: MECHANICAL PROPERTIES, DUCTILE CAST IRON, INVERSE REGRESSION

.

1. Introduction

The ultrasonic testing of the mechanical properties of ductile cast iron [1,2,3] is a common practice in M+C HYDRAULIC.

There are methods of regression analysis are used. In literature there are dependencies between the structural characteristics of the cast iron $(F;P;N_G)$ and its mechanical properties $(E;\nu;N_G;R_m;HB)$, where $(F;P;N_G)$ are appropriate *F*,% - quantity of ferrite and *P*,% - quantity of perlite in the metal matrix, N_G ,% - nodular graphite contain; R_m - ultimate tensile strength; A_5 - relative elongation; *HB* – Brinell's hardness; $(E;\nu)$ - elasticity modulus. The following dependencies are considered [4-11]

(1) $(E;\nu)\Rightarrow(V_L;V_T)$;

(2) $N_G=\eta(V_L)$;

(3) $R_m=\gamma_0+\gamma_1.V_L$; $\quad R_m=\beta.V_L^2.HB$;

(4) $A_5=A_5^{(0)}+A_5^{(1)}.V_L$; $A_5=a.(M.V_L^2/HB)^m$;

(5) $HB=h_0+h_1.V_L$,

where $(V_L;V_T)$ are velocities of longitudinal and transversal ultrasonic waves [8,11]. The coefficients in (2)-(5) $\gamma_0;\gamma_1;\gamma;A_5^{(0)};A_5^{(1)};a;M;h_0;h_1$ are subject to determination and depend on the casting technology and the type of graphite in the casting. The dependencies (2) to (5) are regressions models from type

(6) $(N_G;R_m;A_5)=F(V_L;HB)$

In regression analysis [12] the basic principle is " $(F;P;G)$ defines by $(N_G;R_m;A_5;HB)$", where $(F;P;N_G)$ - microstructure characteristics of, $(N_G;R_m;A_5;HB)$ - mechanical properties for ductile cast iron. In this sense, dependencies (2) to (5) are incorrectly. The correct approach is

(7) $V_L=\Psi(N_G;R_m;A_5;HB)$,

where $(F;P;G)\Rightarrow V_L$. In this article the models with one predictor $X=\chi(N_G;R_m;A_5;HB)$ and order n are considered [12]

(8) $V_L=\sum_{K=0}^{n}\beta_K X^K$.

The condition for choice, at *X* = 1, of order m, is $R^2\rightarrow\max$, where R^2 is coefficient of determination.

Table 1.

m	R^2
$m=1$	$R^2\equiv R^2(m=1)$
$m=2$	$R^2(m=2)\approx(1.05\div1.10).R^2$
$m=3,4,5$	$R^2(m=3,4,5)\approx(1.06\div1.13).R^2$
$m\geq6$	The regression matrix is badly determined.

If $m=1$, then the values of R^2 are relatively low. If $m=2$, then the values of R^2 are rises with $\sim(5\div10)$%. If $m=3;4;5$, then the values of R^2 are rises $\sim(1\div3)$% and efforts to calculate it are not justified. If $m\geq6$, then the regression matrix is badly determined and calculations are not made.

Therefore, the optimal choice of the model (8) is one predictor $X\Leftrightarrow(N_G;R_m;A_5;HB)$, and model order m = 2.

2. Relations for ductile cast iron

2.1. Deterministic dependencies

In the theory of elasticity [10,11] is obtained (9)

$$V_L=\sqrt{\frac{1-\nu}{(1+\nu).(1-2.\nu)}}.\sqrt{\frac{E}{\rho}},$$

where the elasticity modulus $E;\nu$ respectively are Young's modulus and Poison's coefficient, density of ductile cast iron - $\rho, kg/m^3$. The deterministic dependence (9) is reduced to

(10) $E=M(\nu).V_L^2$,

where

$$M(\nu)=\rho.\frac{(1+\nu).(1-2.\nu)}{(1-\nu)},\nu=\frac{0.5-(V_T/V_L)^2}{1-(V_T/V_L)^2}.$$

For most ductile cast iron, the reference values for ν are $\nu\in(0.23\div0.28)$. In fact, for ductile cast iron, Poisson's coefficient changes to a very narrow boundary. By means

reference values $med(\nu)=0.25$, $\rho=7.31 kg/m^3$, M = 6.092 is obtain. Therefore, the dependence (10) is reduced to

(11) $E \approx 6.V_L^2$.

2.2. Stochastic dependencies

According the experimental data, for ductile cast iron, from M+C HYDRAULIC a polynomial models of (8) are considered

(12) $V_L = \sum_{K=0}^{2} \beta_K X^K$,

where $X \equiv (N_G; R_m; A_5; HB)$, $(\beta_0; \beta_1; \beta_2)$ subject to determination. It are direct regression problems.

The inverse regression problems are determine the confidence intervals $(X_L; X_R)$, when V_L is measured. The equations for $(X_L; X_R)$ are [12]

(13) $\mp \chi(X_{L,R}) + V_L = 0$,

where

$\chi(X_{L;R}) = t.S.\left[\frac{1}{n} + \frac{1}{S_{XX}}\left(X_{L;R} - \overline{X}\right)^2\right]^{1/2} - \sum_{K=0}^{2} \beta_K X_{L;R}^K$, number of measures – n, $S_{XX} = (n-1).S$, $(t, S, \overline{X})$, by means Excel, MS Office are obtain.

The equations (13) are non-linear regarding $X_{L;R}$ and solved by the Newton's method using a ZEROIN algorithm [11], on-line C ++ compiler, at a specified root spacing. The ZEROIN algorithm is resistant and fast approaching.

3. Equipment

Image Analyzer Buehler Omnimet, Digital Ultrasonic Flaw Detector Sitescan 150S, Tensile machine Testometric F300, Hardness tester ТШІ- 2М.

4. Experiment

Ten samples were made with varying percentages and graphite morphology and mechanical properties. They were determined for them $(N_G; R_m; A_5; HB)$ and $(V_L; V_T)$. Morphology of graphite (N_G) was determined with a Buehler Omnimet image analyzer at an 8x image magnification. The mechanical properties $(R_m; A_5; HB)$ are determined by mechanical testing. The velocities $(V_L; V_T)$, Fig.1. , according ASTM E 494:2015 are calculated.

Piezo plate with X – cut for longitudinal waves with velocity V_L	Piezo plate with Y – cut for transversal waves with velocity V_T
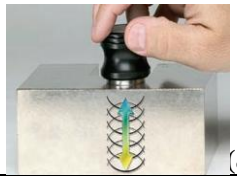 (a)	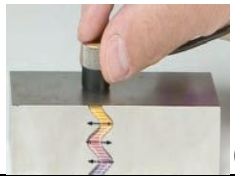 (b)

Fig.1. Ultrasonic L-waves (a) and T-waves (b)

5. Inverse regression tasks

5.1, Polynomial models

According the experimental data, for ductile cast iron, confidence intervals $(X_L; X_R)$, are obtained.

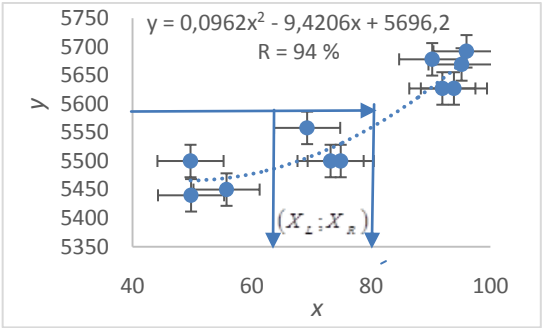

Fig.2. $(x = N_G, \%; y = V_L, m/s)$

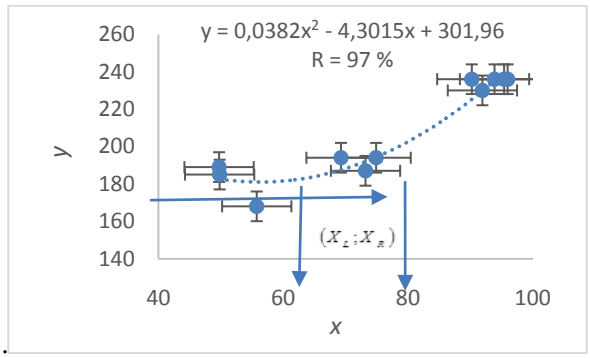

Fig.3. $(x = N_G, \%; y = HB, kgf/mm^2)$

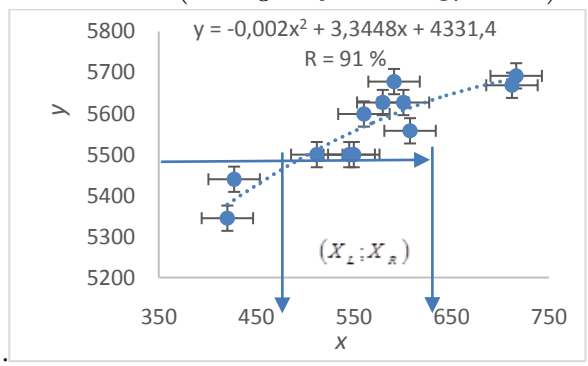

Fig.4. ($x = R_m, MPa; y = V_L, m/s$)

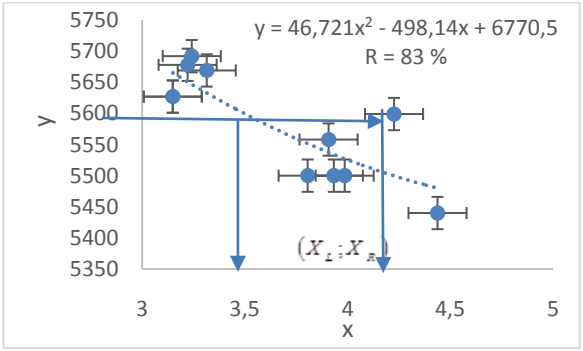

Fig.5. ($x = A_5.\%; y = V_L; /s$)

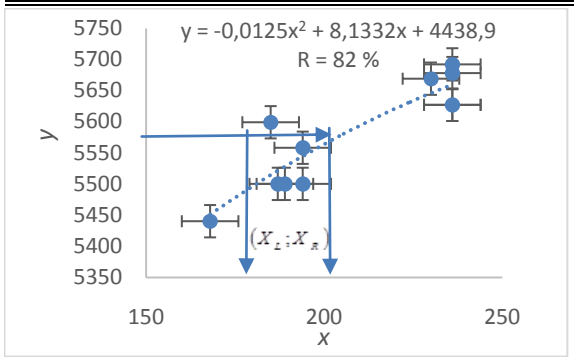

Fig. 6. ($x = HB, kgf/mm^2; y = V_L.m/s$)

5.2. Hybrid models

The introduction of hybrid models in the regression analysis is based on the following assumption. Factor combinations depend on one predictor [4-11]. For example $F(V_L;HB) = A_5$ and $\Psi(V_L;HB) = R_m$. Such an approach is expected R^2 will rise. On Fig. 7. and Fig. 8. specific dependencies are given.

.

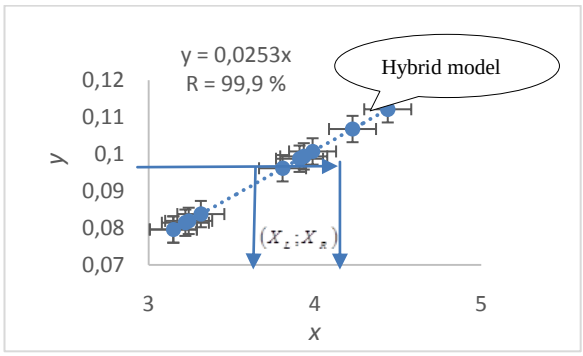

Fig. 7. ($x = A_5, \%; y = 6(V_L^2 / HB)^{4/3}$

.

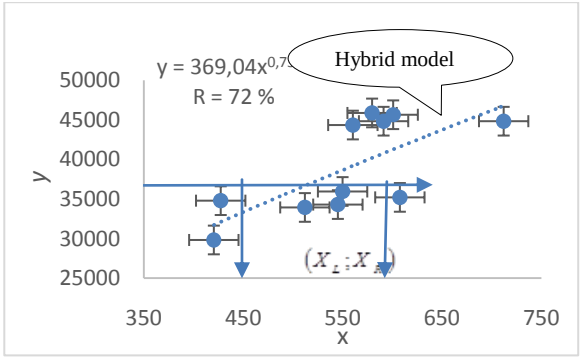

Fig.8. ($x = R_m, MPa; y = 6.V_L^2.HB$)

6. Results

For data from M+C HIDRAULIC Plc the results of inverse regression analysis in Tables 2 - 8. are given. When comparing the results of (Fig.2.) and (Fig.3.), it appears that using the model from (Fig.2.) has less scattering gives a little narrower boundaries evaluation of N_G , %. In this sense, the use of the model from (Fig.2.) is slightly better than the model from (Fig.3.).

Table 3.

A / Polynomial models 95% probability confidence intervals, $(V_L;V_T)$ for *NDE* of N_G ,% by V_L ,m/s and by *HB* ,kgf/mm^2 *Rm, MPa*, A_5 , %, *HB*, kgf/mm^2 by V_L ,m/s			
-	Characteristics of ductile cast iron	(X_L)	(X_R)
Fig.2.	N_G (V_L)	~ 64	~ 81
Fig.3.	N_G *(HB)*	~ 65	~ 80
Fig.4.	*Rm* (V_L)	~ 470	~560
Fig.5.	A_5 (V_L)	~ 3.6	~ 4.4
Fig.6.	*HB* (V_L)	*~ 175*	*~ 213*

Median values are V_L , m/s =5850; *HB,kgf/mm*^{2}=194.

Table 4.

B / Hybrid models 95% probability confidence intervals, $(V_L;V_T)$ for *NDE* of A_5 % , *Rm, MPa* by $\Psi(V_L$,m/s; *HB* ,kgf/mm^2)			
-	Characteristics of ductile cast iron	(X_L)	(X_R)
Fig.7.	A_5 $(V_L;HB)$	~ 3.8	~ 4.1
Fig.8.	*Rm* $(V_L;HB)$	~ 465	~ 595

Median values are V_L , m/s =5850; *HB,kgf/mm*^{2}=194.

7. Conclusion

The paper examined the possibilities and constructed correct models for assessing the degree of ductile iron spheronization and mechanical properties
by measuring the velocity of propagation of longitudinal ultrasonic waves and Brinell hardness. The numerical values of the coefficients of the models were obtained as well as the coefficients for their determination. For this purpose, the respective inverse regression tasks are solved.

8. References

1. Anderson J.C., K.D. Leaver, R.D. Rawlings, J.M. Alexander, Materials Science, Chapman and Hall, London, 1990
2. Guliaev A.P., Material Science, Metalurgia, Moscow, 1986, (In Russian).
3. Arzamatov B.N., &, Materials Science, MGTU "N.E.Bauman", Moscow, 2003, (In Russian).
4. Ivanushkin E.S., G.S. Belay, Ultrasonic Testing of Castings, Technika, Kiev, 1984, (In Russian).
5. Popov Al., Inverse Problems in Solid Mechanics and Ultrasonic Testing , Series "Applied Mathematics and Mechanics", Vol. 9, Institute of mechanics - BAS, Sofia, 2018. (ISSN: 1314-3034), (In Bulgarian).
6. Litovka V.I., Improving the quality of high-strength cast iron in castings, Naukova dumka, Kiev, 1987 (In Russian).

7. Aleshin N.P., &, Acoustical methods for metal testing, Mashinostroenie, Moscow, 1989. (In Russian).
8. Voronkova L.V., Ultrasonic Testing Possibilities of Cast Iron Ingots, Th.2.2.3., ECNDT 2006, Roma, Italy.
9. Hanza S.S., D. Dabo, Characterization of cast iron using ultrasonic testing, Journal of Cr S NDT, No 18, p.3-7, ISSN 1847-9340, 2017
10. ASTM E 494:2015, Standard Practice for Measuring Ultrasonic Velocity in Materials.
11. Sokolnikov I. V., Mathematical theory of elasticity, Nauka i izkustvo, Sofia, 1972 (In Bulgarian).
12. Draper N.R., Smith H., Applied regression analysis, v.1.,v.2.,Finansi i statistika, Moscow, 1986, (In Russian).
13. Forsythe Dj., M Malcolm, K. Molar, Computer methods in mathematical calculations, Nauka i Izkustvo, Sofia, 1986, (In Bulgarian).

ИССЛЕДОВАНИЕ ПОРИСТОСТИ ПЕСЧАНО-СМОЛЯНЫХ ФОРМ, ПОЛУЧЕННЫХ ПРИ ВАРИАТИВНОМ ДАВЛЕНИИ

RESEARCH OF POROSITY OF SHELL FORMS, MADE WITH A VARIABLE PRESSURE

к.т.н., профессор Куликов В.[1], к.т.н., профессор Квон Св.[1], д.т.н., профессор Еремин Е.[2], магистр, докторант Ковалёва Т.[2]
[1]Карагандинский государственный технический университет, г.Караганда, Республика Казахстан
[2]Омский государственный технический университет, г. Омск, Российская Федерация
mlpikm@mail.ru, svetlana.1311@mail.ru, sagilit@mail.ru

Abstract: Increase in pressure in the course of formation of a shell form gives the chance a little to increase density of packing of particles. Comparison of calculation of porosity for the received dependence and a practical curve depending on diameter of grain was carried out. It is defined that use of non-stationary pressure leads to increase in a share of a time of the radius of 1000 nanometers up to 58%, however further increase in pressure leads to decrease in the general porosity.
KEYWORDS: HARDNESS, POROSITY, FORM, SAND, PITCH, A COVER, PRESSURE, PULVERBAKELIT

1. Введение

Способ получения отливки в первую очередь влияет на шероховатость и размерную точность поверхности отливок. Изготовление отливок деталей горно-шахтного оборудования традиционно производится в песчано-глинистые формы (ПГФ). Такая технология имеет как достоинства (относительно низкая стоимость), так и недостатки (высокая шероховатость, значительное пылевыделение при выбивке форм, передвижении отработанной смеси, низкая газопроницаемость ПГФ из-за присутствия глины и влаги, вероятность брака по вине формы). В итоге необходимо искать качественно новые способы изготовления отливок.

Оболочковые формы со смолой в качестве связующего могут использоваться при получении отливок широкой номенклатуры от 0,2 до 300 кг при толщине стенок 3…18 мм из самых различных сплавов. Литьё в оболочковые формы обеспечивает большую геометрическую точность, что зачастую исключает необходимость механической обработки. Также они обладают высокой прочностью и газопроницаемостью, не впитывают влагу, не склонны к осыпаемости и сопротивлению усадке, застывающего металла.

2. Предпосылки и средства для решения проблемы

Повышение количества точек контакта между частицами смеси при возрастании плотности их упаковки обусловлено влиянием давления прессовой плиты, которую прилагают к песчано-смоляной смеси для уплотнения. Внешняя нагрузка необходима для преодоления сил аутогезии и трения, которые препятствуют перераспределению частиц в более плотную упаковку. Чем сильнее требуется уплотнить материал, тем больше должна быть величина прессования.

Увеличение давления дает возможность немного повысить плотность упаковки частиц. Процесс перераспределения частичек смеси, определяемый действием определяется как трением, так и значением сил аутогезии. Таким образом, при воздействии внешнего давления изменяются как прочностные характеристики каждого отдельного контакта, так и количество и упаковка формовочной смеси. Они определяются физико-химическими свойствами материала частиц, а также от их формы и размера.

3. Результаты и дискуссия

Одними из основных стадий, определяющих макроструктуру песчано-смоляной формы, является прессование смеси и спекание оболочки. На данных стадиях формируются такие свойства огнеупора, как пористость и плотность формы, которые во многом определяют такие важнейшие эксплуатационные свойства, как механическая прочность, термоустойчивость и шероховатость поверхности. Пористость оболочки является одним из основных параметров структуры формы, т.к. определяет его газопроницаемость. Если исходить из этих соображений, пористость огнеупора должна быть максимальной. Однако очевидно, что при очень высокой пористости оболочки падает ее прочность. Поэтому необходимо достигать оптимальной пористости, которая обеспечивала бы с одной стороны, достаточную прочность, с другой – позволила бы обеспечить технологически требуемую газопроницаемость. Для выбора оптимальных режимов изготовления оболочковых форм необходимо исследовать влияние режимов технологии на пористую структуру формы.

Для изготовления оболочковой формы и получения в ней отливки важным представляется возможность определения математической зависимости газопроницаемости от условий прессования.

Известно, что газопроницаемость дисперсных материалов можно определить, используя формулу, основанную на законе фильтрации Дарси (1):

$$K = \frac{Q \times h}{F \times \Delta p \times \tau}, \quad (1)$$

где K – газопроницаемость;

Q – объем воздуха, проходящего за время τ через образец с поперечным сечением F и высотой h при перепаде давлений Δp.

Также известно, что газопроницаемость формовочных смесей может быть определена как [1]

$$K = d^2 \cdot \frac{S^2}{96 \cdot (1-m) \cdot \eta}, \quad (2)$$

где d – диметр зерна;

S – площадь просвета между частицами в смесях;

m – пористость ПСС;

η – динамическая вязкость газа.

Приравниваем (1) и (2):

$$\frac{Q \times h}{F \times \Delta p \times \tau} = d^2 \cdot \frac{S^2}{96 \cdot (1-m) \cdot \eta}.$$

Находим $S = \sqrt{\frac{96 \times Q \times h \times (1-m) \times \eta}{d^2 \times F \times \Delta p \times \tau}}$.

Определим пористость (3):

$$\frac{96 \times Q \times h \times \eta}{d^2 \times S^2 \times F \times \Delta p \times \tau} = \frac{1}{1-m} \quad (3)$$

В итоге имеем (4):

$$m = 1 - \frac{d^2 \times S^2 \times F \times \Delta p \times \tau}{96 \times Q \times h \times \eta} \quad (4)$$

В результате ранее проведенных исследований [2-3] предложен следующий технологический процесс: после перемешивания песчано-смоляная смесь засыпалась в бункер машины. После производили опрокидывание бункера со смесью на нагретую до 230 ^{0}C модельную плиту с моделями радиаторов. При этом одновременно через плиту подавалось давление 0,25 МПа. Через 10 с давление снизили до 0,2 МПа, а температуру до 210 ^{0}C. Еще через 10 с температуру нагрева повысили до 0,35 МПа, а температуру до 260 ^{0}C. При этом формировалась оболочковая форма толщиной 10-12 мм. После этого формы спекались в течение 2 минут при температуре 320-340 ^{0}C. Приложение нагрузки в процессе формообразования оболочки повышает не только механические свойства оболочковой формы, но и чистоту поверхности отливок и количество пригара на них.

Было проведено сравнение расчета пористости по полученной зависимости и практической кривой в зависимости от диаметра зерна (рисунок 1).

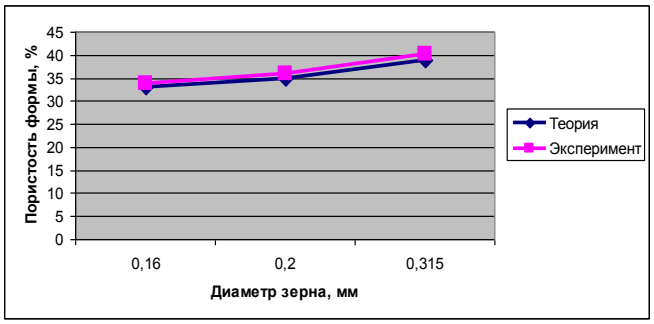

Рисунок 1 *– Зависимость пористости песчано-смоляной формы от величины давления на форму*

По технологии весь период формообразования оболочки из песчано-смоляной смеси продолжается 30-60 с и зависит от величины модели и модельной плиты. Все это время на смесь воздействует тепло, исходящее от модельной плиты и давление, передаваемое посредством прессовой колодки или гибкой диафрагмы (ее можно расположить в бункере). Достижению лучших технологических параметров формы способствует использование вариативного давления. Использованная смесь состояла из наполнителя – кварцевый песок – 94,5 %, связующее – пульвербакелит – 4,5 %; керосин 1 %. Определено, что вначале целесообразно использовать базовое давление, составляющее порядка 0,27 … 0,36 МПа, которое варьируется в течение всего цикла: спустя 9 - 11 с оно понижается на 0,06 - 0,08 МПа, после, через 18 - 22 с увеличивается на 0,08 - 0,12 МПа. В результате, когда сформировалась оболочка толщиной 10 - 15 мм (за 5 - 10 секунд до окончания цикла) давление целесообразно снизить до нуля.

Важным показателем литейных форм является их газопроницаемость. Очевидно, что между газопроницаемостью оболочки и ее пористостью существует определенная зависимость. При этом надо подчеркнуть, что в данном случае надо говорить не о пористости вообще, а только об открытой пористости, т.к. очевидно, что процесс газопроницаемости будет определяться только параметрами открытой пористости. Также надо отметить тот факт, что важно знать не только коммулятивный объем открытой пористости, но и распределение открытых пор по размерам. Это связано с тем обстоятельством, что не все открытые поры доступны для проникновения газов, а только поры определенного радиуса. Для воздуха эта величина составляет около 20 нм, однако состав отходящих газов при сгорании пульвербакелита, в основном представлен фенолом и аммиаком, при заливке расплава образуется СО и др. газы. Молекулы этих газов примерно в 3 раза больше, чем молекула кислорода: например, размер молекулы фенола 0,8 нм, размер молекулы кислорода 0,3 нм. Поэтому условно будем считать, доступным размером, поры радиус которых превышает 60 нм. Как видно из приведенных данных размер доступных пор не равен размеру молекулы, т.к. фактически фиксируется средний размер поры, при этом сама пора может иметь сложное строение типа «бутылки», т.е. входной размер может быть ниже, чем средний. Также надо отметить, что поры радиус которых превышает 1000 мкм являются потенциально «опасными» порами, их присутствие в структуре крайне нежелательно. Поры радиуса больше, чем 1000 мкм, снижают прочность оболочки, ухудшают качество поверхности отливки, нарушают условия равномерного теплообмена [4]. Таким образом, интерес представляет группа пор, средний размер которых находится в диапазоне 60 - 1000 нм. Для удобства обозначим данный диапазон символом А. Данные параметры пористой структуры можно получить только с помощью метода ртутной порометрии. Исследования проводили на ртутном порозиметре системы PASCAL - 400, который позволяет регистрировать поры радиусом до 2 нм. Кроме того, данная система позволяет определять характер распределения пор по размерам, что является очень важным показателем при данном исследовании. Пример получаемых порограмм приведен на рисунке 2.

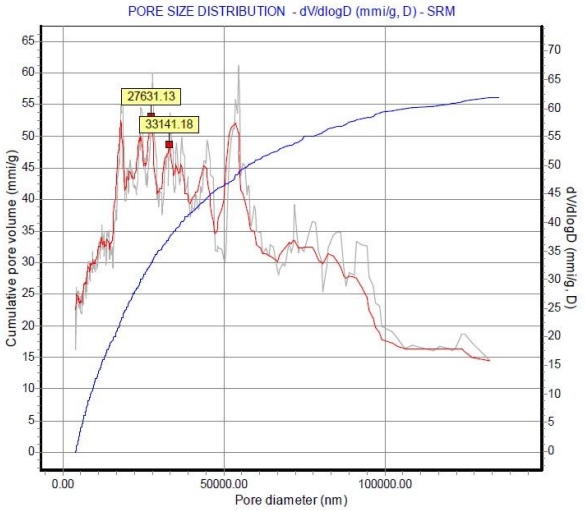

Рисунок 2 *– Распределение пор в оболочковой форме, полученной при вариативном давлении*

4. Заключение

Определено, что применение нестационарного давления приводит к увеличению доли пор радиуса 1000 нм до 58%, однако дальнейшее увеличение давления приводит к снижению общей пористости.

Данные исследования проведены в рамках реализации гранта Комитета науки МОН РК AP05130026 «Разработка и внедрение производства песчано-смоляных форм при нестационарном давлении с целью улучшения качества готовой продукции».

5. Литература

1 Гуляев Б.Б., Корнюшкин О.А., Кузин А.В. Формовочные процессы. – Л.: Машиностроение, 1987. – 264 с.

2. Еремин Е.Н., Ковалёва Т.В., Мозговой И.В. Определение прочности и газопроницаемости литейных форм из песчано-смоляных смесей. Омский научный вестник. - 2016. - № 5 (149). - с. 15-20.

3. Куликов В.Ю., Исагулов А.З., Еремин Е.Н., Ковалёва Т.В. Повышение равномерности плотности и увеличение прочности оболочковой формы. Литейное производство. - 2018. - № 3. – с. 27-29.

4 Нащокин В.В. Техническая термодинамика и теплопередача. Учебн. пособие для неэнергетических специальностей вузов. – М.: «Высшая школа», 1975. 496 с. с ил.

SUPPLY CHAIN PLANNING METHODOLOGY FOR METALS

Ass. Prof., Candidate of Technical Sciences, Solodovnikov V.[1,2]

[1] LOGIS Research and Development Laboratory, Frenstat pod Radgostem, Czech Republic
[2] National Research University Higher School of Economics, Moscow, Russia
E-mail: vsolodovnikov@hse.ru

Absract *The paper contains the results of the study on the systematization and formalization of specialized approaches to planning supply chains of leading metal companies and comparison of these practices with the standard supply chain management models SCOR & CCOR & DCOR and GSCF. The paper defines the main directions of development of the methodology of supply chain planning in terms of its adaptation to the specifics of metals.*
KEYWORDS: SUPPLY CHAIN MANAGEMENT, METALLURGY

1. Introduction

A series of changes in global markets led to a significant transformation of the supply chain management systems of leading metallurgical companies [1,2]. To improve competitiveness companies were forced to restructure their business processes and increase efficiency. Leading metal companies have developed specialized supply chain management approaches which in practice proved to be highly efficient around the world.

These methods in order to be used have to be formalized and studied. In this article, the author formalizes the main directions of development of the methodology of supply chain planning in terms of its adaptation to the specifics of the metals.

2. Preconditions and means for resolving the problem

The result of the survey conducted by the author were the systematization and formalization of the processes and their interactions, a comparison of these processes with the standard supply chain management models like SCOR + CCOR + DCOR [3,4,7] and GSCF [5-7].

The study was based on the analysis of public data of leading steel companies such as TimkenSteel, USA; Trinecke Zelezarny, Czech Republic; Severstal, Russia; MMK, Russia; OMK, Russia; Mechel, Russia; VSMPO-AVISMA Corporation, Russia and many other. A large contribution to this study has made materials from the leading providers of Advanced Planning and Scheduling software for the metallurgical industry: LOGIS, i2 Technologies, and others.

Figure 1 shows the organization of key planning processes in Metals. It is a generalization of the best practices of the abovementioned companies in the area of processes and supporting systems.

3. Results and discussion

From Supply Chain Management (SCM) point of view there are two most common cross-industrial SCM standards in the world: the SCOR model with extensions CCOR and DCOR from Supply Chain Council (SCC) and the model from the Global Supply Chain Forum (GSCF).

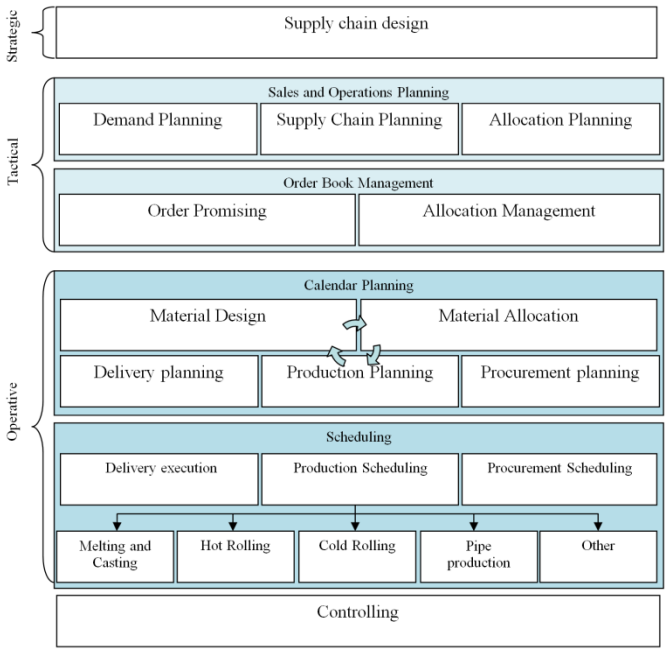

Fig 1 *Organization of key planning processes in Metals*

SCC is an independent, non-profit organization formed in 1996 by the global consulting company Pittiglio Rabin Todd & McGrath (PRTM) and research company Advanced Manufacturing Research (AMR) from Cambridge. At the beginning of its activity, SCC included 69 companies; today the list of participants includes more than 1000 companies.

GSCF under the guidance of Dr. Douglas M. Lambert provides an opportunity for practitioners and theorists to investigate critical issues related to the quality of customer service and operational efficiency, regardless of the specific functional expertise. The professional community of GSCF includes about 14 leading international companies [5,6], recognized as leaders in their industries.

The results of the comparison of the best practices of the organization of business processes of supply chain planning of metallurgical companies with standard models of supply chain management are given in table 1.

For ease of use, the processes of the GSCF model are numbered from 1 to 8 according to the original sequence [6].

For strategic level sub-processes, the suffix S is introduced, for operational level - O.

Table 1. *The results of the comparison of the best practices of the organization of business processes of supply chain planning of metallurgical companies with standard models of supply chain management*

Main process/level	Subprocesses		Model xCOR	Model GSCF
Supply Chain Design	Supply Chain Design		M4SC: SCOR tools could be used for that purpose	4S OF 1S CRM 6S SRM
Tactical planning				
• S&OP	Demand Planning		CCOR:Plan sP1.1	1O CRM 3O DM: forecasting
	Supply Chain Planning		sP1	3O DM: Synchronization
	Allocation Planning		sP1	3O DM: Synchronization
• Order Book Management	Allocation Management		sP1	3O DM: Synchronization
	Order Promising		sD1.2 sD2.2 sD1.3/sD2.3 sD3.3	2O CSM 4O OF
Operative Planning				
• Calendar planning	Production	Material planning/design/technology development	DCOR:Design	7O PDaC
		Material Allocation	sD1.3/sD2.3 sD3.3	4O OF: Process Order
		Production Planning	sP3	5O MFM
	Delivery planning		sP4	4O OF
	Procurement planning		sP2	4O OF
• Scheduling	Production scheduling		sM1.1 sM2.1 sM3.2	5O MFM
	Delivery execution		sD1.3/sD2.3 sD3.3	4O OF
	Procurement scheduling		sS1.1	4O OF
Efficiency evaluation	KPI		sED2 sES2 sEM2	Subprocess «Measure Performance» of corresponding GSCF processes

The presented comparative analysis of the best practices of planning in metallurgy with the known SCM models (SCOR, GSCF) determines the directions of development of these methodologies in terms of their adaptation to the features of supply chain planning of metallurgical companies:

1. Re-engineering the links of existing planning processes according to best practices in metallurgy planning.
2. Consolidating CCOR, SCOR and DCOR models into a single supply chain planning process system.
3. Adding clarification steps of the planning processes, introduction of additional if necessary.
4. Formalization of planning methods and models.
5. Requirements definition for supporting information technologies.

4. Conclusion

The formalization of the best practices of planning in metallurgy given in this article, as well as the results of their comparison with the standard models SCOR+CCOR+DCOR and GSCF, determine the main directions of development of the supply chain management methodology in terms of its adaptation to the specifics of planning in the metallurgical industry.

The need to systematize and develop the planning methodology is determined by the need for its application to ensure the competitiveness of metallurgical companies in a tough struggle in the global market.

5. Literature

[1] PwC, Steel in 2025: quo vadis?, PwC, 2015.
[2] KPMG, Global Metals Outlook, KPMG, 2015.
[3] Supply Chain Operations Reference Model v 10.0, Supply Chain Council, 2010, p. 856.
[4] V. Sergeev, Supply Chain Management, Uright, Moscow, 2015. P. 480. (in Russian)
[5] GSCF http://fisher.osu.edu/centers/scm/members/
[6] D. Lambert, Supply Chain Management: Processes, Partnerships, Performance. 3rd Edition, Supply Chain Management Institute, 2008, p. 431.
[7] H. Stadtler, Ch. Kilger, Supply Chain Management and Advanced Planning. Third Edition, Springer, Berlin, 2004, p. 512.

THE INFLUENCE OF NATURAL AGING AND PRE-AGING ON THE MECHANICAL, PHYSICAL AND MICROSTRUCTURAL PROPERTIES OF THE EN AW-6060 ALUMINUM ALLOY

MSc. Stamenković U., Prof. Dr Ivanov S., Assist. Prof. Marković I., Prof. Dr Mladenović S., Prof. Dr Manasijević D., Prof. Dr Balanović Lj.
University of Belgrade, Technical Faculty in Bor, Bor, Serbia

ustamenkovic@tfbor.bg.ac.rs

Abstract: *The aim of this paper is the investigation of the effect of natural aging on the mechanical, physical and microstructural properties of an EN AW-6060 aluminum alloy. These properties were investigated during different aging treatments. Firstly, the effect of natural aging on properties was investigated, after which the influence of natural aging (room temperature pre-aging) on the artificial aging was studied. The results showed the beneficial effect of natural aging in both sets of experiment. During the natural aging, the hardness increased for around 20 % while electrical conductivity values were slightly higher than in the quenched sample. The hardness of the samples gradually increases up to 25 days of natural aging reaching a plateau state, after which the values of hardness remain the same. Also, room temperature pre-aging had a positive effect on subsequent artificial aging. Samples that were pre-aged for 40 days or more before artificial aging had around a 13 % increase in hardness values compared to the samples that were directly artificially aged. Electrical conductivity had increased by around 1 MS/m in pre-aged samples compared to only artificially aged samples. Optical microscopy investigations confirmed the existence of precipitated phases and their distribution in the microstructure.*

Keywords*: ALUMINUM ALLOYS, EN AW-6060, NATURAL AGING, ARTIFICIAL AGING, HARDNESS, ELECTRICAL CONDUCTIVITY, MICROSTRUCTURE, PRE-AGING*

1. Introduction

Mechanical properties of metallic materials are often improved by various heat treatments. In order to strengthen aluminum alloys, age hardening process is used. This process includes solution heat treatment, quenching to room or below room temperature and aging, which can be either natural (performed at room temperature) or artificial (performed at higher temperatures) [1, 2]. The aging process is responsible for the formation of very fine and evenly dispersed particles that hinder the movement of dislocation thus strengthening the alloy through Orowan mechanism [2]. To attain deeper knowledge of the aging process it is very useful to know the precipitation sequence of investigated alloys. The precipitation sequence is usually found by DSC analysis with combination of some other characterization methods. The largely accepted precipitation sequence for Al-Mg-Si alloys which was found by other authors is given as: α_{ssss} → Mg:Si clusters→ G.P. zones→ β''→ β'→ Si (if excess silicon is present)→ β [3-9]. Precipitates given in this sequence appear at different temperatures and affect the structure differently. Natural aging, as it is performed at room temperature, can only produce the clusters of dissolved elements. In the case of EN AW-6060 alloy the most important clusters are that of Mg and Si, as they are the ones that affect structure the most [10]. The effect of natural aging on the mechanical properties can be summarized as either a positive or a negative one. Low-alloyed alloys or often called lean alloys in this series of aluminum alloys often exhibit the positive effect. This means that natural aging leads to an increase in mechanical properties and also higher peak-aged hardness can be achieved after room temperature pre-aging [11-14]. The negative effect occurs in high solute alloys used in automotive and construction industries [1, 2, 15, 16]. The influence of natural aging is still studied, regardless of numerous studies. In this paper the lean alloy from 6xxx series was investigated (EN AW-6060). The aim was to better understand the influence of natural aging and room temperature storage (pre-aging) on hardness, electrical conductivity and microstructural changes. Also, the investigation of positive or negative effects on subsequent artificial aging was performed.

2. Materials and design

Experimental investigation was performed on EN AW-6060 alloy. The alloy was delivered by "AlCu metali d.o.o." company, in peak aged condition (T6 temper) in the form of extruded rectangular bars. The Table 1 represents the chemical composition of the investigated alloy determined by the optical emission spectrometer "Belec Compact Port". Annealing at 550 °C for 6 hours in the electric resistance furnace Heraeus K-1150/2 removed peak aged condition and obtained the O-temper for all of the samples. After that, solution heat treatment was performed at the same temperature for 1 hour followed by quenching in water with ice in order to obtain a super saturated solid solution (α_{ssss}). After obtaining the super saturated solid solution, the samples were subjected to natural aging for a different time from 3 up to 70 days (referenced as NA samples). One sample was directly aged without any room temperature delay in order to achieve peak hardness state (presented on graph as directly aged AA samples). In order to investigate the influence of natural aging on artificial aging (AA), samples that were naturally aged for 3, 10, 40 and 70 days were chosen and artificially aged in the same manner as the directly aged sample (those samples are referenced as NA+AA samples). All the NA samples were compared to the quenched sample (quenched state on the presented graphs), while all the NA+AA samples were compared to only the artificially aged samples (AA samples).

Table 1: *Chemical composition of the investigated alloy (mass. %)*

Si	Fe	Cu	Mn	Mg	Cr	Ni	Zn
0.49	0.182	0.012	0.006	0.594	<0.003	0.028	0.01
Ti	**Pb**	**V**	**Co**	**Sn**	**Zr**	**Al**	
0.005	<0.003	0.014	<0.003	<0.003	<0.003	98.62	

During the aging treatment, all samples were subjected to various characterization methods. Electrical conductivity was measured using the electrical conductivity tester Sigmatest 2.063". Hardness was measured on the VEB Leipzig Vickers hardness tester using a 10 kg load and a 15 s dwelling time. The ASTM E384 standard was followed during the hardness measurements [17].

3. Results and discussion

Analysis of the graph presented in Fig. 1 shows that hardening was achieved through natural aging. All of the naturally aged samples had higher hardness values in comparison to quenched state. After only 3 days of natural aging hardness rapidly increases, and continues to increase until it reaches hardness saturation after which the curve shows the plateau state where hardness remain almost the same up to 70 days. Hardness has a maximum value after 40 days of aging. This value is around 20% higher than the value for the quenched sample.

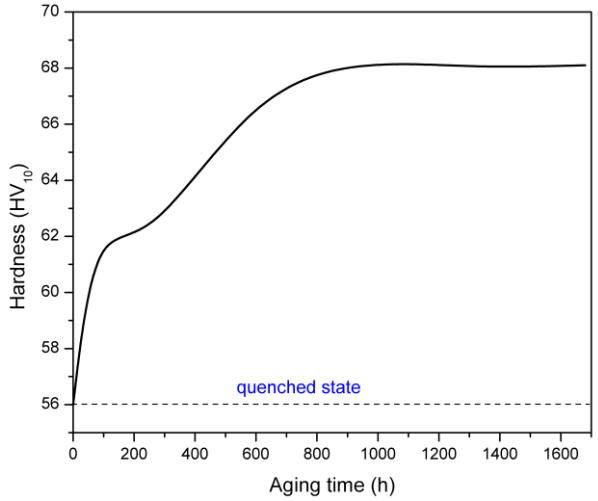

Fig. 1 *Hardness variations of quenched samples during natural aging of EN AW-6060*

During solution heat treatment, Mg and Si atoms dissolved into the Al matrix and remained in the matrix after quenching. Hardness increment was possible due to the formation of magnesium and silicon clusters and co-clusters caused by precipitation during the natural aging process. This formation is causing the restriction of dislocation motion and increasing the hardness of the alloy [1, 2, 10, 16]. The incline of the curve presented in Fig. 1 can be explained by the formation of Mg and Si clusters which occurs after several hours of natural aging discovered through 3D atom probe by L. Cao et al. [18].

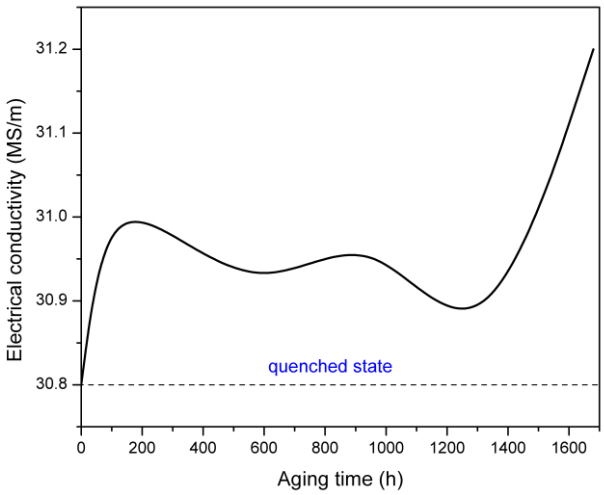

Fig. 2 *Electrical conductivity variations of quenched samples during natural aging of EN AW-6060*

The influence of natural aging on the electrical conductivity of the investigated alloy is presented in Fig. 2. From Fig. 2 it can be concluded that all of the NA samples exhibit slightly higher values of electrical conductivity in comparison to the quenched samples. Electrical conductivity increase can be expected knowing that during natural aging clusters and co-clusters are formed. The quenched solute atoms are released from the super saturated matrix in the form of clusters and co-clusters. This formation is responsible for relaxing the matrix and promoting the free movement of electrons, thus increasing electrical conductivity. The increase in electrical conductivity is not very large due to the fact that this is a lean alloy so the amount of formed clusters cannot have much impact. Usually these clusters have a strong electron scattering effect that can lower the electrical conductivity, but in our case that was not detected [7, 19, 20].

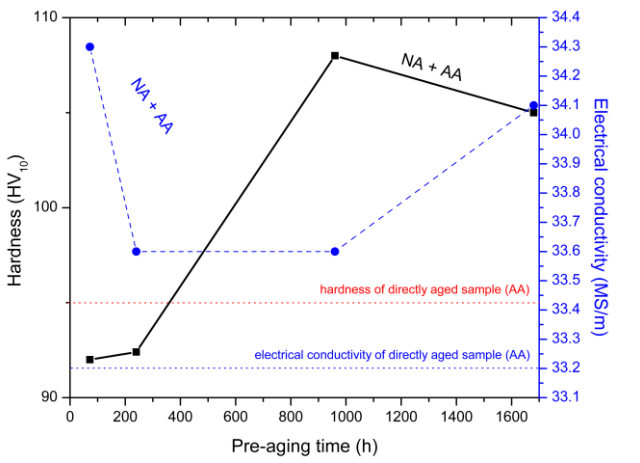

Fig. 3 *The influence of pre-aging on artificial aging on hardness and electrical conductivity of investigated alloy*

In Fig 3 the influence of natural aging (room temperature pre-aging) on the artificial aging has been presented. From the presented graphs in Fig. 3 it can be seen that in both cases, hardness and electrical conductivity, pre-aging had a positive effect on subsequent artificial aging. In order to obtain the highest hardness values the samples need to be peak aged. For the highest values of hardness in peak aged samples the β'' phase is responsible. Any stimulation of the precipitation of this phase results in higher hardness values. In the case of lean Al alloys, clusters and co-clusters formed during the pre-aging help the nucleation of the β'' phase in later precipitation during artificial aging [11, 14]. Samples that were pre-aged for 3 and 10 days had somewhat lower values of hardness in comparison to directly aged samples. In these samples, due to a short period of pre-aging, the nucleation of the β'' phase was not as much affected. Samples pre-aged for 40 and 70 days had enough time to form enough clusters of Mg and Si to stimulate the nucleation, hence the hardness values are higher in comparison to the directly aged ones [2, 6, 10, 11, 14, 15]. In the matter of electrical conductivity, all of the values are higher in the pre-aged samples in comparison to the directly aged sample. This can be ascribed to larger precipitation due to pre-aging and stimulation through nucleation of the β'' phase.

The formation of clusters and the stimulation of precipitation through nucleation sites, caused the β'' phase to appear in the microstructure as finely dispersed particles on the grain boundaries and in the grains, as shown in Fig 4a-b.

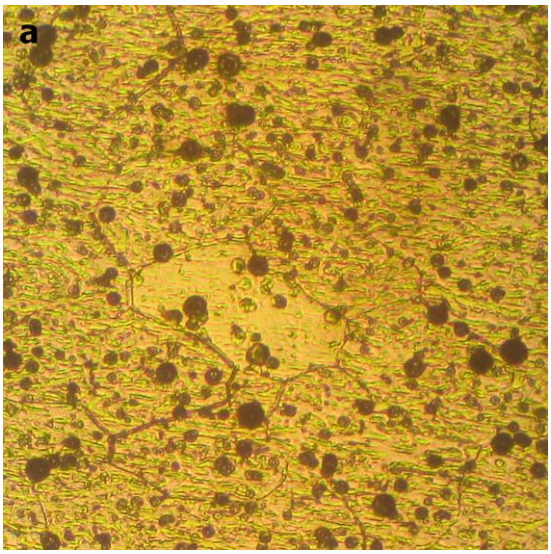

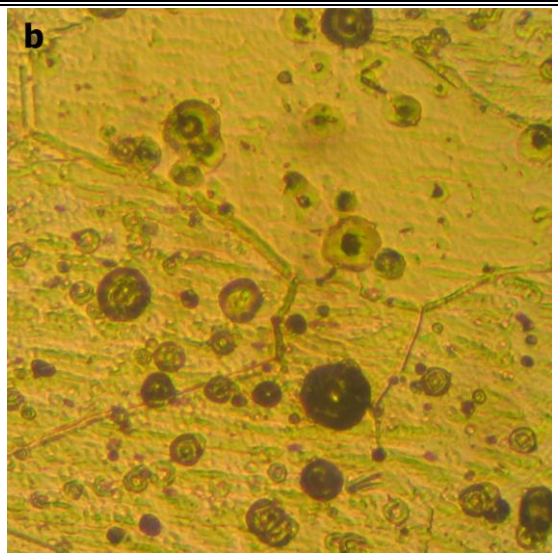

Fig. 4 *Microstructure of the sample naturally aged for 40 days and then peak aged for maximum hardness value; a) magnification x200; b) magnification x500*

4. Conclusions

The influence of natural aging on hardness, electrical conductivity and microstructure was investigated. Key conclusions can be outlined:

- The hardness of the samples naturally aged is higher than those in the quenched state. Maximal hardness is achieved after 40 days of natural aging, after which the hardness goes into the plateau state and hardness remains the same until 70 days of natural aging.
- Naturally aged samples have slightly higher values of electrical conductivity in comparison to the quenched one.
- Natural aging showed positive effect on artificial aging.The nucleation of the β'' phase and the strengthening effect of β'' phase was affected by the formation of magnesium and silicon clusters and co-clusters. The hardness of the pre-aged samples was higher only in the ones pre-aged for 40 and 70 days. Hardness was higher for around 13 % for the pre-aged sample in comparison to the directly aged one. Electrical conductivity was higher in all of the pre-aged samples when compared to the only artificially aged one.
- In the samples that were naturally and subsequently artificially aged, β'' phase appeared in the form of finely dispersed particles.

Acknowledgements

The research results were developed with the assistance of the Ministry of Education, Science and Technological Development of the Republic of Serbia under the projects OI 172037 and TR34003.

References

[1] Pogatscher S., Antrekowitsch H., Leitner H., Ebner T., Uggowitzer P.J., Mechanisms controlling the artificial aging of Al–Mg–Si Alloys - Acta Materialia, Volume 59 (2011), pp. 3352-3363.

[2] Cuniberti A., Tolley A., Castro Riglos M.V., Giovachini R., Influence of natural aging on the precipitation hardening of an AlMgSi alloy - Materials Science and Engineering: A, Volume 527 (2010), pp. 5307–5311.

[3] Milkereit B., Wanderka N., Schick C., Kessler O., Continuous cooling precipitation diagrams of Al–Mg–Si alloys - Materials Science and Engineering: A, Volume 550 (2012) pp. 87-96.

[4] Mrowka-Nowotnik G., Influence of chemical composition variation and heat treatment on microstructure and mechanical properties of 6xxx alloys - Archives of Materials Science and Engineering, Volume 46 (2010), pp. 98-107.

[5] Birol Y., Precipitation during homogenization cooling in AlMgSi alloys - Transactions of Nonferrous Metals Society of China, Volume 23 (2013), pp. 1875-1881.

[6] Gupta A.K., Lloyd D.J., Court S.A., Precipitation hardening in Al–Mg–Si alloys with and without excess Si - Materials Science and Engineering: A, Volume 316 (2001), pp. 11-17.

[7] Edwards G.A., Stiller K., Dunlop G.L., Couper M.J., The precipitation sequence in Al–Mg–Si alloys - Acta Materialia, Volume 46 (1998), pp. 3893-3904.

[8] Shang B.C., Yin Z.M., Wang G., Liu B., Huang Z.Q., Investigation of quench sensitivity and transformation kinetics during isothermal treatment in 6082 aluminum alloy - Materials & Design, Volume 32 (2011), pp. 3818-3822.

[9] Vedani M., Angella G., Bassani P., Ripamonti D., Tuissi A., DSC analysis of strengthening precipitates in ultrafine Al–Mg–Si alloys - Journal of Thermal Analysis and Calorimetry, Volume 87 (2007), pp. 277–284.

[10] Jin S., Ngai T., Zhang G., Zhai T., Jia S., Li L., Precipitation strengthening mechanisms during natural ageing and subsequent artificial aging in an Al-Mg-Si-Cu alloy - Materials Science and Engineering: A, Volume 724 (2018), pp. 53-59.

[11] Chang C., Wieler I., Wanderka N., Banhart J., Positive effect of natural pre-ageing on precipitation hardening in Al-0.44 at% Mg-0.38 at% Si alloy - Ultramicroscopy, Volume 109 (2009), pp. 585-92.

[12] Strobel K., Lay M.D.H., Easton M.A., Sweet L., Zhu S., Parson N.C., Hill A.J., Effects of quench rate and natural ageing on the age hardening behaviour of aluminium alloy AA6060 - Materials Characterization, Volume 111 (2016), pp. 43-52.

[13] Abid T., Boubertakh A., Hamamda S.,Effect of pre-aging and maturing on the precipitation hardening of an Al–Mg–Si alloy - Journal of Alloys and Compounds, Volume 490 (2010), pp. 166-169.

[14] Lai Y.X., Jiang B.C., Liu C.H., Chen Z.K., Wu C.L., Chen J.H., Low-alloy-correlated reversal of the precipitation sequence in Al-Mg-Si alloys - Journal of Alloys and Compounds, Volume 701 (2017), pp. 94–98.

[15] Birol Y., The effect of processing and Mn content on the T5 and T6 properties of AA6082 profiles - Journal of Materials Processing Technology, Volume 173 (2006), pp. 84-91.

[16] Aruga Y., Kozuka M., Takaki Y., Sato T., Formation and reversion of clusters during natural aging and subsequent artificial aging in an Al-Mg-Si alloy - Materials Science and Engineering: A, Volume 631 (2015), pp. 86–96.

[17] Standard Test Method for Microindentation Hardness of Materials, Accessible on Internet: https://www.astm.org/Standards/E384.htm

[18] Cao L., Rometsch P.A., Couper M.J., Clustering behavior in an Al-Mg-Si-Cu alloy during natural ageing and subsequent under-ageing - Materials Science and Engineering: A, Volume 559 (2013), pp. 257–261.

[19] Cui L., Liu Z., Zhao Xi., Tang J., Liu K., Liu X., Qian C., Precipitation of metastable phases and its effect on electrical resistivity of Al-0.96Mg2Si alloy during aging - Transactions of Nonferrous Metals Society of China, Volume 24 (2014), pp. 2266-2274.

[20] Prabhu T.R., Effects of ageing time on the mechanical and conductivity properties for various round bar diamaters of AA2219 Al alloy - Engineering Science and Technology, an International Journal, Volume 20 (2017), pp. 133-142.

ШЛИФОВАЛЬНЫЕ СТАНКИ С ЧПУ – НЕОБХОДИМОЕ ОБОРУДОВАНИЕ В ЛИТЕЙНОМ БИЗНЕСЕ 4.0

CNC GRINDING MACHINES AS A NECESSARY EQUIPMENT IN INTELLIGENT 4.0 FOUNDRY BUSINESS

Msc.Eng. Zaton J., Iron Foundry WULKAN Inc. Czestochowa, Poland
MBA.Msc.Eng. Zaton P., LAWA Ltd., FENIX MACHINES Ltd., Czestochowa, Poland
janusz.zaton@wulkansa.com.pl
piotr.zaton@wulkansa.com.pl

Abstract: *Nowadays when the main stream of castings is oriented on a automotive business, the quality of grinding plays important role. We are presenting high efficient Fenix CNC grinding machine. Fenix CNC grinding machines are designed for castings grinding of mass production, as well as grindnig casts' flashes and residues of gates and riser heads. Additionally machines allow to programme the shape of grinded casts. Our CNC grinding machines does not have any impact on environment in aspect of pollution and works quietly. It's hermetic casing prevents spreading of pollination resulting from the casts grinding process. The machine is equipped with optical safety devices blocking the rotation of loading and processing table while the operator is in the table rotation work zone. We can offer a position with a robot and a grinder, as well as a ready position with a robot grinder and machining machines.*

Keywords: CNC GRINDER, NUMERICALLY CONTROLLED, EFFECTIVE GRINDING, TABLE ROTATION, FIXING UNIT, INNOVATIVE TECHNICAL SOLUTIONS

1. Введение

Мировое производство отливок превысило 104 миллиона тонн в 2018 году и находилось в пределах статистической ошибки на уровне прошлого года. Китай является лидером по производству отливок – его доля составляет 45 % мирового производства. Следует отметить, что особенно в производстве железных сплавов за последние несколько лет произошёл заметный застой. Наблюдается тенденция к увеличению производства отливок на один литейный завод, что является результатом падения малых литейных цехов.

В дальнейшем будем говорить только об отливках из железных сплавов.

Современные литейные заводы поставляют свою продукцию в различные отрасли промышленности, в основном однако для автомобильной. Большинство отливок требует механической обработки, покрытия поверхности покраской, катафорезы или цинкования и т.д. Это предъявляет высокие качественные требования к литейной промышленности с точки зрения не только прочности отливок (качество материала), но и формы и качества поверхности. Кроме того в течение реализации производственных процессов должны учитыватся условия работы, а также забота о натуральной среде.

Это означает, что при производстве отливок следует использовать новейшие технические достижения: автоматические производственные линии, компьютерное управление, роботы, станки с числовым программным управлением.

Литейный бизнес 4.0 означает четвёртую промышленную революцию (индустрия 4.0) – прогнозируемое событие, введение киберфизических систем в производство.

Насколько формовочные линии, цеха для плавки металла, производство формовочной смеси достигли высокого уровня технологий и широко используются в большинстве литейных заводов, то процессы обработки отливок такие как: удаление литниковой системы и питающей бобышки, очистка и шлифование – реализуются в значительной степени используя силу человеческих рук или простых инструментов.

В результате это приводит к низкой эффективности на одного работника в литейном производствие, что делает литейный завод менее конкурентоспособным.

При организации производства в литейном цехе необходимо перейти от мышления «производство отливок» к мышлению «производство продуктов». Это значит, что полученная уже отливка должна быть ошлифована и обработана «до конца» в литейном заводе.

Большинство отливок требует обработки резанием. Практически каждая отливка, предназначена для автомобильной или машиностроительной промышленности, в следующем этапе подвергается обработке резанием.

Эти процессы должны осуществляться в литейных заводах.

Большой проблемой является шлифование отливок. В большинстве заводов оно делается вручную с помощью дискового шлифовального станка. Это неточный метод, требующий много тяжёлой и опасной работы. Есть группа отливок, для которой этот метод соответствует требованиям качества, однако в случае отливок, которые в дальнейшем производстве обрабатываются механически, отливка шлифованная таким образом не сохраняет точности формы, не имеет одинаковых припусков на целой поверхности

механической обработки. Кроме того из-за характера работы - работа тяжёлая и опасная – рынок труда очень ограничен.

Однако самой важной проблемой в случае ручного шлифования является низкая производственная способность. Из-за этого литейные заводы имеют низкую производительность на одного работника и поэтому они не очень конкурентоспособны.

На рис. 1 показана эффективность производства в литейных цехах различных стран Европейского Союза, выраженная в каличестве тонн продукции на одного занятого в литейном заводе.

Основной причиной низкой эффективности является низкий уровень автоматизации и роботизации производственных процессов. Это, в свою очередь, приводит к низкой производительности процессов шлифования отливок.

Рис. 1 *Эффективность производства отливок из железных сплавов (ферросплавов) в некоторых европейских странах*

2. Шлифовальные станки FENIX

Станки Fenix SZK это машины предназначены к шлифованию отливок железных сплавов весом до 15 килограмм. Шлифовальный круг имеет способность передвигаться в трёх плоскостях, а стол, на котором закреплена отливка, имеет возможность оборота. Следовательно, это четырёхосевая машина.

Это даёт возможноть удалять заливы на разделительных поверхностях и следы оставшиеся после питающей бобышки практически в каждой отливке.

Использовано систему управления машиной FANUC.

3. Характеристические свойства машины FENIX:

- машина имеет чугунные корпуса, которые редуцируют колебания и гарантируют высокую точность шлифования.

- рабочее пространство машины является изолированным от окружающей среды, что обеспечивает экологическую нейтральность процесса, а также гарантирует хорошие условия работы обслуживающего персонала.

Машина имеет наружную и вентиляционную установку, которая обеспечивает баланс воздуха в рабочем пространстве, а также позволяет – благодаря системе фильтров - очищать воздух от чугунной и графитовой пыли, возникающей во время шлифования.

Эта установка удаляет пыль с подузлов и элементов машины (корпуса подшипников, подвижные элементы и т.п).

- высокое качество и эффективность шлифования

У шлифовального круга обороты в пределах 3000 – 6000 оборотов на минуту. Система управления обеспечивает получение любой траектории движения круга в пространстве, приспособление соответствующей скорости шлифования, что даёт возможность шлифования отливки любой формы с высокой точностью. В машине использовано запатентованное решение оборота стола (патент РП номер П. 424701), которое позволяет очень точно позиционировать стол относительно шлифовального круга. Всё это гарантирует высокое качество шлифования.

Кроме того в машине использовано инновационное решение для закрепления обрабатываемых предметов типа кольцо

(патент РП номер П. 421493), что даёт возможность достигнуть высокую производительность и, одновременно, позволяет подключить станок к роботу.

На рис. 2 показано работизированная высокопроизводительная станция шлифования колец ремённых шкивов для автомобилей. Станция состоит из двух станков FENIX, двух роботов и системы подачи отливок.

(фильм представлен во время доклада)

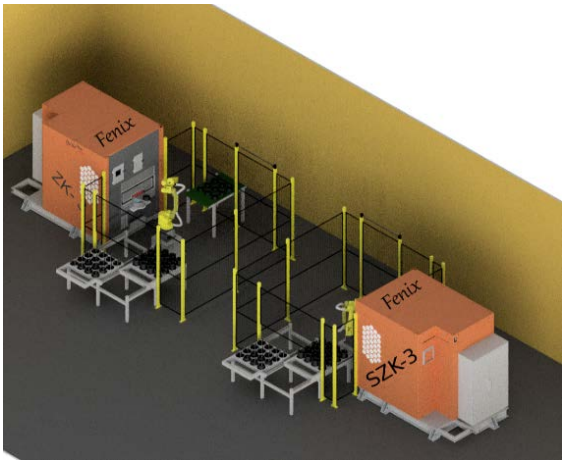

Рис. 2 *Роботизированная станция для шлифования отливок Fenix*

Рабочая станция обслуживается одним работником и достигает производительности в 4,5 раза выше, чем в случае ручного шлифования.

- станок позволяет создавать роботизированные станции для шлифования и обработки резанием чугунных отливок. (Рис.3)

(фильм представлен во время доклада)

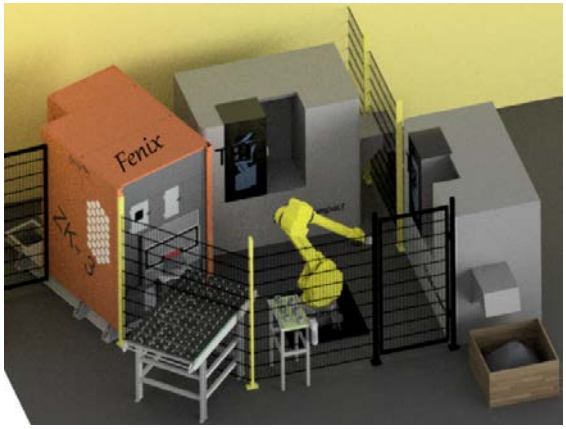

Рис. 3 *Гнездо для шлифования и механической обработки отливки*

Следует отметить, что эта станция в течение рабочей смены в состоянии ошлифовать и обработать резанием 1200 штук продуктов и обслуживается одним работником. (Эффективность самого шлифования в ручном режиме составила 400 штук в одну смену).

Эта станция заменяет работу 5-ти людей и гарантирует самое высокое качество.

- станок FENIX соответствует индивидуальным ожиданиям клиентов.

Модульная система компонентов машины позволяет адаптироваться к потребностям клиента относительно технических параметров (разнообразие отливок).

4. Заключение

Чтобы литейное производство могло быть индустрией 4.0 нельзя обойтись без шлифовальных станков с ЧПУ.

Шлифовальные станки FENIX должны быть необходимым оборудованием для литейного производства железных сплавов, потому что:

- гарантируют высокое качество шлифования отливок;

- позволяют добиться высокой эффективности шлифования, что повышает конкурентоспособность фирмы и в результате приводит к повышению производительности продукции на одного работника;

- даёт возможность создавать роботизированные отделочные станции для шлифования и механической обработки отливок;

- исключают тяжёлую и опасную работу;

5. Литература

1. WFO Industry Report 2017. Actual situation of the Worldwide Casting Industry. WFO, September 2017;

2. Report CAEF, 2017;

INVESTIGATION OF THE STRUCTURE AND SOME OF PHASE TRANSFORMATIONS IN WEAR-RESISTANT CAST ALLOYS

ИЗСЛЕДВАНЕ НА СТРУКТУРАТА И НЯКОИ ФАЗОВИ ПРЕВРЪЩАНИЯ В ИЗНОСОУСТОЙЧИВИ ЛЕТИ СПЛАВИ

Assoc. Prof. PhD eng. Gavrilova R. Vl. *, eng. Lazarova V. K.

Faculty of Metallurgy and Materials Science
University of Chemical Technology and Metallurgy – Sofia
Bulgaria

r.gavrilova@abv.bg

***Abstract**: The study of phase transformation processes in wear-resistant alloys from Fe-Cr, Fe-Ni-Cr, Fe-Cr-Mn base systems has not only a fundamental, but also a practical significance, especially with regard to alloys with a chemical composition with difference from the conventional one - this is an interesting scientific and applied direction. The importance of this type of researches is motivated by fact, that in the available literature there is insufficient data on the structure and properties of non-standard iron-based materials, with variation amount of alloying elements (as well as additional alloying or modification) not only in the cast state, but also after thermal or plastic treatment. That`s why, the aim of the present study is to obtain data on alloys with the most mass application that have increased carbon and reduced chromium content relative to stainless deformable steels.*

Keywords: WEAR-RESISTANT CAST ALLOYS, STRUCTURE TRANSFORMATIONS

1. Introduction

The choice of materials is motivated by their most extensive application for body parts and components in responsible constructions or apparatures [1, 2, 5, 6] operating under special conditions - their working environment is loaded with abrasive wear, aggressive corrosive environments, cavitation, impact loads, ets.

Chemical compositions of the examined alloys are shown in Table 1. From each alloy, 11 samples were obtained and further processed.

***Table 1.** Chemical compositions of the alloys*

Alloys composition	C, %	Mn, %	Si, %	Cr, %	S, %
1 (406)	0.43	14.17	0.32	5.48	0.011
2 (408)	0.92	14.85	0.21	6.12	0.011
3 (410)	1.48	15.05	0.23	5.8	0.011
4 (412)	1.98	14.43	0.21	5.8	0.012
5 (414)	2.35	15.05	0.28	5.72	0.012

2. Experiment

Experimental tasks are carried out in the following order:

2.1. Heat treatment under different modes

- The heat treatment of the samples was carried out in two stages in a laboratory furnace.
- Homogenization for austenization at 1150°C, retention time of 2 hours and quench hardening of the samples in water are provided, to be fixed the high temperature state and probably the most higher rate of carbon uptake from the decomposed carbide phases, [2-4, 7, 8].

The spesimens are treated to heating regimes shown in Table 2.

***Table 2.** Regimes of heat treatment*

Heat treatment regimes			
Alloys	Temperature, [°C]	Time, [h]	Cooling conditions
1 (406)	1150	2	H_2O
2 (408) 3 (410) 4 (412) 5 (414)	350 550 750	5, 10, 20 5, 10 5, 10	H_2O

2.2. Rockwell hardness testing

Each stage of the heat treatment to the samples is accompanied by a measurement of changes in their macrohardness according to a standard Rockwell method (HP-250 combined hardness meter, penetration depth 1Rc=0.002mm), [3, 5]. The obtained results are averaged from all testing spesimens. They are shown at Fig.1.

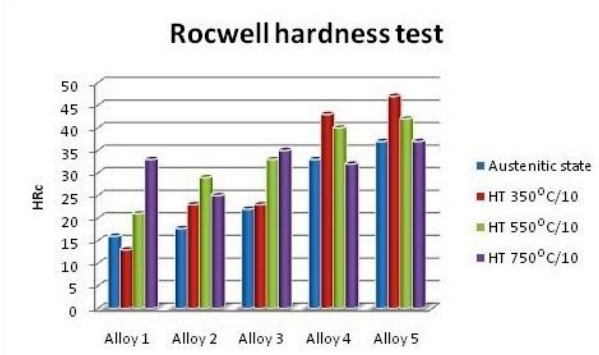

***Fig.1.** Data for macrohardness of the alloys*

2.3. X-ray structural analysis

The phase composition of the alloys is determined from the interplanar distance data, which gives different lines on X-rays.

The results are compared with literature data on the basic carbide phase lines and the solid solutions in the matrix of the alloys [1, 4, 7].

The anode of the X-ray tube is the lightest element of the

system under study - Cr-radiation with wavelength $\alpha = 2{,}29092$ Å is used. To achieve accuracy, unfiltered radiation is applied, i.e. the characteristic X-ray spectrum of chromium consists four lines ($\alpha_1, \alpha_2, \beta_1, \beta_2$). Strong alpha lines have a very near wavelength and

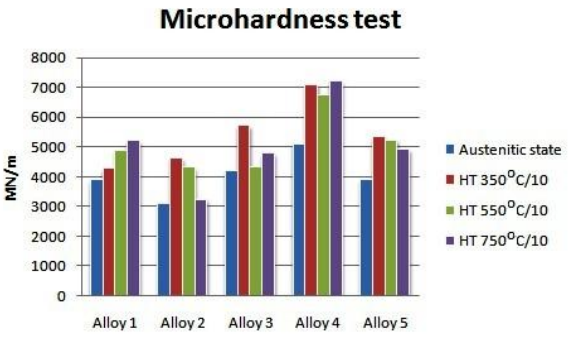

Fig. 3. *Datas for the microhardness of the alloys*

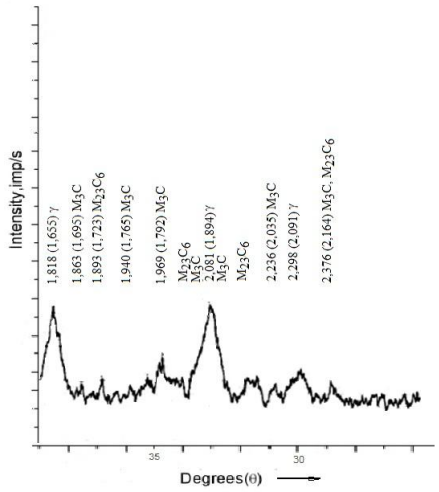

Fig. 2a. *X-ray diffraction of the alloys after homogenization*

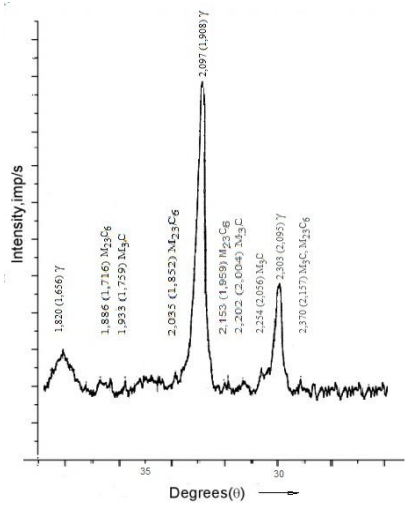

Fig.2b. *X-ray diffraction of the alloys after HT*

count as a single line. The intensity of the β_2 line is very weak and absent from the X-rays. The data for α_1 and β_1 are taken from tables [4]. Some of the X-rays diffraction patterns are shown in Fig. 2a and 2b (Alloy 3, homogenized and after 550°C/10 h). Results of analysis of the examined alloys are shown in Table 3.

2.3. Metallographic examination

The preparation of specimens is standard - mechanical grinding and polishing. Surfaces are etching with nital (1.5% solution of HNO_3 in ethyl alcohol) and ammonium persulfate (10% solution of $(NH4)_2S_2O_8$) in water [3]. The mycro-photographs are taken at a 300x magnification with a camera, attached to the Epigraph-2 metallographic microscope. Some of important transformations, seems on the spesimen`s structures are shown in Fig.4, (see the next page).

2.4. Microhardness testing

Microhardness testing carried out using a Neophot-2 metallographic microscope equipped with a additional equipment. For calculation it was found that 20 divisions of the micro-scale corresponded to a load equal to 46.95 grams. The calculations are made according to the formula:

$$(1) \qquad H_\mu = \frac{1{,}8544\ P}{d^2\ 9{,}806}, \quad [MPa]$$

where **P** is load size of kg; **d** is the arithmetic mean of the length of the two diagonals, resulting from the penetration of hardness indentor, [6]. Measurements are performed at different locations in the main solid solution. The results, as measurment values are presented in Table 3. Graphically, the changes of microhardness as a result of heat treatment for all examined alloys are shown at Fig. 3

Table 3. *Datas for the matrix structure of the alloys, separated phases in time of the heat treating and results for microhardness*

Alloy	Heat treatment T°C/time	Metal matrix	Carbid phases	Microhardness of the solid solution, MN/m
1	1150°/2	α, γ	Me_3C	3886
	350°/10	α, γ	Me_3C	4270
	550°/10	α, γ	Me_3C, possibly limited $Me_{23}C_6$	4897
	750°/10	α, γ	Little quantity Me_3C	5205
2	1150°/2	γ	Me_3C, $Me_{23}C_6$	3117
	350°/10	α, γ	Me_3C, $Me_{23}C_6$	4622
	550°/10	γ	Me_3C, $Me_{23}C_6$	4329
	750°/10	γ	Me_3C, $Me_{23}C_6$	3246
3	1150°/2	γ	Me_3C	4210
	350°/10	α, γ	Me_3C	5720
	550°/10	γ	Me_3C, $Me_{23}C_6$	4350
	750°/10	γ	Low carbid lines of Me_3C	4787
4	1150°/2	γ	Me_3C	5108
	350°/10	γ	Me_3C	7100
	550°/10	γ	Low carbid lines of Me_3C	6729
	750°/10	γ	Me_3C, $Me_{23}C_6$	7221
5	1150°/2	γ	Me_3C	3912
	350°/10	α, γ	Me_3C, $Me_{23}C_6$	5341
	550°/10	α, γ	Me_3C	5235
	750°/10	α, γ	Me_3C	4921

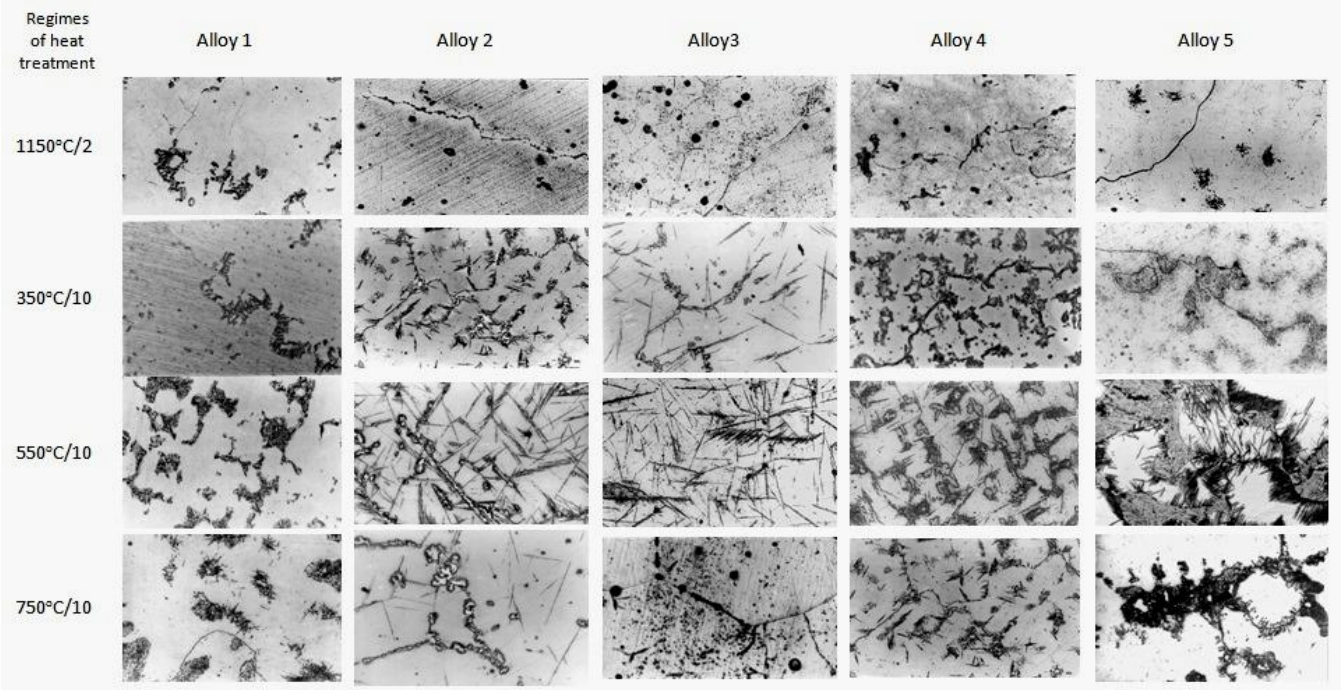

Fig. 4. *Microstructures of the alloys after heat treatment* (HT), *300x*

3. Results and Discussion

After austenization all compositions of the alloys have an austenitic matrix structure, with the exception of the 0.43%C composition, that containing ferrite. According to the carbon content of the alloys, an increase in the volume of the second phase and the coalescence of the carbides start at lower temperatures. At a temperature range between 550 to above 700°C, the decomposition of the solid solution proceeds with separation, formed from pearlite-like colonies.

As separations at 750°C are maximum for all investigated alloys, with a longer retention time at this temperature, for example 10 hours, starts the process of re-dissolving the second phase in the austenitic matrix [9]. This trend is most pronounced in alloys with 1.98 and 2.35% carbon. With defined carbon content of 1.48 and 1.98%, a needle-like phase formation in the temperature range of 550-750^{o}C is observed.

By increasing the retention time, Rockwell hardness (HRc) increases. The highest values are fixed at 10 hours for a temperature of 550°C. With temperatures up to 750°C, a hardness reduction was observed for all tested compositions with 0.92 to 2.35% carbon. Studies show that hardness increases due to different mechanisms:

- After austeniation and rapid cooling, the hardness increase is due to the dissolved carbon and the residual carbide phases in the matrix.
- The increased hardness as a result of the additional heat treatment is probably due to the presence of residual carbide phases of type Me_3C and $Me_{23}C_6$, as well as to the formation of new phases with specific quantity and morphology.

4. Conclusion

The received results will be useful in future researches and projects, related to the stages of structure formation, separations of strengthening phases in state of time of the thermal processes, mechanical and exploitation properties, and application of this type of metal materials.

5. References

[1] Modern Physical Metallurgy and Materials Engineering, *Science, Process, Applications*: R. E. Smallman, R. J. Bishop, Woburn, MA 01801-2041, A division of Reed Educational and Professional Publishing Ltd, Sixth edition 1999.
[2] Bogatcev, I. N., Ergolaev, V. F., Struktura I svoystva jeleza-margantsevih splavov, "Metalurgiya", Moskva, 1993.
[3] Kay Geels, Metallographic and Materialographic Specimen Preparation, Light Microscopy, Image Analysis and Hardness Testing, Printed in U.S.A., ASTM, No. MNL46, 2007.
[4] H. Schumann, Metallographie, VEB DVG, Leipzig, 1997.
[5] Metallic Materials: Properties Development and Standardization (MMPDS) Handbook, 2003.
[6] Structure, Deformation and Integrity of Materials: Volume I: Fundamentals and Elasticity/ Volume II: Plasticity, Visco-elasticity, and Fracture, 2 Volumes, Gijsbertus de With, ISBN: 978-3-527-31426-3, 2006.
[7] Steel heat treatment handbook, II^{-nd} edition, *Metallurgy and technologies*, Taylor and Francis Group, UC, 2006.
[8] Heat Treatment of Metals (English), ISBN: 9781410203052, Publisher: Univ. Pr. of the Pacific, December, 2002.
[9] Gavrilova, R. Vl., Petkov R. I., Koleva E. M., Study the influence of alloying elements on the structure of iron-based alloys with high content of carbon, manganese and chromium in modes of heat treatment, *International Journal Materials Science, Non-equilibrium Phase Transformations*, ISSUE 2/2016 YEAR II, ISSN 2367-749X, 13-16.

VIBRO-ACOUSTIC APPROACH FOR REGISTRATION AND EVALUATION OF TECHNICAL DEVIATIONS IN ALUMINUM CASTINGS

Prof. Kolarov I. PhD.
Higher School of Transport "Todor Kableskov", Sofia, Bulgaria

ikolarov@vtu.bg

Abstract: *Superficially masked internal discontinuities in the aluminium casting during the manufacturing process occurs often. As a result of dynamic loadings in the process of operation, it is possible the occurrence of leakage in the machines. The application of classical methods of non-destructive testing of internal discontinuities in parts with relatively complex geometric dimensions requires a significant resource or is not always possible.*

A vibro-acoustic study for express diagnosis of internal discontinuities in aluminium castings is shown in the work.

The resonance behaviour of a part depends on its specific shape and material properties of the elastic medium. This allows diagnostic approaches for registration of different technical deviations, estimating an equivalent size of internal discontinuities, to be created.

Classical theory of resonance is used for scientific justification of study. It is suitable in spatial parts of complex shape the theoretical results to be obtained for each particular construction by means of the constructive model in CAD environment. The possible technical deviations are created in the geometric model by software. The model is divided into elementary parts and a detailed description of their properties and the elastic connections are described by the Finite Element Method (FEA). This allows diagnostic models for registration of discontinuities, incl. for assessing its equivalent size in a particular section of the casting to be created rapidly.

A study of an aluminium part by a universal acoustic apparatus is shown in this work. The samples are separated into factory conditions of „suitable" and „unsuitable" after machining of the joining dimensions. Typical areas of occurrence of discontinuities in the casting process are defined. The „suitable" samples are divided according to the specific elastic characteristics of the material used. Insignificant scattering (2-6 Hz) of resonant frequencies in the range 20 Hz to 20 kHz is measured. Discontinuities in the typical areas of registration in the real parts are formed successively in the CAD model. The resonances are calculated in FEA. Diagnostic signs for registration and evaluation of an equivalent size of discontinuity according to its disposal are created. Discontinuities of irregular shape are created in part of the „suitable" samples and the resonances are registered again; the changes of resonances are determined. The principle consistency between theory and experiment is assessed. A good compliance is obtained.

The work may be used to assess the technical condition of castings by manufacturers of such parts.

Keywords: ALUMINUM CASTING, INTERNAL I DISCONTINUITIES REGISTRATION AND SIZE EVALUATION

1. Introduction

As a result of technological deviations in the process of aluminum parts casting superficially masked internal discontinuities occurs often[1]. The problem with internal discontinuities is significant for thin-walled details, from which both mechanical strength and tightness are required. As a result of internal discontinuities accidents of product leakage after a certain period of dynamic load during the operation are possible.

Internal discontinuities can be recorded by well established non-destructive methods. For each method a scientifically justified sensitivity threshold is defined, ie. the minimum amount of discontinuities that can be registered. There are also specific requirements for the shape of the parts in order to realize the study.

In parts with relatively complex geometric shapes nonconformities with different locations are possible. For their registration, technical devices have been developed to explore the subject from different sides and make 3D computer images. This makes the application of classical methods for non-destructive testing of internal discontinuities to require a significant resource or is not always applicable.

The resonance behavior of a part depends on its particular shape and material properties of the elastic medium [2]. An opportunity to assess the technical condition, incl. the registration of internal discontinuities in aluminum castings gives the analysis of some characteristic resonant frequencies, excited in the parts. The vibrations are recorded quickly by means universal acoustic equipment and no highly qualified personnel is needed to determine resonant frequencies [3]. The vibro-acoustic method is not universal in terms of diagnostics of machine elements. This defines it as a highly effective method for controlling the technical condition of concrete parts after a specialized procedure to demonstrate its application.

The aim of the work is to show a vibro-acoustic express diagnostic approach of internal discontinuities in aluminum castings.

2. Stages of the study

To clarify the resonance phenomenon in theory, mathematical dependencies are usually presented for simple bodies. For example, the basic (first) critical angular velocity of one shaft is given by the dependence [2]:

$$\omega = \sqrt{\frac{k}{m}} \quad . \qquad (1)$$

Here k is stiffness on the shaft, m - mass. For each body, resonant modes of a specific nature exist; they are determined by the major deformation in the material, such as: transverse, longitudinal, twisting, etc. In complicated parts, consisting of simple interconnected bodies, there are conditions for the simultaneous stimulation of more resonances. In fact these are systems of elements with elastic connections between them, which make their theoretical description difficult. The shape of complex details is easily described using engineering CAD and strength analysis (FEA) software, widespread in engineering. Once created, the geometric model of a part in a CAD is used for technological purposes, and can also be used for vibro-acoustic control of the productions. In a CAD environment, it is appropriate to work on the model to create some technical deviations that are found experimentally. After translating into FEA environment, the revised geometric variants are separated to elements by software, and the elastic properties of the material are set. Depending on the complexity of the model and the level of computer equipment, the time for calculating the resonant frequencies is 2 - 60 minutes, followed by an analysis of the results obtained with respect to the change of frequencies compared to those of the model without technical deviations.

One of the frequent reasons for changing the resonant frequencies in serially produced parts is the permissible deviation of the elastic characteristics of the metal. These deviations are difficult to record by non-destructive methods, such as an ultrasonic method, but they change the resonant frequencies of the part. It is appropriate for the "elastic medium" factor to be read in advance so as to achieve a good recognition of unacceptable technical deviations.

The theoretical results are evidenced by comparing theoretical results with experiments with details with artificial discontinuities, which repeat the CAD deviations, as well as with details with proven discontinuities. Difficulties in proving the theoretical results create the possibility in a part with the recognized discontinuities by leakage to exist other inconsistencies / deviations.

2.1. Preparation for Vibro-Acoustic Control:

- Demonstration of the metrological accuracy of finished products in one series - this activity is performed by comparing the deviation of resonant frequencies in a series;

- Analysis of typical sections with a discontinuity in the parts;

- Modeling of the dependence between the resonance frequency deviation and an equivalent degree of discontinuities in the way $\Delta f_i = F(\delta)$, i - the number of the resonance, Δf_i - its frequency deviation from the technical variance; or reverse function - $\delta = F(\Delta f_i)$;

- Creating samples with artificial discontinuities and verifying the theoretical results;

- Setting standards to control for registration and diagnosis of inconsistencies.

2.2. Control procedure

- Distribution of parts in batches, e.g. by mass measurement or reference resonance frequencies;

- Recording resonance frequencies and analysis by comparing with selected standards for recording inconsistencies in typical sections;

- In case of suspected frequency deviations, conclusions are drawn about the location and the extent of the discontinuities.

This sequence helps to quickly create diagnostic signs for registration of technical deviations, such as geometric deviations, deviations in product density.

3. Example of illustrating the approach

An example of a study of an aluminum piece shown in Fig. 1 a) with a universal vibration-acoustic apparatus is shown in this paper. In factory conditions the samples are processed to the exact size, after which they were tested for leakage. The typical areas of discontinuities in the casting process are selected [5]. The good samples are separated into groups according to the specific elastic characteristics of the material used. Insignificant scattering (2-6 Hz) of resonant frequencies in the range 20 Hz to 20 kHz is determined and higher resonances have greater scatter. In addition, higher-frequency resonances require extra attention on excitation and analysis.

The mass of samples was examined and a change of 2.8% was found.

3.1. Preparation of the test sample

In the constructive model of the sample are formed consecutive irregularities in the typical areas of registration in real details. Part of the sample models are modified by irregularities in the sections established by practical studies, established by practical research and changes Δf of some resonance frequencies are registered $\Delta f = f - f_{def}$; f - frequency of sample with normal quality, f_{def} - frequency of sample with discontinuities. Frequency variation Δf depends on the equivalent depth δ of discontinuities and on the particular disposition of the discontinuities. For the specific detail, four sections are found [5]. They are shown in Fig. 1 b). In the first stretch the possibility of double-sided leakage, indicated as I and I ', is established. When the depth of discontinuities ranges from 0 to 3 (6) mm, some resonant frequencies change significantly (above 10 Hz). They are shown in Table 1. It is appropriate to use them as informative it is appropriate to use them as informative features for registration of discontinuity and for determine its equivalent depth.

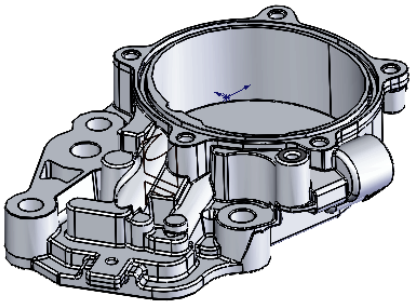

a)

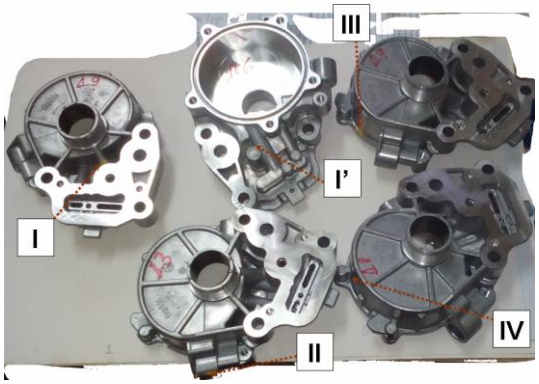

b)

Fig. 1. *3D model of research example (a) and typical sections with discontinuity in the real samples (b).*

Resonance 4 changes insignificantly (up to 10 Hz) in case of discontinuities in section IV, and otherwise does not change and is suitable to be selected as a benchmark for assessing the quality of the parts.

Tab. 1. *List of resonant frequencies up to 10 kHz, which changes in case of discontinuity according to the section.*

Section №	Significant change in the resonant frequencies, №	Minor change in resonant frequencies, №
I	1, 3, 10, 11, 12	5
II	26*, 37*	-
III	2, 7, 8	3, 5, 12
IV	2, 3, 5 – 10, 12, 13	1, 4, 11
Note: * Resonances specified are only informative and are outside the frequency range.		

A statistical analysis of the frequency of occurrence of discontinuities in the different sections of the sample is done. The most common cases of leakage (about 60%) are recorded in section I. Sections I and IV are used here as examples of creating

diagnostic signs for registration and evaluation of equivalent discontinuity dept.

Theoretical results for the frequency variation Δf of resonances with conditional serial number (№) in sections I (a) and IV (b) depending on their serial number are shown in Fig. 2.

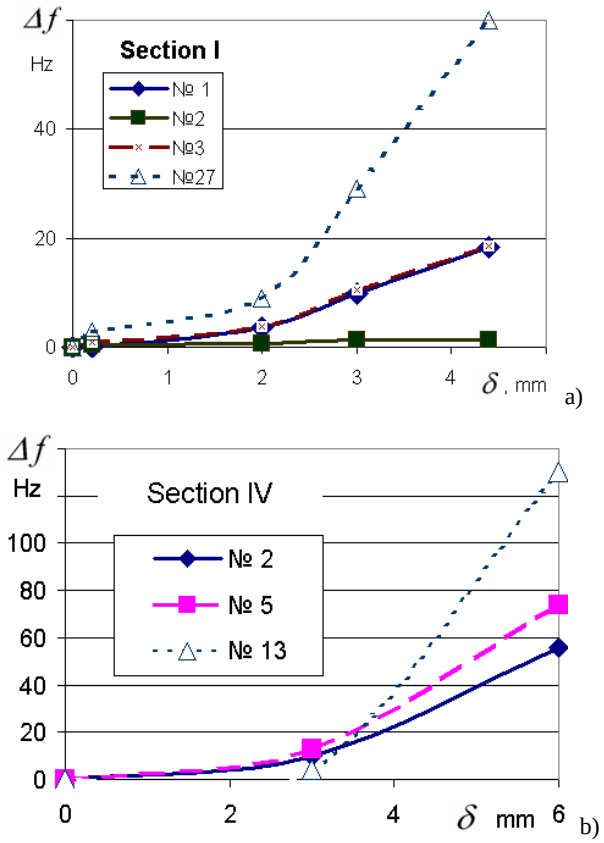

Fig. 2. *Results for variation of Δf in section I (a) and IV (b) depending on the serial number (No) of the resonant frequency.*

Diagnostic signs for registration and assessment of an equivalent depth δ of discontinuity according to its location were created on the so-called nomograms as follows:

For section I

$\Delta f = = -0{,}1288\delta^4 + 0{,}8485\delta^3 - 0{,}2947\delta^2 + 0{,}026\delta + 6.10^{-11}$ for resonance № 1

$\Delta f = -1{,}1666\delta^4 + 9{,}9951\delta^3 - 22{,}643\delta^2 + 19{,}138\delta + 2.10^{-10}$ for resonance № 27

For section IV

$\Delta f = 2\delta^2 - 2{,}6667\delta + 6.10^{-14}$ - for resonance № 2

$\Delta f = 2{,}6667\ \delta^2 - 3{,}6667\delta + 6.10^{-14}$ - for resonance № 5

Here Δf is in Hz, and δ - in mm. These equations are processed to the following:

For section I

$\delta = 0{,}002\ \Delta f^3 - 0{,}0649\ \Delta f^2 + 0.735\Delta f + 0{,}1$ - for resonance № 1

For section IV

$\delta = -0{,}0042\Delta f^2 - 0{,}3419\Delta f + 3.10^{-14}$ - for resonance № 2

$\delta = -0{,}0025\Delta f^2 - 0{,}2627\ \Delta f + 1.10^{-14}$ - for resonance № 5

The main criteria for selection of informative resonance frequencies are:

- Target sensitivity of the analysis, which determines the minimum recognizable value of Δf and is related to the scattering of the results for one batch of parts;

- Recognition of resonance; this problem is typical for close-to-order resonances for which overlapping is possible. In this case, the inspection body may make a wrong conclusion. The results of processing multiple experiments show that lower frequency resonances are easier to analyze. For example, the resonance change № 27 of depth incoherence δ in section I shown in Fig. 2 (a) has a theoretical meaning due to difficulties with its registration.

The main factors of scattering for a batch are related to:

- Variations in geometric dimensions of the parts due to technological reasons;

- Non-metal inclusions and porosity of the material (in case the study does not have a purpose for their registration).

3.2. Experimental results

The experimental results were obtained by universal acoustic equipment and were realized in a soundproofed room. Audio signals are recorded in the 20 Hz - 20 kHz range and they are they are entered and saved on a computer via a USB. The samples are suspended on a perfectly flexible and unstretchable thread and are dynamically excited by impulse. Attention is paid to the relatively uniform amplitude excitation of resonant frequencies over a wide frequency range. Registration and frequency analysis of signals is done in digital form by software for a recording time range 0.5 s.

In Fig. 3. a typical experimental result of the resonance recording is shown. By software the exact measured values of the resonant frequencies are determined and the values of Δf are determined according to the depth of discontinuities.

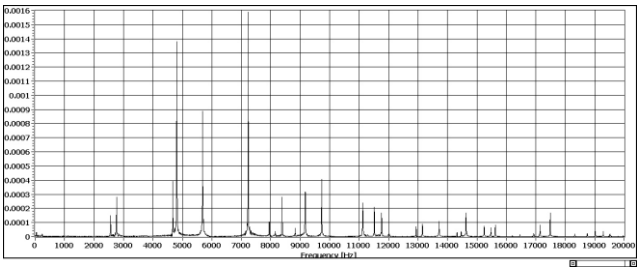

Fig. 3. *A typical result obtained by experimental study of resonant frequencies.*

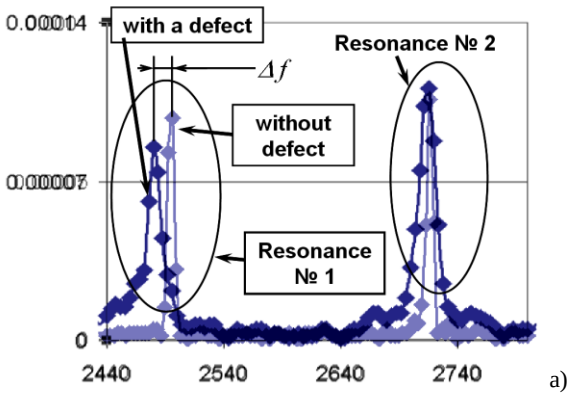

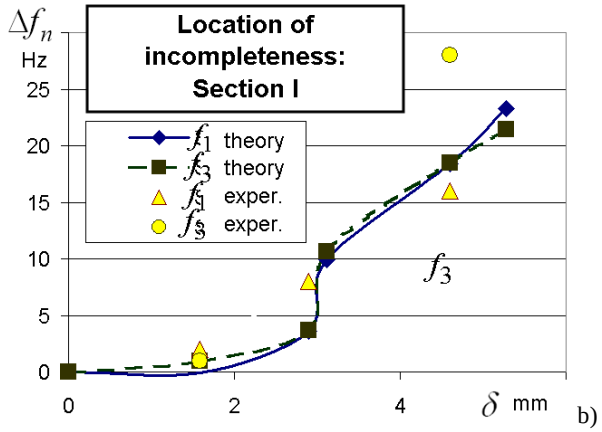

Fig. 4. *Stages of the study; a) - to determine the frequency resonance change, b) - to confirm the theoretical results.*

A comparison of the resonance frequencies №1 and №2 obtained for detail without deviation (used as etalon) and for detail with discontinuity 2.5 mm depth in section I is shown in Fig. 4 (a). The figure is shown for illustrative purposes and it is obtained by overlaying screen images of recorded signals and formatted for the same frequency range (2440 to 2780 Hz). It is noted that for the part with discontinuity the first resonance is lower (13 Hz is reading) from the etalon and for the second resonance the both frequencies are equal. Basically, these results correspond to the theoretical values shown in FIG. 2 (a).

A quantitative comparison between theoretical and experimental results in case of discontinuities in section I is made. For this purpose discontinuities with different depth δ are formed in the section of a series part and the frequency difference Δf for each modified part has been measured. The results of the comparison of resonance frequencies № 1 and № 3 are shown in Fig. 4 (b). Principal coincidence between theoretical and experimental results is observed. This allows resonances 1 and 3 to be used for registration and determination of equivalent depth of discontinuities in section I.

4. Conclusion

The approach described above for vibro-acoustic assessment of internal incompleteness in aluminum castings is illustrative and object-oriented. For its application, no specialized knowledge and further continuing training in non-destructive testing is required. The approach is based on general engineering fundamental knowledge in the field of defectology and software products widely used in engineering. It can be applied using affordable acoustic equipment. The assessment of the technical condition of the products is made by comparing the reference resonance frequencies of the studied parts with those obtained for good quality products.

The approach is not universal and requires considerable theoretical and experimental work to demonstrate its validity. But it provides an opportunity for an express assessment of the technical condition of the parts and is cost-effective.

The work may be used for self-assessment by manufacturers of technical condition of cast parts.

Bibliography

1. The Aluminum Automotive Manual. European Aluminium Association. Version 2002.

2. Harris' shock and vibration handbook. Allan G. Piersol, editor.—5th ed. McGRAW-HILL. 2002. ISBN 0-07-137081-1.

3. Коларов И. Диагностика на повреди в машинни елементи чрез модален анализ. Стр. 138, София, 2015 г. ISBN 978-619-90083-4-8.

4. NX Nastran. Basic Dynamic Analysis User's Guide. Siemens Product Lifecycle Management Software Inc. 2008.

5. Коларов И., Д. Добрев Виброакустично регистриране на типични дефекти в алуминиев корпусен детайл за сглобяване на помпи. Научни известия на НТСМ. NDT days 2017"/ „Дни на безразрушителния контрол 2017. Брой 1 (216). ISSN 1310-3946.

NEW POSSIBILITIES FOR IMPROVEMENT AND OPTIMIZATION OF THE CASTING TECHNOLOGIES IN THE LATEST VERSION OF THE MAGMASOFT SOFTWARE PACKAGE - MAGMA5.4

Ass. Prof. Dr. Georgi Evt. Georgiev
Institute of Metal Science, Equipment and Technologies with Hydro-aerodynamics Centre "Akad. A. Balevski"-BAS

НОВИТЕ ВЪЗМОЖНОСТИ ЗА УСЪВЪРШЕНСТВАНЕ И ОПТИМИЗАЦИЯ НА ЛЕЯРСКИТЕ ТЕХНОЛОГИИ В ПОСЛЕДНАТА ВЕРСИЯ НА СОФТУЕРНИЯ ПАКЕТ MAGMASOFT – MAGMA5.4

Доц. д-р Георги Евт. Георгиев
Институт по металознание, съоръжения и технологии с център по хидроаеродинамика "Акад. А. Балевски"-БАН,

Abstract: The newest features of the latest version of the world-famous software package MAGMAsoft - MAGMA5.4 for simulation and optimization of casting technologies are presented. The provided tools and skills are illustrated by a number of casting examples for various casting methods which handle optimization tasks for both the casting system and casting feeding during crystallization. It shows the capabilities of the software for automatic improvement and optimization of the casting-mold system and the casting technology for forming high-quality castings.
KEY WORDS: COMPUTER SIMULATION, CASTING FORMATION, OPTIMIZATION OF CASTING TECHNOLOGIES

Резюме: Представени са най-новите възможности на последната версия на световно известния софтуерен пакет MAGMAsoft - MAGMA5.4 за симулиране и оптимизация на леярските технологии. Приведеният инструментариум е илюстриран с помощта на редица примери от леярската практика на различни методи на леене, които третират задачи за оптимизация както на леяковата система, така и на храненето на отливката по време на кристализацията. Показани са възможностите на софтуера за автоматично усъвършенстване и оптимизация на системата отливка-форма и леярската технология за формиране на висококачествени отливки.
КЛЮЧОВИ ДУМИ: КОМПЮТЪРНО СИМУЛИРАНЕ, ФОРМИРАНЕ НА ОТЛИВКИ, ОПТИМИЗАЦИЯ НА ЛЕЯРСКИ ТЕХНОЛОГИИ

1. Увод

Леярството е много старо изкуство, но с бурното развитие през последните тридесет години на математическото моделиране и компютърното симулиране в областта на материалознанието, то вече се е превърнало в бързо развиваща се в различни направления наука[1]. Навлизането на компютърния софтуер в световната леярска практика отдавна вече не е екстравагантна украса за ефектно представяне на изделията, а се е превърнало в неразделна част от научно-изследователската, проектантската и развойната дейност, свързана с прецизирането и оптимизирането на леярските технологии, създаването на отливки с високи експлоатационни качества, снижаване на разхода на метал, реализирането на енергетични икономии, рязко съкращаване на времето за цикъла проектиране-реализация, бърза и точна, качествена и количествена диагностика на широка гама от евентуални дефекти.

Един от световно известните софтуерни пакети за такива цели е известен под името **MAGMAsoft.** Той е създаден от фирмата **MAGMA Giessereitechnologie** със седалище гр.Ахен, Германия[2]. Пакетът се развива и обогатява непрекъснато от сътрудниците на фирмата, посредством разработката на множество научни проекти с различни звена на водещи немски институти като Института по леярство в гр. Ахен, Макс Планк институт и др. Математическите модели, заложени в програмата, се обновяват непрекъснато като в тях биват отразявани повечето от най-съществените научни разработки в областта на материалознанието, били те обект на докторски дисертации или научни публикации. Разширяват се и се усъвършенстват както математическите модели, обхващайки все по-широк кръг от явления и процеси, така и базата данни, която позволява третирането на все по-широк кръг от материали и сплави, а така също и методите на леене. Общопризнат факт е, че **MAGMAsoft** няма конкуренция по отношение на вградената база от данни в пакета. По такъв начин, тя успешно се конкурира с най-известните и мощни програми от бранша, като ABBACUS, PROCAST**,** ANYCASTING, NOVACAST, 3D-FLOW, LM- FLOW, PATRAN и др.

В тази връзка следва да се отбележи, че в нашата страна и по-точно в Института по металознание, съоръжения и технологии с център по хидроаеродинамика при БАН "Акад. А. Балевски" (ИМСТЦХА-БАН) в гр. София се разполага с **MAGMAsoft** от повече от 10 години. Първоначално, програмният пакет бе предоставен за научни изследвания, като резултат от успешно съвместно изпълнение на проект "COPERNICUS" – една от водещите европейски програми за научно развитие. От 2005 година насам, ИМСТЦХА-БАН е изключителен и официален дистрибутор на програмните продукти на MAGMA GmbH за България и разполага с последните им версии. Той е оторизиран както да продава лицензи за ползване на програмите, така и да сключва договори за оказване на технологична помощ и реализиране на конкретни проекти с извършване на симулации и оптимизации на конкретни леярски технологии. Настоящото изложение има за цел да представи най-новите възможности на последната версия на софтуера **MAGMA5.4** за компютърна симулация и оптимизация на леярските технологии.

2. Методи за усъвършенстване и оптимизация на леярските технологии

Развитието на методи и подходи за оптимизация на леярските технологии е естествено продължение и надграждане на математическото моделиране и неговата алгоритмизирана версия – компютърното симулиране[2,5]. Първоначално интензивно се развиват итеративно-интерактивните подходи [6,7], при които оптималното решение се достига чрез последователност от симулации след промени, осъществявани от компютърният оператор.

2.1. Илюстрация на принципите на итеративно – интерактивния подход

Тук е представен общ подход за оптимизация на леярските технологии, базиран на инструментариума на MAGMA5.4 за симулиране на леярските технологии. Той е илюстриран на примера на технологично решение за формиране на автомобилна джанта по метода за леене с газово противоналягане или при леене под ниско налягане, но с успех би могъл да се прилага и при кокилно леене. Подходът се

състои в прилагането на последователност от компютърни симулации на запълването и кристализацията на отливката, при които се осъществяват целенасочени промени в технологията на база на анализ и оценка на получените резултати. Процесът стартира с така наречената „натурална симулация“, при която формирането на отливката се осъществява във форма с максимално проста геометрия – паралелепипед или цилиндър. В MAGMA5.4 тя се генерира с инструмента “*Automatic mold*”. Резултатите от такъв тип симулация дават представа за характера на запълването на кухината на леярската форма с течен метал и вида на кристализацията, произтичаща главно от геометрията на отливката. Те очертават и основните евентуални дефекти, дължащи се на геометричните особености и свързаното с тях разпределение на масите в отливката. На базата на анализа на тези резултати се предприемат и първите промени в технологията с цел елиминиране на дефектите.

На Фиг.1 е представена геометрията в 3D на автомобилната джанта. Използваната сплав за отливката е AlSi7Mg с начална температура на леене 700^{o}C. За формата е избран паралелепипед, обхващащ отливката с еднаква дистанция във всички посоки. За целите на симулациите тя се предполага изработена от сплавта X38CrMoV5_1 с начална температура 300^{o}C. На Фиг.2 е илюстриран полученото с MAGMA5.4

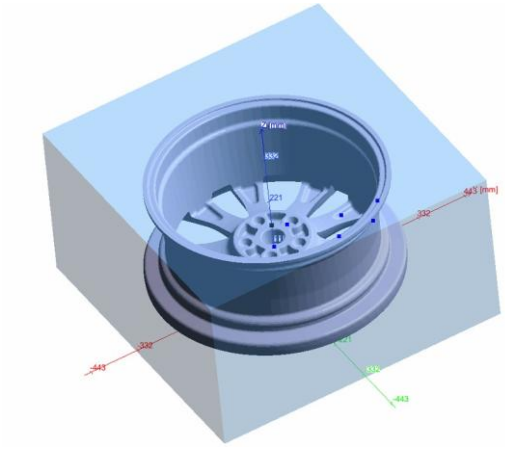

Фиг.1. Геометрия за „Натурална” симулация

разпределение на газовата пористост в отливката.

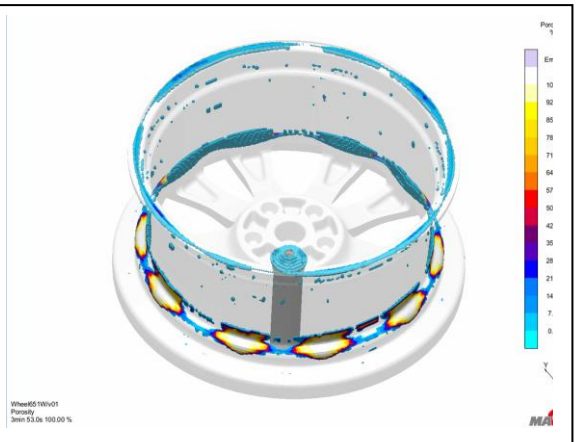

Фиг.2. Критерий “Porosity” при „натурална” симулация

Първият фактор, с който може да се влияе на хода на кристализацията е разпределението на масите на формата. Например, за да се осигури насочена кристализация в посока от рима към спиците на джантата следва да се оформят странични вложки с по-голяма маса при рима и периферията на спиците. Формата в средата около спиците следва също да бъде изтънена за да работи на по-висок температурен режим от останалите части. Целта е спиците да кристализират последни и то в посока от периферията към леяка. Следвайки този анализ и съобразявайки се с характерните изисквания на механиката на технологията, бяха оформени две сърца – горно и долно, четири вложки и един разсекател. Геометрията на новите формообразуващи е показана на Фиг.3. Така се стигна до нов

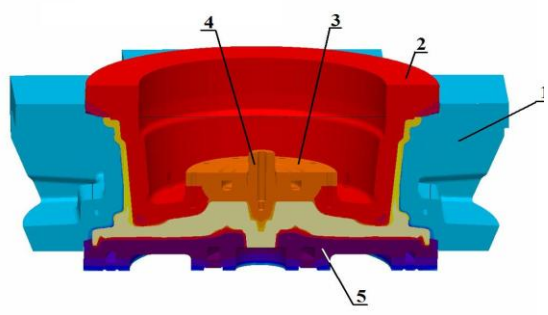

Фиг.3. Геометрия на формообразуващите.
1. Странични вложки; 2. Горно сърце1; 3. Горно сърце 2; 4 Разсекател; 5. Долно сърце.

вариант на технологията, чийто резултат за критерия “Porosity” на MAGMA5.4 е показан на Фиг.4. Вижда се, че избраното

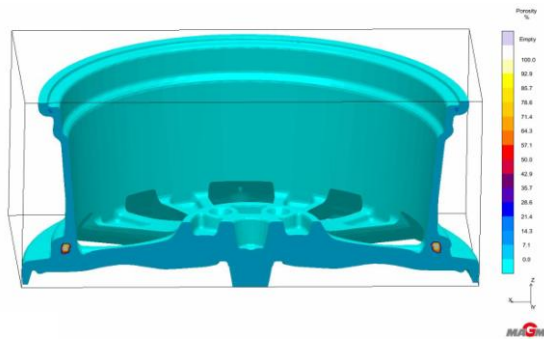

Фиг.4. Критерий “Porosity”. Вариант 2.

разпределение на масите във формообразуващите е редуцирало съществено пористостта в рима до незначителна степен и е осигурило желания характер на кристализацията в спиците, но не е успяло да елиминира проблемните зони в периферията на джантата (термичните възли на Фиг.4). По-нататъшно подобрение на технологията обикновено се търси със система от охладителни канали, като показаните на Фиг.5. Ефектът от

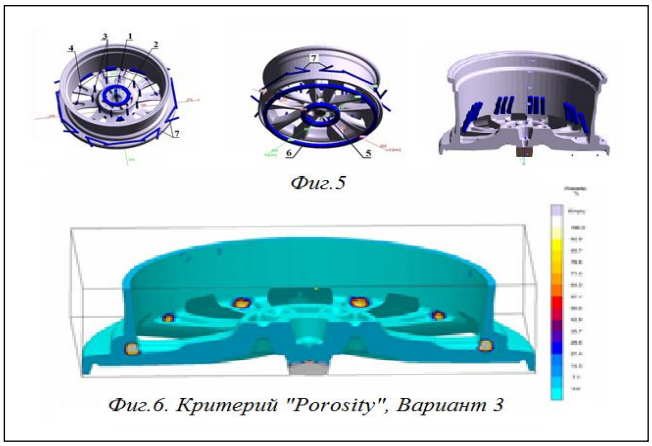

Фиг.5

Фиг.6. Критерий "Porosity", Вариант 3

тяхното влияние е илюстриран на Фиг.6 с полученото разпределение на газовата пористост. Наблюдава се желаното преместване на термичните възли в посока към питателя, но не и елиминирането им. Явно влиянието на охладителните канали не успява да преодолее съотношението на масите, формирано от геометрията на отливката. Ето защо при следващият вариант (№4) бе въведено диференцирано обмазване на формообразуващите, показани на Фиг.7. Неговият ефект, както

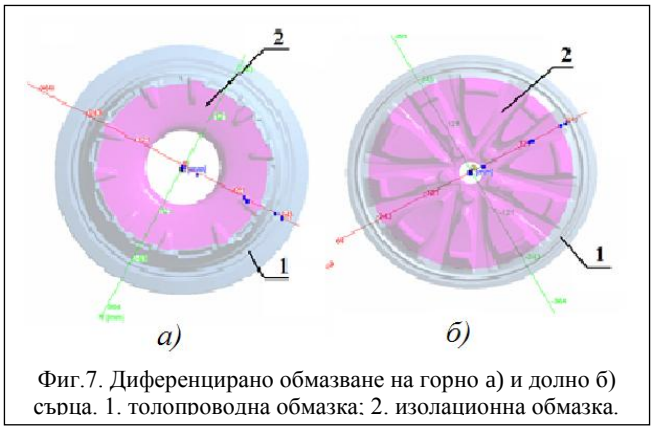

Фиг.7. Диференцирано обмазване на горно а) и долно б) сърца. 1. топлопроводна обмазка; 2. изолационна обмазка.

се вижда от пористостта на Фиг.8 бе достатъчен за да се преодолеят термичните възли и да се получи една навсякъде плътна, качествена отливка. За последното свидетелства и

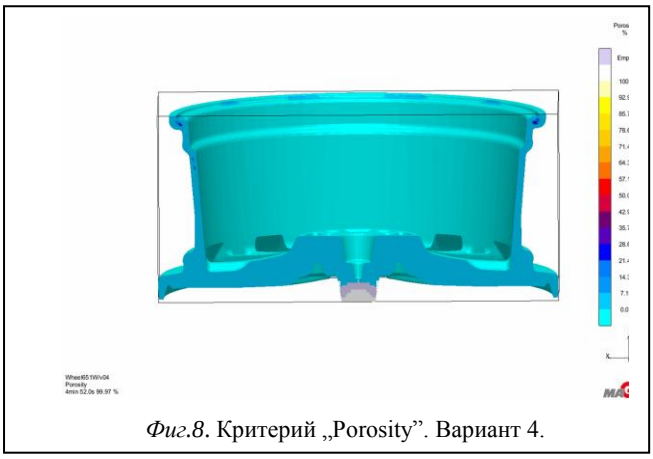

Фиг.8. Критерий „Porosity". Вариант 4.

Критерия на MAGMA5.4 – "Microporosity" на Фиг.9.

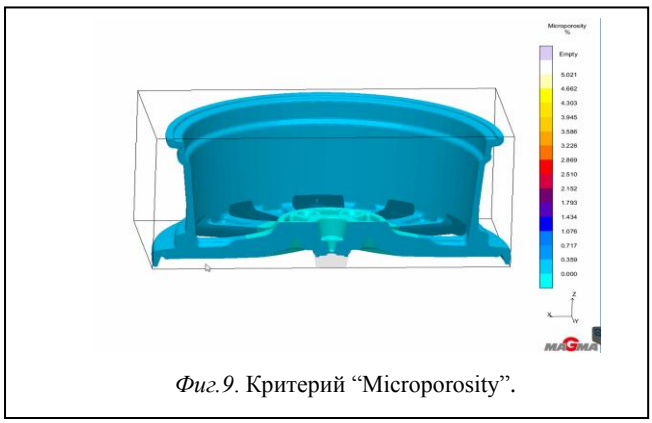

Фиг.9. Критерий "Microporosity".

2.2. Метод за автоматична автоматизация в MAGMA5.4

По-нататъшно развитие итеративните подходи намират в симулиране на варианти на технологията в крайно множество от точки във фазовото пространство на определящите технологията параметри. Това могат да бъдат както геометрични така и технологични параметри. Във всяка от тях се пресмята стойността на предварително подбрана за целите на оптимизацията целева функция, след което с различни математически методи се намират нейните екстремуми (глобални минимуми или максимуми) [8,9].

Към такъв клас от подходи следва да причислим и предлаганият в MAGMA5.4 метод за автоматична оптимизация. Той е базиран на генерирането на множество от варианти на третираната леярска технология. За целта е въведен нов геометричен обект – параметризирани геометрични обекти. Това могат да бъдат всички компоненти на системата отливка-форма: мъртви глави, сърца, компоненти на леяковата система и др. Техните размери се задават не с конкретни димензии, а в параметричен вид. По този начин при генерирането на варианти на технологията тези параметри могат да пробягват краен брой значения.

2.2. Автоматична оптимизация в MAGMA5.4

По-долу ще изложим подхода за автоматична оптимизация, възприет в MAGMA5.4. Той изисква параметризиране на обектите, които ще се варират.

2.2.1. Параметризиране на геометрични обекти

Ще илюстрираме подхода за параметризация на примера на цилиндрична мъртва глава за леене. На Фиг.10 е представена геометрията на мъртва глава в сечение по нейния диаметър.

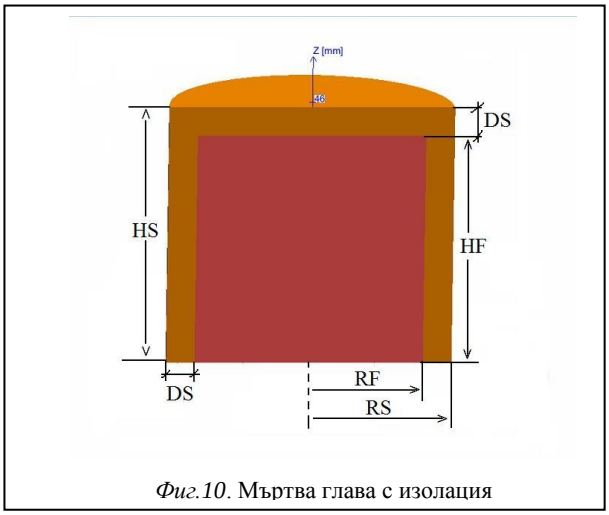

Фиг.10. Мъртва глава с изолация

Радиусът на мъртвата глава е означен с RF, а височината ѝ с HF. Дебелината на изолацията е представена като DS. Всички изброени до тук означения са параметри, които могат да заемат различни значения независими едно от друго значения. Радиусът на изолацията RS и нейната височина HS се явяват функции на RF и DS, и на HF и DS, съответно, а именно RS = RF + DS и HS = HF + DS. На Фиг.11 е показан прозорецът на MAGMA5.3, в който се виждат означенията на изброените параметри. Буквата "x" означава, че величината след нея е независим параметър, а знакът "$f_{(x)}$", че следващият параметър е функция на други параметри. По този начин мъртвата глава е

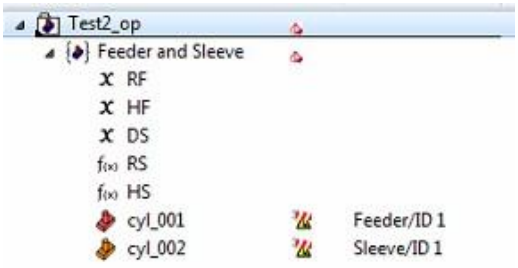

Фиг.11. Параметри и функции

параметризирана и готова за използване при генериране на нейни варианти. По подобен начин се третира всеки геометричен обект, който следва да бъде вариран при оптимизацията.

2.2.2. Създаване на групи от параметризирани обекти

Геометричният моделиер на софтуера дава възможност от създаване на групи от еднотипни параметризирани геометрични обекти разположени по кръг или дъга, по отнапред избрана траектория или повърхност. На Фиг.12 това е илюстрирано на примера на стоманен пръстен, при който се варират броя и разположението на мъртвите глави и два вида

охладители. В този случай, освен че се променят размерите на охладителите, те могат да бъдат включвани или изключвани при генерирането на варианти от технологията. Софтуерът дава възможност да се симулира по пълната генерация от варианти, но предлага и метод за генериране, наречен "SOBOL", който спестява големия брой варианти на пълното комбиниране, като същевременно осигурява сходимост към оптималния резултат.

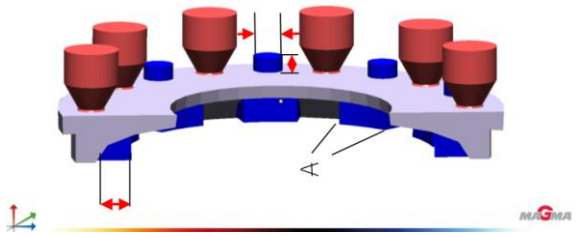

Фиг12. Оптимизация на технология за формиране на стоманен пръстен.

2.2.3. Целеви функции и инструментариум за избор на оптимален резултат

В алгоритъмът за оптимизация могат да бъдат включени както критериални функции, изчислявани от софтуера при симулиране на отделните варианти като „Porosity", "Microporosity", "Soundness", "Cooling Rate" и други, така и дефинирани критерии от потребителя. Те представляват целите, които следва да се достигнат при оптимизацията. След като са пресметнати всички варианти на технологията, MAGMA5.4 предлага набор от диаграми, таблици и корелационни матрици за бърз и удобен избор на оптималното решение. За илюстрация на казаното ще разгледаме пример със стоманена отливка във формата на пресечена пирамида – Фиг.13. В горния й край е позиционирана параметризирана мъртва глава с изолация.

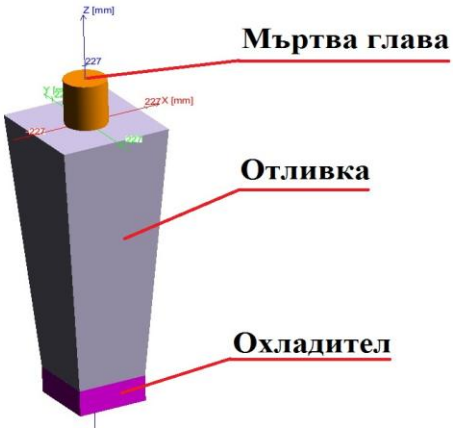

Фиг.13. Пример със стоманена отливка, формирана в пясъчна форма

Варират се нейният радиус и нейната височина, както е показано на Фиг.14. Охладителят също взима участие в оптимизацията кат бива включен или изключен при генериране на вариантите.

Design Variables

	Design Variable	Lower Limit (mm)	Upper Limit (mm)	Step (mm)
☑	Geometry RF - Radius na MG	50.0	200.0	50.0
☑	Geometry HF - Visochina na MG	150.0	600.0	150.0
	Design Variable			
☑	Geometry cube2_001 - active			

Фиг.14. Параметри на оптимизацията

Софтуерът сам генерира геометрично вариантите и симулира формирането на отливката при всеки от тях съгласно дефинираните условия. На Фиг.15 вариантите са представени

Start Sequence

Design ID	Geometry RF - Radius na MG (mm)	Geometry HF - Visochina na MG (mm)	Geometry cube2_001 - active
1	50.0	150.0	0.0
2	100.0	150.0	0.0
3	150.0	150.0	0.0
4	200.0	150.0	0.0
5	50.0	300.0	0.0
6	100.0	300.0	0.0
7	150.0	300.0	0.0
8	200.0	300.0	0.0
9	50.0	450.0	0.0
10	100.0	450.0	0.0
11	150.0	450.0	0.0
12	200.0	450.0	0.0
13	50.0	600.0	0.0
14	100.0	600.0	0.0
15	150.0	600.0	0.0
16	200.0	600.0	0.0
17	50.0	150.0	1.0
18	100.0	150.0	1.0
19	150.0	150.0	1.0
20	200.0	150.0	1.0
21	50.0	300.0	1.0
22	100.0	300.0	1.0
23	150.0	300.0	1.0
24	200.0	300.0	1.0
25	50.0	450.0	1.0
26	100.0	450.0	1.0
27	150.0	450.0	1.0
28	200.0	450.0	1.0
29	50.0	600.0	1.0
30	100.0	600.0	1.0
31	150.0	600.0	1.0
32	200.0	600.0	1.0

Number of designs: 32 Unfeasible: 0 Duplicate: 0

Фиг.15. Генерирани варианти. Параметри.

със своите параметри. Последният параметър в таблицата от Фиг.15 представя участието на охладителя. При „0" той не участва в процеса на формиране на отливката, а при „1" присъства и участва като охладител.

Като първи резултат от оптимизацията тези от вариантите, които удовлетворяват поставените цели се маркират със зелено квадратче и се извеждат на първа позиция в списъка – фиг.16.

Rank	Design	Reduce Porosity (-)
Rank 1	Design 12	0.0
Rank 1	Design 16	0.0
Rank 1	Design 28	0.0
Rank 1	Design 32	0.0
Rank 1	Design 8	0.0
Rank 6	Design 24	2.15
Rank 7	Design 11	127.18
Rank 8	Design 31	150.58
Rank 9	Design 27	164.08
Rank 10	Design 15	176.02
....	....	....

Фиг.16. Варианти, постигнали целта

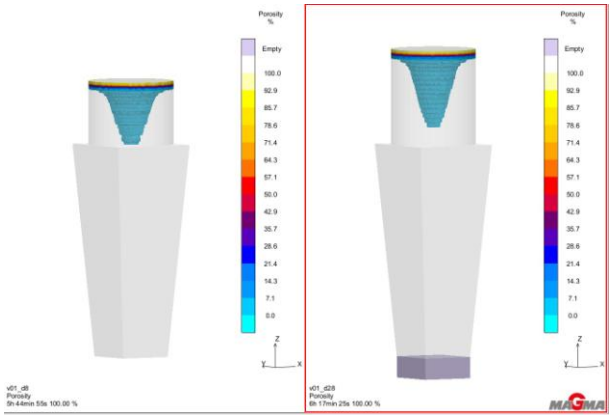

Фиг.17. Критерий "Porosity" за варианти 8 и 28

В конкретния случай поставената цел е реализирането на минимална пористост и тя е постигната, както добре се вижда, при пет от вариантите. Софтуерът предлага и детайлна информация за резултатите от симулацията при всеки от третираните варианти. На Фиг.17 такава информация илюстрира газовата пористост при два от успешните варианти от Фиг16. MAGMA5.4 предлага няколко информативни диаграми, които помагат на потребителя да получи максимална информация за получените резултати. На Фиг.18 вариантите са представени графично посредством подходящи траектории.

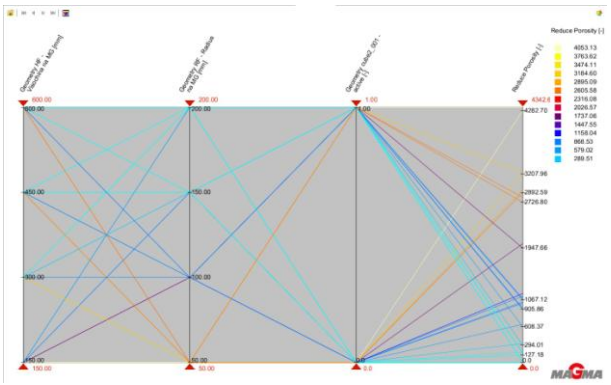

Фиг.18. Вариантите, представени като траектории

Целевата функция, пористостта е разположена върху последната вертикала. Посредством плъзгача във вид на червено триъгълниче можем да вариираме стойностите на пористостта като го движим по вертикалата. Траекториите, на вариантите, които реализират пористост над избраната стойност отпадат от диаграмата. По този начин плъзгайки триъгълничето отгоре надолу елиминираме вариантите с по-висока пористост, а остават само тези с по-малка. Накрая остават само тези с минимална пористост. Тази ситуация е показана на Фиг.19. Предлага се и диаграма (Фиг.20), която

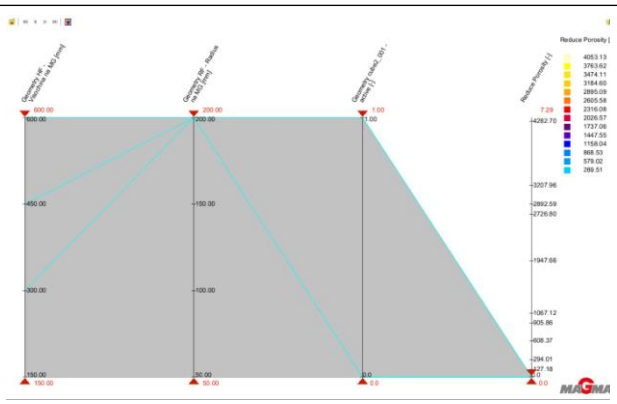

Фиг.19. Редукция на вариантите до оптималните

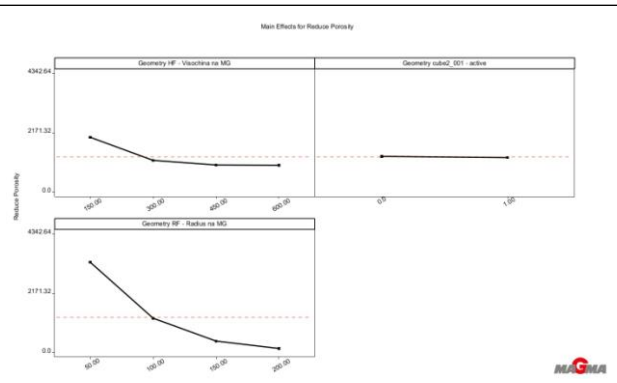

Фиг20. Оценка на степента на влияние на отделния параметър

показва влиянието на всеки от отделните параметри върху целевата функция. Вижда се, например, че радиусът на мъртвата глава оказва най-силно влияние, докато охладителят е с най-слабо такова. Друг вид диаграма пък показва корелациите между участващите величини – Фиг.21.

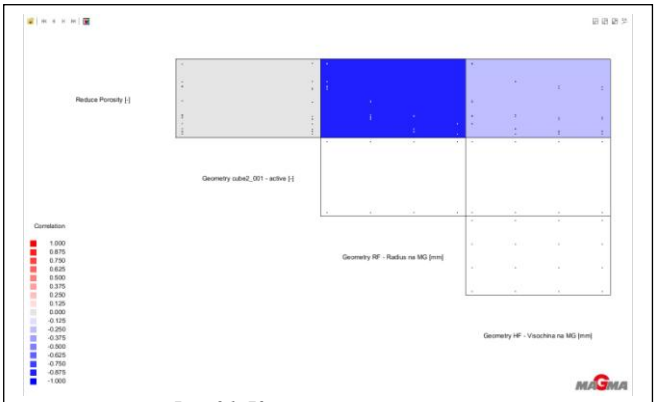

Фиг.21. Корелационни матрици

Окончателно, измежду вариантите, реализиращи нулева пористост, следва да се избере икономически най-изгодният. В случаят, това е Вариант 8, тъй като при него рандеманът на отливката е най-висок.

3. MAGMA5.4c+m

От повече от две години MAGMA GmbH предлага на пазара новия си модул ***MAGMA5.4c+m*** за симулиране на процесите при формиране на пясъчни сърца и оптимизиране на технологиите за тяхното производство. Той моделира адекватно както процесите на изстрелване на формовъчния пясък и газовите потоци така и процесите на свързване и втвърдяване.

Модулът предлага следните възможности:

- симулиране на формирането на пясъчни сърца с органични и неорганични втвърдители;
- моделиране на потоците на газа и формовъчния пясък в пясъкоструйните дюзи и вентилационни канали;
- симулиране и оценка на формираната якост в пясъчните сърца както при органични свързващи вещества, така и при неорганични.

На базата на моделирането на основните физически процеси при формиране на пясъчните сърца ***MAGMA5.4c+m*** предлага множество резултати и критерии, които дават всестранна представа за протичащите процеси и качеството на формираните изделия. Един от важните фактори се явява налягането на газа в системата. Неговото разпределение може да се види във всеки момент от процеса, както е показано на Фиг.22.

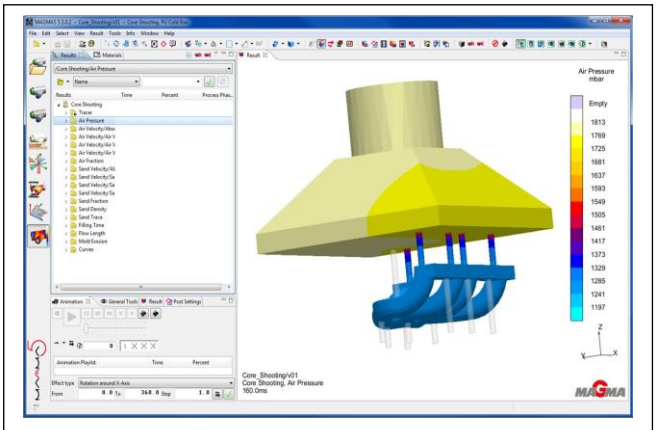

Фиг.22. Налягане на газа в системата

Софтуерът предоставя възможност детайлно да се проследят скоростите както на пясъчните частици (Фиг.23), така и на газа – Фиг.24.

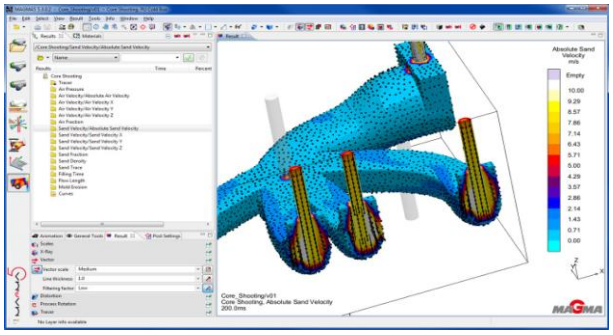

Фиг.23. Скорост на пясъчните частици

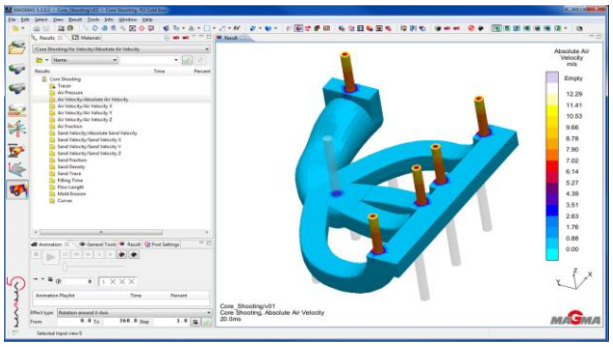

Фиг.24. Скорости на газа

Цитираните величини имат отношение към първата фаза на процеса – запълването на формата. Те са свързани и с еродиията на последната, за която софтуера предлага специален критерий –"Mold Erosion", представен на Фиг.25.

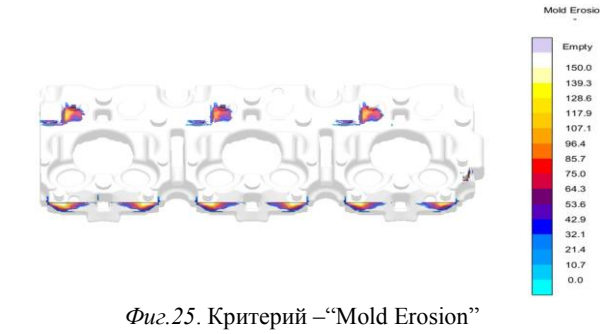

Фиг.25. Критерий –"Mold Erosion"

Подобни критерии за оценка на втората фаза – втвърдяването се предлагат за различните процеси на свързване. Например, за PU Cold Box процеса критерия "Absorbed Curing Gas", представен на Фиг.26 дава представа за степента на втвърдяване на сърцето.

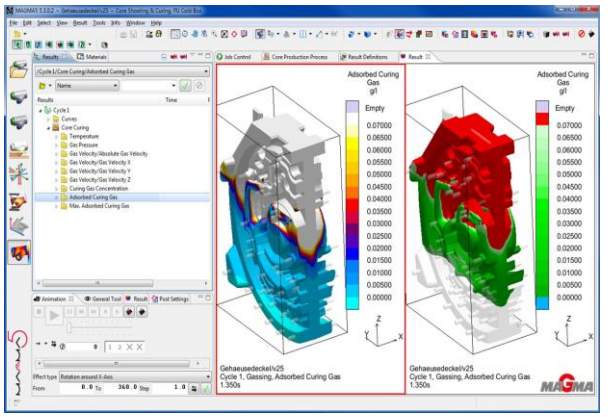

Фиг.26. Относителен дял на абсорбирания газ

4. Заключение

Авторът се надява, че изложеното по-горе е убедително доказателство за това, че **MAGMA5.4** изключително ефикасен и универсален инструмент за намиране на оптимални технологични решения, осигуряващи висококачествени отливки, както и за значително повишаване на ефективността на проектантско-развойната дейност, а също така и за постигане на високи производствени резултати с минимален разход на средства. Следователно той се явява и мощен инструментариум за повишаване на конкурентоспособността на използващите го леярски фирми.

ИМСТЦХ-БАН е изключителен и официален дистрибутор на програмните продукти на MAGMA GmbH за България, включително и на MAGMA5.4. Той е оторизиран както да продава лицензи за ползване на програмите, така и да сключва договори за оказване на технологична помощ и реализиране на конкретни проекти с извършване на симулации и оптимизации на конкретни леярски технологии.

5. Литература

1. Flemings, M.C., Solidification Processing, NY, Massachusetts Inst. of Technology,1974.
2. Sahm P. R., P. N. Hansen, Numerical Simulation and Modelling of Casting and Solidification Processes for Foundry and Cast-house", CH-8023, Zurich, CIATF,1984.
3. Huang, H., J., T. Berry, T.S. Pivonka, The use of Criteria Functions to predict Porosity in aluminum Alloy Investment Castings, 40-th Annual Technical Meeting, Investment Casting Institute,1992.
4. Popov J. Criteria Functions for Porosity Prediction in low-pressure aluminum Alloy Castings. Journal of material science and technology, NO.1,2002.
5. Sahm, P.R., P.Stojanov, A.Bührig-Polaczek, T.Zeuner, Y.B.Arsov, G.Gueorguiev, K.Daskalov, L.Drentchev, I.Katzarov, J.Popov, G.Batchvarov, R.Kovatcheva, S.Kluska-Nawarecka, A.Fajkiel, H.Polcik, M.Warmuzek. Casting of High Quality Cast Parts by the Gas Counter-Pressure Casting Process Using Numerical Simulation. Part IV: Optimization and Control of the Casting Process. J. of Materials Science and Technology, **6**, 1998, No.1, 17-26.
6. Georgiev, G. Contemporary Comprehensive Approaches for Computer Simulation and Optimization of the Processes of Casting Formation. J. of Material Science and Technology, **13**, No.1, 2005, 10-19.
7. Georgiev, G., G.Ivanov. New Interactive and Automatic Optimisation Procedures Offered of the Recent Foundry Simulation Software. MTM'07, 28-29.03.2007, 95-98.
8. Popov, J., G.Georgiev, L.Drenchev, K.Daskalov, Y.Arsov, P.Stoyanov, T.Zeuner, A.Buehrig-Polaczek, P.R.Sahm. A Comprehensive Approach to the Mathematical Modeling of Counter Pressure Casting of High Quality Details. Giesserei Forschung, **51**, 1999, No.1, 21-34.
9. Georgiev, G., Y. Arsov, Contemporary Computer Tools and Approaches for Optimization of the recent Casting Technologies, Comptes rendus de l'Academie bulgare des Sc., **61**, № 9, 1181-1188, 2008.

ИЗСЛЕДВАНЕ ВЪЗДЕЙСТВИЕТО НА ФЛЮСИ ВЪРХУ ТВЪРДОСТТА ПО БРИНЕЛ (HB) НА СПЛАВ AlSi12CuNiMg

RESEARCH OF THE IMPACT OF FLUXES ON BRINELL HARDNESS (HB) OF AlSi12CuNiMg ALLOY

A. Velikov, Y. Boichev, K. Petrov, B. Ivanova, R. Rangelov
* BAS - Institute of Metal Science, Equipment and Technologies
with Hydroaerodynamics Center "Akad. A.Balevski", 67 "Shipchenski Prohod" Blvd., Sofia.
** TU - Sofia
E-mail:anmabg@yahoo.com

Abstract: *In the work was studied the influence of different fluxes on the Brinell hardness (HB) of piston aluminum alloy AlSi12CuNiMg. Analysis and conclusions were made.*
KEYWORDS: *ALUMINUM ALLOY, BRINELL HARDNESS (HB), PISTON ALUMINUM ALLOY*

Въведение

Физико-механичните и технологични свойства на алуминия и алуминиевите сплави в много голяма степен зависят от съдържанието на неметални включения в тях [1]. Газове, оксиди, карбиди, нитриди, части от футеровката на пещите и др. нарушават плътността на отливките, намаляват якостните им показатели, херметичността им, влошават леярските свойства на сплавите и механичната им обработка и т.н. Неметалните включения са една от основните причини за брака по отливките, особено за отговорни такива.

Използването на флюси за намаляването на загубите при топене и предотвратяване на брака е основен метод.

Използваните флюси за алуминиеви сплави трябва да отговарят на следните изисквания:

1.Да предпазват метала от окисление и газонасищане.
2.Да отстраняват неметалните включения в стопилката.
3.Да не променят състава на сплавта чрез отстраняване на някои елементи от нея или внасяне на такива.
4.Да се отделят лесно от топилния агрегат и от стопилката, при минимални загуби на механически включен в шлаката метал.
5.Да са минимално хигроскопични и да запазват качествата си продължително време.
6.Да не взаимодействат с футеровката на пещите и леярските устройства за заливане (кофи, черпаци и др.) или с тиглите, в които се топи сплавта.
7.Да бъдат безопасни за здравето на работния персонал.
8.Да имат точка на топене, близка до тази на алуминиевите сплави.
9.Да не са силно летливи.
10.Да са със сравнително ниска цена.

Постигането на всички гореизброени качества не е възможно. За различните случаи се налага прилагането на флюси с различен състав. Действието на флюсите е предмет на непрестанно изследване [2].

Цел

Целта на настоящата работа е да се изследва влиянието на различни по процентно
съдържание на NaCl, KCl, Na_3AlF_6 и CaF_2 флюси, върху механичните показатели на бутална сплав AlSi12CuNiMg. Въпросната сплав е подбрана поради това, че при производството на бутала (особено при гравитационно запълване на метални форми), след механична обработка , загубите от стружки, леякова система, мъртви глави и преливници е съществена. В предишно изследване[2] бе използвана сплав AlSi6Cu7Mg, която също като AlSi12CuNiMg е бутална, но получените резултати бяха за якост на опън и линейно удължение.

За оползотворяване на метала, остатък след механична обработка, е необходимо неговото стопяване, обработка и последващо използване. Тук се проявява ролята на гореописаните флюси.

Експериментална част

Изследванията се проведоха по следната методика:

Металната шихта се състоеше от свеж метал, обрезки (леяци, мъртви глави и преливници) и стружки, в съотношение 3:1:1, като вторичният метал не бе подлаган на предварително обезмасляване и сушене. Топенето се проведе в тиглова електросъпротивителна пещ с чугунен тигел. Тигелът бе предварително обмазан с огнеупорна обмазка, за да се предотврати разтварянето на желязо в стопилката.

Таблица 1.

№ на флюс	Състав в теглови %			
	NaCl	KCl	Na_3AlF_6	CaF_2
I	50	50	-	-
II	60	25	10	5
III	60	25	15	-

Флюсите бяха подбрани по състав в тегловни проценти, чиито стойности са поместени в табл.1.

Бяха проведени осем плавки, като две от тях- без флюсова обработка, а всеки две от останалите плавки бяха обработени с флюсове I, II и III, в количество 15 % от количеството на металните отпадъци и металните стружки. Плавките бяха по две, за да се получи известна повторяемост и от там- по-голяма достоверност на резултатите.

След стопяване, сплавта от шесте плавки бе третирана със съответния флюс при температура на метала 730^0C.

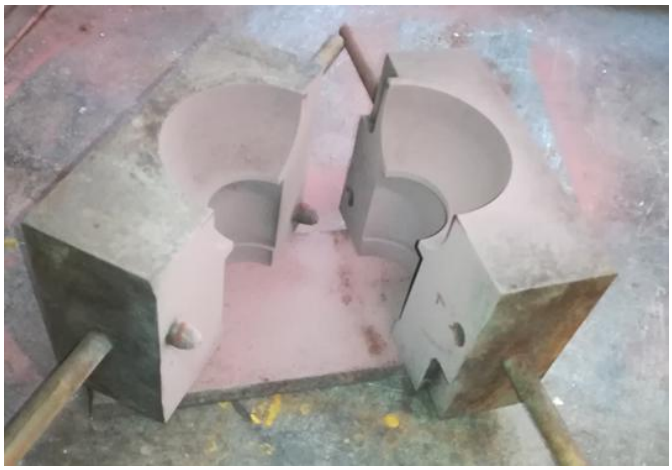


Фиг. 1.

Пробните образци, тип „гъба“, бяха отляти в специално изработени метални форми (фиг.1), подгряти до температура 200^0C.

На фиг.2 са показани от различен ракурс отляти пробни образци.


Фиг. 2

Всеки един от опитните образци бе разрязан през центъра на цилиндричната част на отливката. Долната част от отреза бе механично обработен за постигането на подходяща повърхност. След механичната обработка на заготовките за опитни образци, те бяха изпитани с уред за твърдост по Бринел „EQUOTIP” в ИМСТЦХА-БАН. Всяка повърхност бе изпитана в четири различни точки, отстоящи на 5 мм от външната повърхност на отливката и разположени на 90 градуса една от друга.

Резултатите от изпитанията на НВ са поместени в табл.2.

Таблица 2.

№ на плавката вид флюс	НВ				
	точка 1	точка 2	точка 3	точка 4	средно
1, 2 (без флюс)	90	91	90	91	90,5
3, 4 (флюс I)	92	93	93	93	92,75
5, 6 (флюс II)	93	93	94	93	93,25
7, 8 (флюс III)	95	95	95	96	95,25

Изводи:

1.При сплав AlSi12CuNiMg ясно личи положителното въздействие на флюсовата обработка върху твърдостта по Бринел (НВ).

2.Резултатите от изследванията са по-добри при флюси II и III със съдържание на криолит (Na_3AlF_6) 10- 15%.

Литература:

1.Славов Р. и др. „Наръчник за леене на цветни метали и сплави“.“Техника“.С.1976.

2. Великов Ангел *, Явор Бойчев *, Крум Петров **, Рангел Рангелов **.”Изследване въздействието на флюси върху якостните качества на сплав AlSi6Cu7Mg”. XXV МЕЖДУНАРОДНА НАУЧНО ТЕХНИЧЕСКА КОНФЕРЕНЦИЯ „МЕТАЛОЛЕЕНЕ 2018”.18-20 април 2018. Плевен. Р България.

ПОВЫШЕНИЕ ИЗНОСОСТОЙКОСТИ ЛИТЫХ ДЕТАЛЕЙ МАШИН

IMPROVEMENT THE WEAR RESISTANCE OF CAST PARTS

д.т.н., профессор Фурман Е., к.т.н. Фурман И.Е., аспирант Усольцев Е.
Уральский федеральный университет имени первого Президента России Б.Н. Ельцина, г. Екатеринбург, Российская Федерация
El.furman@urfu.ru, foundry@inbox.ru, e.a.usoltcev@urfu.ru

Abstract:. *The results of the investigations of methods to improve the steel and cast iron parts wear resistance are presented.*
***KEYWORDS**: WEAR RESISTANCE, SURFACE WETTING, SURFACE ALLOYING, STRENGTHENING*

1. *Введение*

Большое количество деталей машин выходят из строя из-за поверхностного износа. Существуют различные способы повышения износостойкости деталей, такие как наплавка, напыление износостойких материалов на поверхность деталей, поверхностная закалка и т.д. Наиболее дешевым способом придания поверхности литых деталей специальных свойств является метод поверхностного легирования, позволяющий совместить процесс изготовления отливки и упрочнения её наиболее изнашиваемой части путём нанесения на поверхность литейной формы упрочняющего покрытия, которое взаимодействует с заливаемым металлом и переходит на поверхность отливки.

2. *Результаты и дискуссия*

Изучены особенности процессов, протекающих при упрочнении поверхности отливок порошками, наносимыми в виде обмазки на поверхность формы. В этих целях применялись карбиды вольфрама, титана и циркония, бориды титана и циркония, нитрид титана, а также сплавы ВК8, Т15К6, Т50N50 и различные марки феррохрома. Как известно, при использовании крупнозернистых тугоплавких порошков ведущей стадией формирования упрочненного слоя является капиллярное проникновение расплава в межзеренные промежутки [1]. Этот процесс существенно зависит от условий смачивания металлом используемых материалов. Краевые углы смачивания, измеренные с помощью видеофиксации в конце процесса растекания капли расплава по пластинке, приведены в таблице 1. Видно, что при использовании WC, TiC, ВК8, Т15К6, феррохрома формирование композиционных слоев может происходить без приложения дополнительного давления за счет капиллярных сил.

Поскольку время контакта жидкого металла с обмазкой литейной формы ограничено, представляют интерес кинетические закономерности проникновения расплава в поры. При высокотемпературной пропитке продвижение расплава рассматривается как вязкий процесс, который описывается уравнением

$$(1)\ l^2 = \frac{\sigma r \cos\theta_p}{2\eta\aleph} t,$$

где l – глубина пропитки; σ и η – поверхностное натяжение и вязкость жидкости; r – радиус пор; ℵ – структурный коэффициент; t – время. При этом предполагается, что краевой угол имеет равновесное значение θ_p, а мениск вогнут и давление в нём понижено.

Исследование кинетики пропитки пористых образцов (пористость 37-45%) из WC, TiC, ФХ800, ВК8 расплава на основе железа проводили методом непрерывного взвешивания. Результаты некоторых опытов представлены на рис. 1.

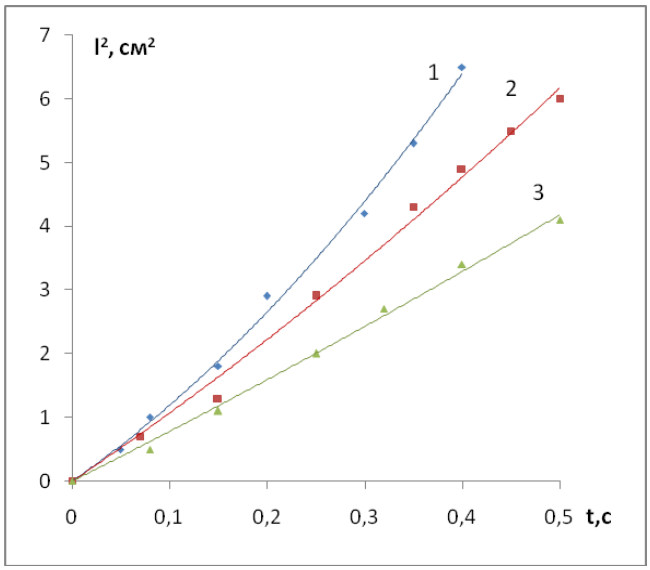

***Рис. 1.** Кинетические кривые пропитки образцов из ВК8 (1); ФХ800 (2) и WC (3) чугуном с 3,5 мас. % С при 1300 ℃*

Пропитка происходит весьма быстро (скорость порядка 10-50 см/с). Видно, что зависимость (1) соблюдается лишь на конечных стадиях процесса. В начальные моменты (~0,1с) наблюдается постоянство скорости пропитки. Это, по-видимому, связано с тем, что объем расплава в капилляре весьма мал и вязкое сопротивление невелико. В таких условиях жидкость почти беспрепятственно поступает к мениску, ликвидируя его вогнутость, т.е. перепад давлений. Поверхность становится плоской, а фактический краевой угол $\theta_ф$, формируясь в условиях натекания, приближается к 90°. При этом процесс сдерживается ограниченной скорость смачивания

***Табл. 1.** Краевые углы смачивания расплава на основе железа тугоплавких материалов, град.*

Расплав	WC	TiC	ZrC	TiB_2	ZrB_2	TiN	ВК8	Т15К6	Т50N50	ФХ800	ФХ025
Fe (карбонильное)	3	51	82	84	86	93	16	31	88	7	11
Fe+0,5% C	15	53	89	92	106	-	21	35	92	19	23
Fe+1% C	31	56	92	-	-	-	29	43	104	24	33
Fe+2% C	36	61	99	-	-	-	36	54	117	31	46
Fe+3% C	45	72	103	-	-	-	41	62	126	38	55
Fe+4% C	64	86	121	-	-	-	58	70	132	49	64
Сталь 35Л	24	60	81	83	86	98	15	38	63	12	21
Серый чугун (3,5% C)	53	82	119	98	105	115	44	61	74	30	52

жидким металлом поверхности капилляра. Перемещение периметра смачивания происходит под действием неуравновешенного натяжения $\Delta\sigma=\sigma(\cos\theta_р - \cos\theta_ф)$ со скоростью

$$(2)\quad \frac{dl}{dt}=\frac{\Delta\sigma\Omega l^{-E/kT}}{kT\tau_0}=\frac{v_0\cos\theta_p}{\cos\theta_p+1},$$

где v_0 – скорость смачивания в начальный момент; Ω – атомный объем; k – постоянная Больцмана; τ_0 – период колебания атомов.

По мере пропитки увеличивается высота (l) столба движущейся жидкости и вязкое сопротивление в её объеме, скорость доставки расплава к периметру смачивания уменьшается.

Добавление в железо поверхностно-активных кислорода и серы мало сказывается на скорости пропитки в первые моменты времени, что связано с быстрым обновлением поверхности расплава. На конечных стадиях процесса эти элементы успевают адсорбироваться, уменьшают поверхностное натяжение и скорости проникновения.

При поверхностном легировании отливок жидкий металл соприкасается с холодной поверхностью форм. Это может внести изменения в закономерности пропитки. Была создана установка, позволяющая приводить в соприкосновение холодный образец из материала обмазки с перегретым до определенной температуры расплавом и фиксировать глубину пропитки во времени. Опыты проводились как на воздухе, так и в контролируемой атмосфере.

Также были изучены кинетические закономерности неизотермической пропитки пористых образцов различной высоты (от 5,0 до 25,0 мм) из релита, феррохрома и сплава ВК8 расплавами системы железо-углерод при температурах 1250-1550 ℃(рис.2).

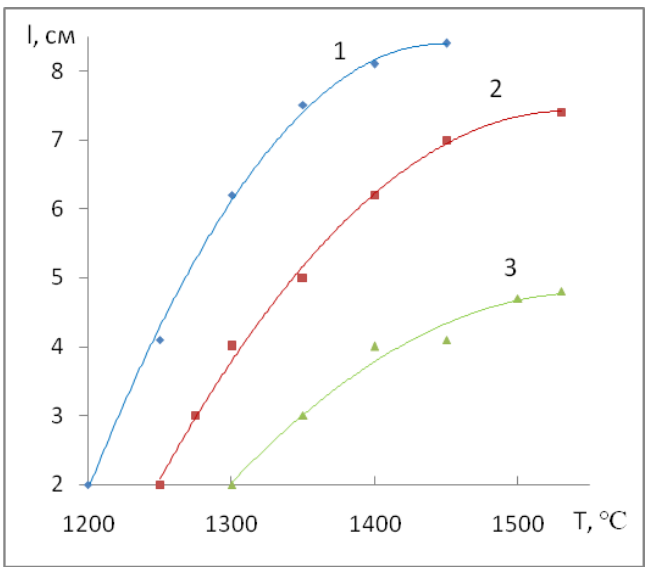

Рис. 2. *Влияние температуры заливки серого чугуна на глубину легированного слоя из релита при различной температуре стенок*
1 – 50 мм; 2 – 30 мм; 3 – 10 мм

Вначале наблюдается инкубационный период. Его продолжительность увеличивается с ростом толщины пластинки и высоты пористого образца и уменьшается с повышением температуры расплава. Наличие инкубационного периода показывает, что смачивание наступает лишь после прогрева образца до определенной температуры. Затем происходит пропитка, скорость которой заметно меньше (порядка 0,1 см/с), чем в изотермических условиях даже при температуре плавления сплава. Течение процесса описывается линейным законом. Скорости пропитки увеличиваются с повышением температуры металла и с уменьшением высоты образца, что указывает на существенное влияние теплопередачи. Опыты показали, что скорость пропитки образцов из релита и феррохрома расплавом Fe+3,0%C выше, чем Fe+4,0%C, хотя их теплофизические свойства близки. Это указывает на важную роль смачивания не только при постоянной температуре, но и в условиях теплообмена.

В работе [2] рост глубины неизотермической пропитки при повышении температуры металла объяснен только большим временем пребывания последнего в жидком состоянии. Однако опыты показали, что в указанных условиях величина скорости примерно на один порядок ниже, чем в изотермических. Это указывает, что смачивание имеет место при неравенстве температур стенки капилляра и металла. Повышение температуры расплава и пористого образца, а также изотермической скорости смачивания увеличивает скорость пропитки в неизотермических условиях.

Изучена пропитка чугуном (2,95% C; 0,16% Si; 0,5% Mn) образцов из релита, феррохрома и сплава ВК8, содержащих примерно 0,2% этилсиликата, алюмофосфата, жидкого стекла, пульвербакелита, сульфитно-спиртовой барды или фенолформальдегидных смол ОФ-1 и КФ-90. Флюсами служили сода, бура, хлористый калий и натрий. В нейтральной атмосфере и на воздухе образцы с алюмофосфатной связкой и этилсиликатом не пропитываются, что связано с обволакиванием частиц твердыми пленками, не смачиваемыми чугуном. В защитной атмосфере скорости пропитки образцов, содержащих органические связующие, а также жидкое стекло, практически не отличаются от таковых для спеченных материалов без связующих. Иная картина наблюдается при взаимодействии расплавов с легирующим покрытием на воздухе. Образцы без связующих и содержащие смолы ОФ-1 и КФ-90, пульвербакелит и сульфитно-спиртовую барду пропитать не удаётся. Это связано с тем, что тонкий слой связующего за короткое время успевает разложиться и сгореть и, таким образом, не защищает релит от окисления. Образовавшаяся окисная пленка затрудняет пропитку. При введении флюсов в образцы с органическими связующими скорость и глубина пропитки на воздухе увеличиваются. Эффективность действия флюсов возрастает ряду Na_2CO_3, NaCl, KCl, $Na_2O\cdot B_2O_3$. Наибольшая глубина проникновения наблюдается при введении в образцы 0,5% буры. В этом случае пропитка на воздухе происходит с почти такой же скоростью, как в защитной атмосфере. При добавках жидкого стекла (0,15%–0,2%) скорости процесса в нейтральной атмосфере и на воздухе одинаковы. Жидкое стекло по отношению к релиту выполняет роль не только связующего, но и флюса и защищает его зерна от окисления. Поэтому при поверхностном легировании чугунных отливок релитом целесообразно использовать в качестве связующего жидкое стекло. Применение других связующих нежелательно, так как требуется дополнительное введение флюсов, которые, как правило, приводят к засорению композиционного слоя неметаллическими включениями.

Влияние толщины стенки отливки и температуры заливки на глубину легированного слоя представлено на рис. 2. Так же, как в опытах, проведенных в неизотермических условиях, пропитка обмазки в форме начинается, когда чугун перегрет не менее чем до 1250℃. С увеличением толщины стенки и температуры глубина легированного слоя возрастает. Приведенные на рис. 2 данные позволяют определять температуру заливки, необходимую для получения на поверхности отливок композиционного слоя заданной толщины.

Проведено сравнение износостойкости образцов с упрочненной поверхностью из серого и высокохромистого (ИЧХ28) чугунов и стали 35Л. Испытания проводились газоабразивной струей, а также закрепленным и незакрепленным абразивом [3]. В отличие от обычных материалов процесс износа образцов состоял из двух этапов. В первые моменты времени происходит приработка поверхности, которой соответствует максимальная скорость износа. При этом наблюдается интенсивное истирание матрицы между твердыми зернами. Поверхность становится шероховатой. Далее износ замедляется благодаря так называемому теневому эффекту выступающих зерен. В случае закрепленного и незакрепленного абразива стойкость чугунных образцов, упрочненных релитом, соответственно в 28 и 17 раз выше стальных (35Л) и в 33 и 20 раз выше стойкости чугунных (СЧ18-36). В случае газоабразивного воздействия при малых углах атаки (~10°) износ упрочненных образцов ниже, чем стальных (35Л), в 5,7 раза и чугунных (СЧ18-36) в 9,6 раза, а при больших углах (~90°) – в 15 и 16 раз соответственно.

3. Заключение

Определены режимы получения износостойких слоев на поверхности стальных и чугунных отливок из обмазки с порошками карбидов тугоплавких металлов и высокохромистого чугуна типа ИЧХ28. Изучение износа упрочненных образцов показало значительное увеличение износостойкости упрочненных образцов при различных режимах изнашивания.

4. Литература

1. Михайлов А.М., Ахметов Г.Ш. Поверхностное легирование стальных отливок. – Известия вузов. Черная металлургия, 1965, №7, с. 175-179.

2. Иткис З.Я., Васин Ю.П. Аналитическое решение задачи проникновения жидкого металла в поры формы. – В кн.: Прогрессивные методы изготовления литейных форм. Челябинск: НТО МАШПРОМ, 1968, с. 63-77.

3. Хрущев М.М., Бабичев М.А. Абразивное изнашивание. – М.: Наука, 1970. – 252 с.

MATERIALSCIENCE – MATHEMATICS AND PHYSICS FOR EVALUATION OF LIQUIDS IN FOUNDRY

Chi. Ass. Eng. A. Maheva, PhD., Ass. Prof. Eng. St. Bushev, PhD.,
Institute of Metal Science, Equipment and Technologies With Hydro- and
Aerodynamics Center „Acad. A. Balevski“
Sofia 1574, 67 „Shipchenski prohod“ blvd. Bulgaria
Bulgarian academy of sciences
anna13@abv.bg, stbushev@abv.bg

Abstract *The base process was obtained: 3D hardening temperature field for the K-test under heat transfer at conditions with maximum intensity. A methodology for determining macro-level defects in aluminum alloys. It is definitely the placement of the K-test method in the process of creating the first order phase transition in a casting technology. The idea of interaction between the classical theory of crystallization and quantum mechanics for the processes of structure formation at casting was introduced by Stefan's task in volume with nano-size.*

Keywords: MATHEMATICS, PHYSICS, MICROSTRUCTURE, ALUMINIUM ALLOY, TASK OF STEFAN IN NANO-SPHERE

1. Introduction – mathematical basis of the foundry; material evaluation (metal, alloy (primary, secondary), ceramic casting)

The basic processes of material science are: casting and heat treatment, collectively called die-casting. On Fig. 1 presents a diagram of methodology and connectivity of the most important fundamental scientific areas for high-tech production of the smallest producer (detail).

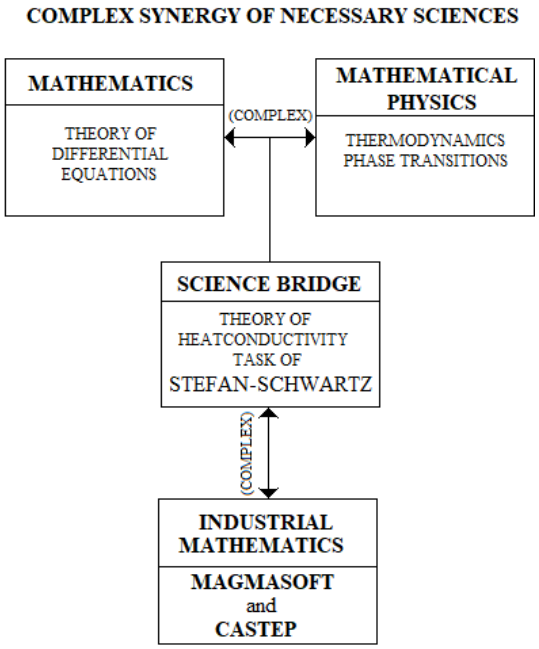

Fig. 1 *Synergy (a complex combination) of high-tech foundry science of a single manufacturer (detail). The connection between mathematics and mathematical physics is a science bridge between software MAGMASOFT [26] and CASTEP (first-principles calculation) [27].*

The working properties of the materials are determined by the structures, which have to describe their creation through the connection between mathematics and mathematical physics from the science bridge (Fig. 1). Fundamental knowledge in industry is used through computational software (Fig. 1).

Mathematics we present in general with work [1] and today it is used everywhere; in research it has become a working language because every science is differentiated through it. Work [2] and the whole development of mathematics has shown that there is no complete (mathematical) mathematics, but it develops itself from an inner necessity without the use of physical experiments. Methods of advancement in theoretical physics are presented in [3]: The principles of quantum mechanics are new ideas observed in experiments and described through mathematical formalism (mathematical theories). The functional link [4] entropy (S) and the probability of the state (π) of the system is eq. of Boltzmann in general with a constant for determining $S = k\ln\pi + \text{const}$, where k is a Boltzmann constant. The difficulty in determining this constant is the separation of the set of dynamic states of the phase space (∞^{2f}), where f – the number of degrees of freedom of the system. Трудностите за определяне на тази константа е разделяне на множеството от динамични състояния на фазовото пространство (∞^{2f}), където f – брой на степени на свобода на системата. Thus (∞2f) is separated into very small cells of the same (hyper-volume) τ: 1. Classical statistical mechanics - indefinite multiplier in π; 2. Quantum mechanics - introduces discrete quantum states: the division of (∞^{2f}) is of cells with hyper-volume hf, where h - the plane of Planck. In [4] is presented the atomic heat capacity based on the Debye temperature quantum mechanics.

Experimentally, a reduction in nanocrystalline Cu and Pd grain size reduction was observed [5].

The material science we present on [6, 7, 8, 9, 10, 11, 12, 13, and 14]: 1. Metal science and hardening [6, 7] - from the electronic structure of the atoms, between atomic bonds, crystal structure, defects and real crystal, properties, X-ray analysis, crystallization and solidification of metals and their alloys; 2. Solid State Theory and Physics of Metal [8, 9, 10, 11,] Atomic view of building-properties from classical physics and quantum mechanics. We note a natural methodological connection from a fundamental point of view between works [6÷11]. Work [12] is an important development for a generalized pattern of strength properties - toughness and resistance to demolition materials; 3. The history of material science is presented by work through separate editions of [13] i.e. a dynamic process of developing learning to teach. We are interested in the theory of alloys. In different editions, the emphasis is on the inclusion of new knowledge of competition in the economy. A problem is a release of knowledge; 4. Principles and system of stereometric metallography methods are presented in [14].

The mathematical experiment is a basic tool besides for research [15] (in pure mathematics discoveries, supporting theorems, and last but not least appraisal of applications [1, 2]). The mathematical experiment was imposed in the industry through the rapid development of mathematical modeling [16]. The [17] is a presentation of the need of using modern computer technology as an active tool in mathematical research. For example, MAGMASOFT is based on modern computer technologies that are constantly being upgraded for high competition. Work is [18] a fundamental example of industrial mathematical physics - nano-particles of gold become corrosively unsustainable. Mathematics is generally a tool that is often stimulated by need for hypothesis assessment and/or predictive discovery (in mathematical and theoretical physics).

Modern Quantum Theory of Solids [19] and modern ideas such as quantum fluctuations and strong electronic correlations. Different topics are dealt with: the general theory of phase transitions, harmonic and anharmonic grids, Bose condensation and superfluidity, modern aspects of magnetism including resonant valence bonds, electrons in metals, and strong electron correlations are seen in terms of ordering and elementary excitement.

The theory of the solid body [20] (or the physics of condensed matter) evolved after the discovery of quantum mechanics. It deals with problems related to materials from **fundamental** to **technological** problems (**quantum mechanics industry**). The progress of industrialized countries is largely a consequence of quantum mechanics [20]. Condensed matter (solids) consists of atomic nuclei (ions) and electrons arranged in an elastic recess. Describe their interaction. Typical scales known from atomic and molecular systems are: Radius length of Bohr; Energy: Hartree with a constant for fine structure. The fundamental theory of common origin of states is sought: electrons interact with each other and through ionic coulombic interaction. Effective (reduced) theories are formulated as an important step (part) of the condensed matter physics of various common Earth states: metal theory, semiconductors, superconductivity.

In [21] are presented the main ideas and methods for the current applications of the variation theory in theoretical physics and chemistry. The known variational principles of classical mechanics and optimization theory are addressed by the variation principles, formalism, and computational methodology of connected and continuous quantum states of interacting electrons in atoms, molecules, and condensed matter

From the works [19, 20, and 21] follows the mandatory use of quantum mechanics in the industry. For example, 34% of the US economy is based on quantum mechanics. The application of quantum mechanics in foundry as a first step in Bulgaria is the methodological proximity of works [6 and 9].

The use of quantum mechanics in the foundry should be from the preparation of the material to the casting and more important structural factors influencing the properties of Al-alloys are [24]: ***macro size of the grains of the solid solution and the state of their boundaries; the amount, shape and temperature of the eutectic crystallization; the amount and size of the secondary phases and their interaction with the solid solution during the heating process***. Physics-chemical properties affecting the casting strength: ***micro-resistance of the solid solution; energetic state of the crystalline lattice of the solid solution (interatomic interaction forces, character state); atomic diffusion coefficient of aluminum and diffusion of the atoms of the alloying elements and impurities in the crystalline grid of the solid solution; quantity and nature of distribution of crystal lattice defects (vacancies, dislocation, impurity atoms) and their interaction with the atoms of the alloying elements***. Quantum numbers are: the quantum number is n and accepts only positive values n = 1, 2, 3, …; an orbital quantum number l = 0, 1, 2, 3, … , n-1, $0 \le l \le n-1$; magnetic quantum number m_i = 0, ±1, ±2, … , ±l, $|m_i| \le l$; spin quantum number s - which occupies only ± 1/2 and defines the moment of impulse of the electron $P_s = \hbar\sqrt{s(s-1)}$. Pauli's principle: In the metal, every possible state of the electron can be occupied by an electron. The electronic state is uniquely defined by the four quantum numbers; there are no two electrons of conductivity with the same four quantum numbers. Not to be taken into account ⇒ Pauli's principle is: each state is described by three quantum numbers and can be encountered twice; it is understood that the two electrons in this state must have the opposite spin. In the electronic gas the impulses p_s (or p) do not have a forward direction, so all p are located within a sphere with max radius p_0 and volume $(4/3)\pi p_0^3$, where p_0 is the maximum impulse corresponding to the energy of Fermi's energy E_0: $E_0 = p_0^2/2m$, where m – electron mass. [10]. The p_0 and E_0 dimensions are defined by Pauli's general quantum theorem: At any state of any z-dimensional system corresponds volume $\hbar^z$ in the phase space (in the impulse space and coordinates). The aim of work is shown in Fig. 2

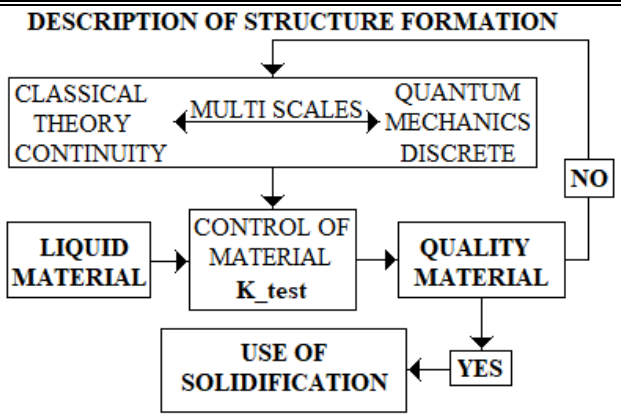

Fig. 2 *The place of the K-test in the process of forming the structure in a first-order phase transition in a casting technology.*

2. Computational Physics - Melt Solidification Temperature Range in the K-Test

The mathematical model for the calculation of the hardening temperature field is the 3D task of Stefan-Schwarz realized with the finite element method at the dates: $\alpha_{C|M}$ = 56000 w/m^2 K, $\alpha_{M|Ar.media}$ = 28000 w/m^2 K, λ_L =104 w/m K, c_L = 30,54 J/kg K, ρ_L = 2500 kg/m^3, λ_S = 83 w/m s K, c_S =30,54 J/kg K, ρ_S = 2500 kg/m^3, $T_m \pm \Delta$= 554 ± 3,5 ° C, Q_L = 160000 J/kg $T_{0|M}$ = 20 ° C, $T_{0|C}$ = 558 ° C

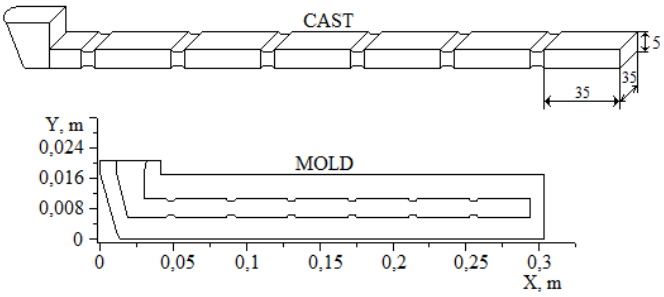

a) Cast and mold for K-test;

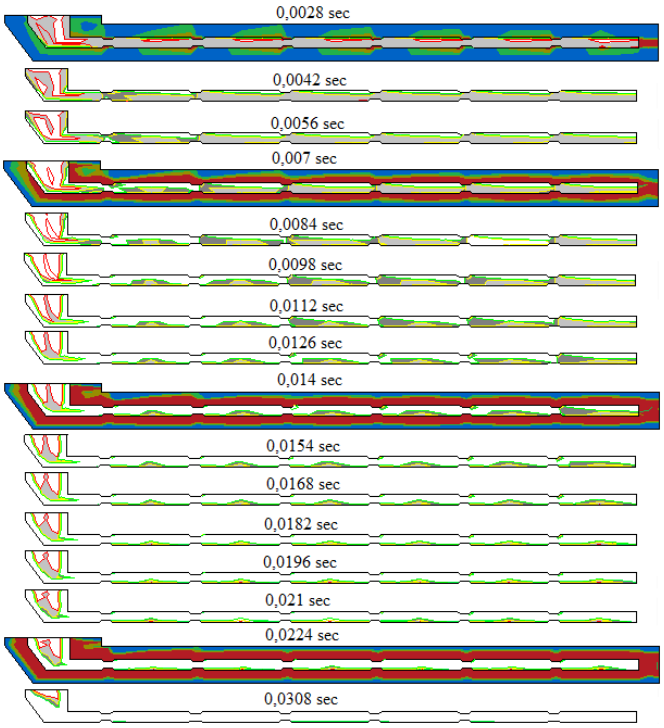

b) Temperature field of solidification in K-test;

Fig. 3 *The role of K-test for the first order phase transition before every castings is the give important technological information.*

The K-test is a visual estimate of the number of non-metallic inclusions of the rapidly-validated sample castings (Figure 3a) from a casting grade. Repeat gravitational flooding in a molten metallic form is done several times. The transverse grooves on the top and bottom surfaces of the slab form the places of rupture. It is believed that the retention of non-metallic inclusions from the melt increases in the channels due to some retention effect.

In Fig. 4 are represented by: a rapid crystallized test sample for the K-test (Fig 3a) and the resultant casting structure of a type of care wheel

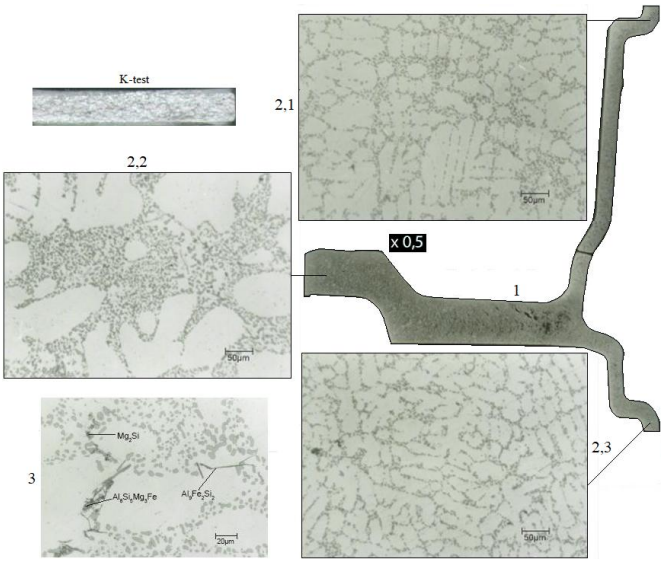

Fig. 4 *Lom on the K-test for visual observation. Polycrystalline structures obtained in local casting volumes: 1 macro-grinding; micro-grindings: (2,1 2,2 2,3); Phases in solid material 3.*

Fig. 3 is the most important information: K-test of liquids → phase transition of first order → real structure of solid body → work properties. Fig. 4 introduced **mathematical experiment**: numerical investigation of the solidification and results **Local solidification velocity.** Stefan-Schwartz task is the bridge (Fig. 1) and it is bridge between theoretical thermodynamics and (metal physics + theory of solid body).

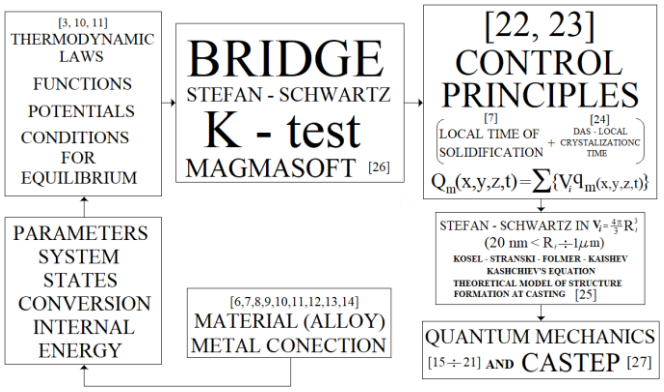

Fig. 5 Mathematical experiment and Computational physics.

Types of Chemical connection: Ion crystals Ion crystals - the crystal lattice is composed of oppositely charged ions connected by an ionic bond; Valence crystals - the atoms are connected in a crystal lattice with covalent (or homeopolar) bonds; Metals - a crystalline lattice made up of positive ions, whose repulsive senses are counterbalanced by free electrons; Molecular crystals - a grid built of separate molecules or atoms interconnected with intermolecular (of Van der Waals) forces. It is well known, that electrostatic nature of chemical connection is attraction and repulsion of electrical charges [9]. Chemical connection are defined from electron structure of the interaction atoms and effects of quantum character of the electrons movement: The energy of ionization J of a neutral atom is the difference with a negative sign (-) between the energy of the atom in its basic state and the energy of the single (+) ion (also in the basic state). J (measured eV), associated with the electronic structure, and the periodic change of the properties of the chemical elements; Energy of the kernel of electrons (electronic affinity) ζ. Many atoms of chemical elements are connected to an additional electron by releasing energy equal to the difference between the energy of the neutral atom in basic state and the energy of the basic state of the corresponding negative ion; Electro-negative based on J and ζ characterizes the ability of atoms in a molecule to attract electrons to itself, atom A associates an electron by cleavage from atom B. When $J_B - \zeta_A < J_A - \zeta_B$ or $J_A + \zeta_A > J_B + \zeta_B$ the electron will strive to move from atom B to atom A i.e. $J_A + \zeta_A$ or the semi-sum $x = (J_A + \zeta_A)/2$ (Mulliken) is a quantitative measure of electro-negative. The energy of the ionic (chemical) bond U is the difference from the interaction energy W and the difference $(- J + \zeta)$ needed to form neutral positive and neutral ions $U = W - (- J + \zeta) = W + J - \zeta$. The energy of the ion crystal lattice between *i-th* and *j-th* ions is sum: a potential energy of interaction W_{ij}; repulsing forces; potential energy of coulomb interaction $W_i = \Sigma_j W_{ij}$. If the surface effects are neglected, the full energy U of a crystal composed of 2N ion or N molecules is: $U = NW_i = NW$. *Methodology for application is* – the necessary work φ spent on approaching two charges or half a crystal ($\varphi_{K/2}$) is: $\varphi = q_1 q_2/4\pi\varepsilon_0 r$, $\varphi_{K/2} = e/4\pi\varepsilon_0 r(-e/1\ e/2 - e/3 + e/4 - \cdots) = (-e^2/4\pi\varepsilon_0 r) ln2$, or $\varphi_{1/2} \equiv (-e^2/4\pi\varepsilon_0 r)\Phi$, where Φ corresponds of $ln2 \Rightarrow$ there is a need for work to create a 3D lattice of a large number of particles, among which only coulomb forces $E_{Lattice} = (-e^2/4\pi\varepsilon_0 r)\Phi$, where $E_{Lattice}$ is the lattice energy, Φ is constant of Madelung [10].In the metal bond, valence electrons are also called generic. They move in the force field of the atoms of the lattice, forming the lattice; are not localized around their atoms but move freely; and interact with one another. In their movement electrons do not disturb the chemical properties of metals. The number of electrons of each atom does not change. The energy of each individual bond in the metal grid is smaller than in a two-atom metal molecule, and the inter-atomic distances are correspondingly larger. Metal alloys are solid solutions. The crystal lattices of the alloys can be: substitution solutions at comparable sizes of different atoms; incorporation solutions when smaller size atoms are introduced into the crystal lattice by atoms of larger size. For describing the structures and properties of metals and materials in general, quantum mechanics is used to search for the corresponding solutions of the Schrödinger equation

$$-\hbar^2\nabla^2\psi(\boldsymbol{r})/2m + V(\boldsymbol{r})\psi(\boldsymbol{r}) = E\,\psi(\boldsymbol{r}),$$
$$\psi_{\boldsymbol{k}}(\boldsymbol{r}) = exp(i\boldsymbol{k}.\boldsymbol{r})u_{\boldsymbol{k}}(\boldsymbol{r}),$$
$$u_{\boldsymbol{k}}(\boldsymbol{r}) = u_{\boldsymbol{k}}(\boldsymbol{r} + T_n),$$

where m is the mass of the electron; $\hbar$ is a Planck constant; *V* is the periodic potential of the interaction electron/(all other electrons); ψ is a wave function, a solution to the Schrödinger equation; $\boldsymbol{k}$ is a vector defined by the vector base $\mathbf{t}_1$, $\mathbf{t}_2$ and $\mathbf{t}_3$ of the crystal Brave lattice $\mathbf{T}_{n_1n_2n_3} = n_1\mathbf{t}_1 + n_2\mathbf{t}_2 + n_3\mathbf{t}_3 \equiv \mathbf{T}_n$, n is the number of the ordered numbers (n_1, n_2, n_3); u_k is a periodic function with the period of *V*.

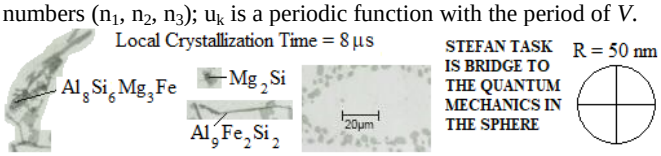

Fig. 6 *Character phases (Fig. 4, 3); sphere R = 50 nm which cannot see in the scale 20 μm; Local Crystallization Time LCT = (20/10)³=8 μs.*

Stefan's task in a sphere with a radius of R_{nm} = 50 nm is our proposal for a bridge between the task of Stephen-Schwartz (the first-order phase transition) and the general theorem of Pauli's quantum mechanics [10]. V is volume in Euclidean space; N is the sum of the electrons of the conductivity (e-gas) n = N/V and:

$$\left(\frac{4\pi}{3}p_0^3V = \frac{N}{2}\hbar^3;\ p_0 = \hbar\left(\frac{3n}{8\pi}\right)^{1/3};\ E_0 = \frac{\hbar^2}{2m}\left(\frac{3n}{8\pi}\right)^{2/3}\right) \leftrightarrow V_{nm} = \frac{4\pi}{3}R_{nm}^3, \quad (1)$$

for a particular material (alloy), a necessary geometric matching is sought for the formation of the polycrystalline structure in the die by Stefan's task in the sphere volume with radius R = 50 nm:

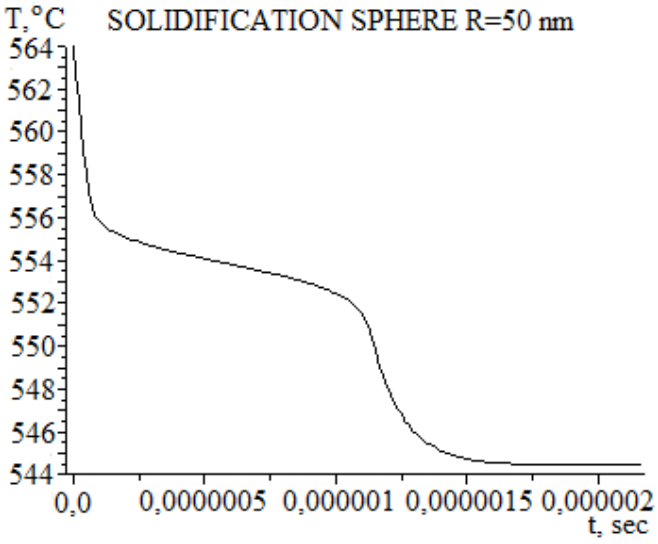

Fig. 7 *Time-temperature curve of solidification of nano-sphere from melt of aluminum alloy (Fig. 3), i. e. conditions of local solidification.*

The process of solidification in a radius sphere, 50 nm is a convenient tool for connecting foundry (MAGMASOFT) and Quantum mechanics (CASTEP) software (first-principles). This software are convention for using the methodology of mathematical experiment and computational physics [16, 17]. Application of CASTEP (or other software) to form a real polycrystalline structure is an important manufacturing tool.

3. Conclusions

1. A 3D Stefan-Schwartz mathematical model is applied in heat transfer with maximum intensity for a K-test. It is obtain the basic process in the real casting volume: the non-stationary temperature field of solidification (separating the latent heat) in the real macro-geometry in the phase transition zone.

2. Stephen's task in nano-volume was chosen as a bridge between software of quantum mechanics to description of structure formation at casting and for example MAGMASOFT.

4. References

1. B. Russell, The principles of mathematics, Taylor & Francis e-Library, 2009 ISBN 10: 0-203-86476-X

2. Gödel's Proof of Incompleteness - English Translation - James R Meyer, *https://www.jamesrmeyer.com/pdfs/godel-original-english.pdf*

3. E. Fermi, Thermodynamics, Prentice-Hall, INC, New York, 1937, Second stereotype edition, Publish house Harkov University, 1973.

4. P. A. M. Dirac, The principles of quantum mechanics, 3-rd edition, University Oxford press, Oxford, 1948.

5. A.H. Chokshi, A. Rosen, J. Karch, H. Gleiter, On the validity of the Hall-Petch relationship in nanocristalline materials, Scripta METALLURGICA Vol. 23, pp. 1679-1684, 1989.

6. A. Balevski, Metalscience, Technics, Sofia, 1962. (In Bulgarian)

7. M. Flemings, Solidification Processing, Peace, Moscow, 1977. (In Russian)

8. J. Blakemore, Solid state physics, Metallurgy, Moscow, 1972. (In Russian)

9. M. Borisov, K. Marinova, Introduction of physics of the solid body part I, Science and Art, Sofia, 1977. (In Bulgarian)

10. G. Schulze, Physics of metals, Peace, Moscow, 1971, (In Russian)

11. Ts. Uzunov, Physics of metals, Technical University, Sofia, 2004. (In Bulgarian)

12. S. Vodenicharov, Dynamic destruction of metals structures, Bulged Ltd. (In Bulgarian) ISBN 978-954-92552-3-2

13. W. D. Callister, Materials Science and Engineering: an introduction, John Wiley & Sons, Inc., New York, 2007. ISBN-13: 978-0-471-73696-7

14. S. A. Saltikov, Stereometric metallography, Metallurgy, Moscow, 1976. (In Russian)

15. R. H. F. Jackson, P. T. Boggs, S. G. Nash, S. Powell, Guidelines for reporting results of computational experiments. Report of the ad not committee, Mathematical programing 45 (1991) 413-425, North Holland.

16. T. Chernogorova, These of Professor, The method of computational experiment to processes from metallurgy, laser physics, ecology and financial, Bulgarian academy of sciences, Institute of Mathematics, 2013. (In Bulgarian)

17. U. Landman. Materials by numbers: Computations as tools of discovery, PNAS, May 10, 2005, vol. 102, no. 19 6671–6678.

18. D. H. Bailey and J. M. Borwein, Experimental mathematics: Examples, Methods and Implications, Notice of the AMS, volume 52, Number 5, 2005.

19. D. I. Khomskii, Basic Aspect of the Quantum Theory of Solids, Cambridge University Pres, 2010, ISBN-13 978-0-511-78832-1

20. M. Sigrist, Solid State Theory, Lecture website http://www.itp.phys.ethz.ch/education/fs14/sst

21. K. R. Nesbet, Variational principles and methods in theoretical physics and chemistry, 2002, eBook ISBN 0-511-04162-4

22. S. Bushev, These of PhD, Controllability problems of crystallization process in casting, TU – Sofia, 1993.

23. S. Bushev, G. Moumdjian, A possibility to influence the dynamics of a phase transition of first order during casting in open thermodynamic systems, Comptes rendus de l'Académie bulgare des Sciences, Tome 46, N^{o} 7, p.27-30, 1993.

24. A. Maneva, These of PhD, Investigation of the structure and properties of castings from subeutectic aluminum alloys depending on the ratio of primary and secondary alloys, Bulgarian academy of sciences, Institute of metal science, equipment and technology with hydro- and aerodynamic center „acad. A. Balevski", Sofia, 2013. (In Bulgarian)

25. S. Bushev, Theoretical model of structure formation in die casting, XXII International scientific technical conference „FOUNDRY 2015", 16-17 April 2015 Pleven, Bulgaria (In Bulgarian)

26. G. Evt. Georgiev, The new Tools for Automatic Optimization of Casting Technologies in the Latest Version of MAGMASOFT – MAGMA5.3.7, Proceedings of Sixth National Conf. with Int. Participation "Material science, Hydro- and Aerodynamics and National Security", May, 29-30, **ISSN 1313-8308,** pp.145-149, 2017.

27. CASTEP, www.tcm.phy.cam.ac.uk/castep/oxford/castep.pdf

MATERIALSCIENCE – ADDITIVE OF MATERIAL AND TECHNOLOGIES

Ass. Prof. Eng. St. Bushev, PhD., Ass. Prof. Eng. L. Stanev,
Institute of Metal Science, Equipment and Technologies With Hydro- and
Aerodynamics Center „Acad. A. Balevski“
Bulgarian academy of sciences
Sofia 1574, 67 „Shipchenski prohod“ blvd. Bulgaria
stbushev@abv.bg, stanev@ims.bas.bg

Abstract: *This paper proposes the idea of a "small volume" in which to consider complicated processes to create structures in phase transitions of first and second order in the foundry. The small volume is chosen based on the classical theory of crystallization and its use for quantum mechanics. A numerical solution of Stefan-Schwarz's task was presented by obtaining the temperature field of solidification of a composite cast in a squeeze casting. This little volume we proposed for a good possibility in the direction for a theoretical possibility of hybridization of production and technology.*

Keywords: „LITTLE VOLUME“, SOLIDIFICATION COMPOSITE, 3D PRINTING, ADDITIVE, MICROSTRUCTURE

1. Introduction – science

The phase transition from the first order is an irreversible process and flows into an open thermodynamic system (OTS). The dynamic state of the particles in it is represented by the generalized entropy function [22]:

$$S=k\ln \pi, \quad (1)$$

where, k is Boltzmann constant. We applied [8] the second low of thermodynamics in the form of the extend of I. Prigogine [11]

$$\left[\frac{Entropy\ of\ OTS}{Time}\right]=\left[\left(\begin{array}{c}Internally\ entropy\ production\ of\\ irreversible\ processes\\ (crystallization)\ in\ OTS\end{array}\right)/Time\right]+\left[\left(\begin{array}{c}Externally\ entropy\\ flow\ by\\ interaction\ OTS\\ with\ environment\end{array}\right)/Time\right]$$

or $\frac{dS}{d\tau}=\frac{dS_I}{d\tau}+\frac{dS_{EX}}{d\tau}$. (2)

At the interphase surface (front) is the limited the change of properties and the thermodynamic state is introduce by Gibbs-Lengmure isotherm

$$d\sigma/d\ln\alpha_i = -\left(RT\Gamma_i^0 K_i'\alpha_i\right)/\left(1+K_i'\alpha_i\right) \quad (3)$$

where σ- surface tension; $K_i'\alpha_i$ is chemical activity of *i*-componentм; Γ_i^0 is maximum concentration at the front. The measure of metastability of phases is the different (Δμ) between chemicals potentials (call driving force) while the change is local equilibrium from anisotropy of surface energy with relation to isotropic is being determined by Gibbs-Thomson equation:

$$\Delta\mu=\mu_L-\mu_S \quad ; \quad \mu_L-\mu_S=\alpha\upsilon_S\left(R_1^{-1}+R_2^{-2}\right) \quad (4)$$

where μ_L, μ_S – are chemical potentials of phases on both sides of surface front; R_1, R_2 – curve radii on surface for location; υ_S – specific volume (of one molecule) of crystals phase; α - surface energy [8]. Theory of Kossel-Stransky-Folmer-Kaishev molecular-kinetic theory. The solution of thermodynamic of equation of Gibbs-Thomson

$$\ln\left(P_{\alpha_3}/P_\infty\right)=\left(\varphi_{1/2}-\bar{\varphi}_{\alpha_3}\right)/kT, \quad (5)$$

where $P_{\alpha 3}$, P_∞ – the pressure of the surface of the crystal and environment; $\varphi_{1/2}$ – the energy for separation (incorporation) of a particle from semi-crystal state; $\bar{\varphi}_{\alpha_3}$ – the average energy used for a particle. The equation much more general [8]. The functional relation between kinetic motion and velocity of crystallization v_{crys} is driving force of crystallization ΔT_k at three growth mechanisms: 1. 2D nucleus formation V_{crys}~ΔT_k; 2. through screw dislocation V_{crys}~ΔT_k^2; 3. Continuous growth V_{crys}~ΔT_k. Character macro- and micro-scales on the base of [11] in [8 and 9] is obtained: $\Delta v_{corr}=l_{corr}^d\tau_{ch}^{-1}=D\Delta v^{-2/d}\quad d=1,2,3$ (6)

where Δv_{corr}, l_{corr}^d are correlations scales and local characteristics volume and time τ_{ch} d is growth directions; and from [2] we accept

$$\tau_{ch}=t_f \Leftrightarrow \Delta\vartheta^{2/d}/D=\Delta\mu/\Delta T_f V_f, \quad (7)$$

where D, ΔT_f, V_f are coefficient of diffusion, locals temperature gradient and velocity of solidification.

The aim of this work we present through paragraphs 1.1 additivity, and 1.2 Synergic.

2.1 Additive – know how

Additive It is known that in a production cycle we have a compulsory sequence of technologies shown in Fig. 1

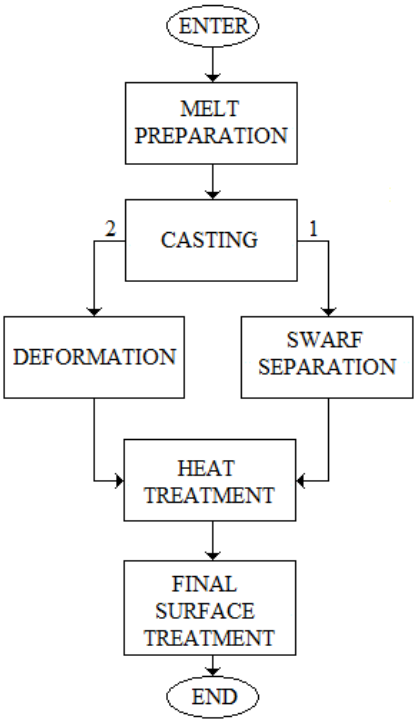

Fig. 1 *Know How – Technological additive on the basis of the two basic processes of material science, casting and heat treatment, where 1 (2) are two real technological circuits, and various well-known combinations of technologies can be made.*

From Fig.1 we add the technology 3D printer.

3.2 Synergic – unification of sciences and technologies

If Material-science is understand full knowledge we introduced on Fig.2: by the through the concepts of science, materials, structure, properties, article, market, product life, material of processing:

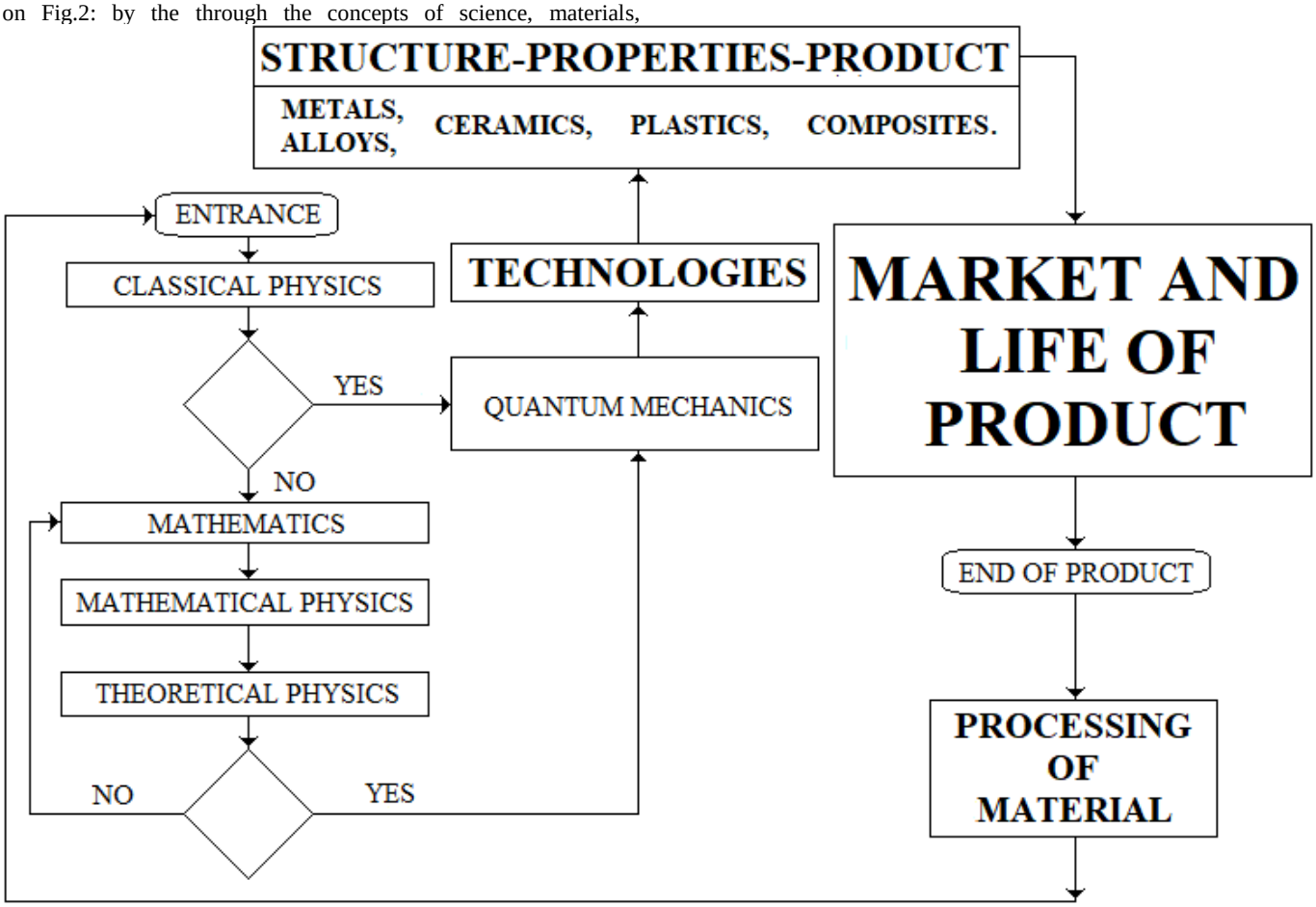

Fig.2 *Synergic the least knowledge of the material science needed for the participation of a family or large foundry company in a* ***circular economy****. Material science is* ***unification of sciences****: classical physics; mathematics; mathematical physics; theoretical physics, quantum mechanics.* ***Integration*** *of casting technology to produce an article whose material has a particular structure and working properties for the longest possible life of the product.* ***Integration of Foundry Technologies we consider as hybrid technology - a combination of foundry machines and 3D printers [].***

4. Materials science in foundry – sciences and technologies

Composite technologies allow new materials to be obtained whose working properties are generally represented by the definition on the base of well-known results [1, 2, 3, 4] and [5; 6, 7] is:

Each composite material is non-homogeneous on a micro scale because it consists of two or more components of different chemical composition and a clear boundary between them but is homogeneous (in properties) on a macro scale. (**WPC**)

Bridge to unite science and technology in materials science is the basic process - the phase transition of the first order. That is the fundamental task at foundry Stefan-Schwarz problem (St-Sch). The mathematical model of foundry in 3D case is

-equation of heat conductivity

$$c_{EF}\rho\frac{\partial T}{\partial \tau}=\lambda\frac{\partial^2 T}{\partial x^2}+\lambda\frac{\partial^2 T}{y^2}+\lambda\frac{\partial^2 T}{\partial z^2}\ in\ V_{OTS}\equiv\begin{cases}V_C^{Al}\cup V_2\cup V_M\\ or\\ V_C^{Al}\cup V_C^C\cup V_M\end{cases},\quad (SS,\ 1)$$

-initials conditions at τ=0:

$$T_C(x,y,z,t=0)=\mathrm{const}_1\ \text{and}\ T_M(x,y,z,t=0)=\mathrm{const}_2,\quad (SS,\ 2)$$

-boundary conditions at τ ≥0:

$$at\ \Gamma:\ \lambda\frac{\partial T}{\partial \vec{n}}=\alpha_\Gamma[T_\Gamma(x,y,z,\tau)-T_{Envirtonment}],$$
$$at\ W_S:\ \lambda\frac{\partial T}{\partial \vec{n}}=\alpha_{Ws}[T_{\Gamma S}(x,y,z,\tau)-T_M(x,y,z,\tau)],\quad (SS,\ 3)$$

,

the thermal coefficients of the OTS for a time interval Δτ, including the filling time of the melt form τ = 0 until the application of the pressure τ = τ_{FP}:

$$\begin{cases}1-\lambda_M,\rho_M,c_M & for\ T_{EL}(\tau) & \forall\tau\\ 2-\lambda_2,\rho_2,c_2 & for\ T_{EL}(\tau) & \forall\tau\\ 3-\lambda_L,\rho_L,c_L & for\ T_{EL}(\tau)\geq & T_m+\Delta T\\ 3-\lambda_L,\rho_L,c_L+Q_F\dfrac{dS_F[T(\tau)]}{dT} & for\ T_{EL}(\tau)\in & [T_m\pm\Delta T(\tau)]\\ 3-\lambda_S,\rho_S,c_S & for\ T_{EL}(\tau)\leq & T_m-\Delta T\end{cases},\quad (SS,\ 4)$$

from the time of application of pressure to solidification of the composite casting

$$\begin{cases}1-\lambda_M,\rho_M,c_M, & for\ T_{EL}(\tau) & \forall\tau\\ 3-\lambda_L,\rho_L,c_L, & for\ T_{EL}(\tau)\geq & T_m+\Delta T\\ 3-\lambda_L,\rho_L,c_L,=c_L+Q_m\ dS_F\ [T(\tau)]/\ dT & for\ T_{EL}(\tau)\in & [T_m\pm\Delta T(\tau)]\\ 3-\lambda_S,\rho_S,c_S, & for\ T_{EL}(\tau)\leq & T_m-\Delta T\\ 3_C-\lambda_L^C=k_{Al}\lambda_L+k_2\lambda_2\rho_L^C=k_{Al}\rho_L+k_2\rho_2, & c_L^C=k_{Al}c_L+k_2c_2 & for\ T_{EL}(\tau)\geq\ T_m+\Delta T\\ 3_C-\lambda_L^C,\rho_L^C,c_L^C=c_L^C+Q_m\ dS_F\ [T(\tau)]/\ dT & for\ T_{EL}(\tau)\in & [T_m\pm\Delta T(\tau)]\\ 3_C-\lambda_S^C=k_{Al}\lambda_S+k_2\lambda_2\rho_S^C=k_{Al}\rho_S+k_2\rho_2, & c_S^C=k_{Al}c_L+k_2c_2 & for\ T_{EL}(\tau)\leq\ T_m-\Delta T\end{cases},(SS.5)$$

the function of the heat source is approximated by δ-type function

$S_F(T) = \frac{1}{D\sqrt{\pi}} e^{-\left(\frac{T-Tm}{D}\right)^2}$, $D \in \Delta T\,(\tau) \equiv (Tm - \Delta T, Tm + \Delta T)$, at (SS, 6)

$\int_{T_m-\Delta T}^{T_m+\Delta T} S_F(T)dT = 1 \Leftrightarrow erf\left(\frac{\Delta T}{D}\right)$ and at $\frac{\Delta T}{D} > 2$.. (SS, 7)

The following symbols are used in this model: thermophysical coefficients λ, ρ, c − thermal conductivity, density and thermal capacity for the individual parts of the OTS according to the indices used M - mold, 2 − preform (corundum), L and S − melt and solid phase of pure Al, lower index C - casting, upper index C - composite area; lower index EL − final element; k_{Al}, k_2 − percentage of pure Al and corundum fibers in the composite area; x, y, z - coordinates of OTS; heat transfer coefficients α_{WS} and $\alpha_{\Gamma M}$ − at working and external surfaces of the Q_F − heat of phase conversion; T_m − phase transition temperature, the same for the composite and Al-casting areas; ΔT – temperature range of T_m; D − dispersion of the S_F function; $T_{AR.M.}$ − ambient temperature; V_2 volume of preform (carborundum) which after filling with Al melt is the volume of the composite area, − volume of pure Al; V_M − mold volume; W_S and Γ − working and external surfaces of the mold.

On Fig. 2 we present General Scheme of the experiment for production of *composite casts by squeeze casting*; and Fig. 3 present solidification of *composite at squeeze casting technology*:

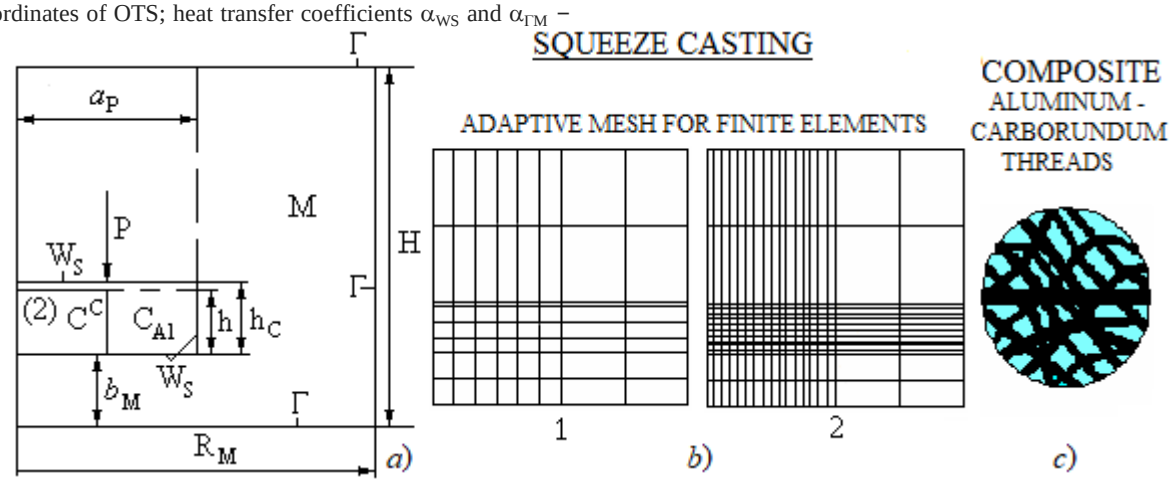

Fig.2 *General Scheme of the experiment for the production of composite casts (square slab) of aluminum base by semi-die-casting at pressure P = 150 Mpa: a)* ***cast*** *C – dimensions: h_C, h – cast heights and composite areas, square base with side $2a_P$; mold M – dimensions R_M – radius, H – height, b_M - distance from the base of the casting to the shape of the mold; W_S, Γ – working and outer surfaces of the form; b) a grid of fined elements for solving the Stefan Schwarz task – 1 for cast with composite area and 2 for cast from pure Al; c) microstructure of the composite where* ∿ *- randomly intertwined carborundum strands,* ■ *– a solid melt of pure Al.*

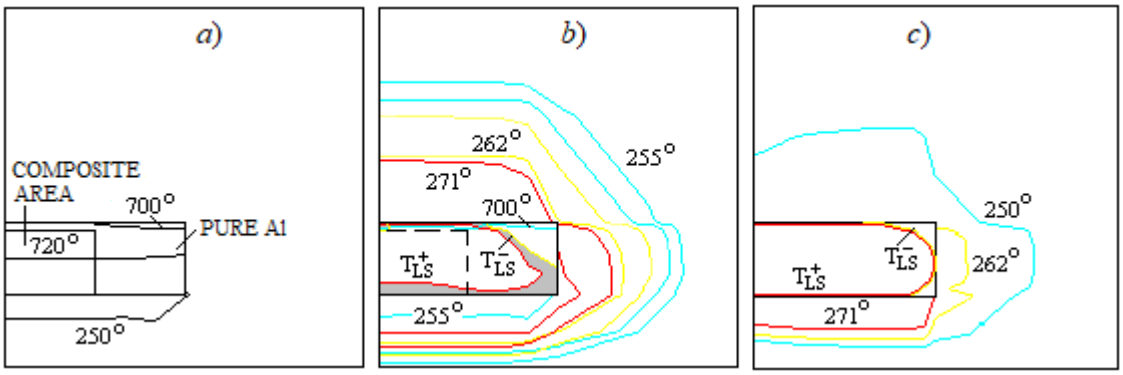

Fig.3 *Temperature fields at different moments of time with perfect contact of the preform – melt and composite – melt or hard composite – hard metal: We use the following numerical values for the above values: H = 0,1m; R = 0,1m; b_M = 0.02m; a_P = 0,05m; h = 0,02m; h_C = 0,037m; for the mold - λ_M = 54,28 w/mK, c_M = 460,548 J/kgK, ρ_M = 7860 kg/m^3; for cast - preform k_2 = 15%, λ_2 = 0,2125 w/mK, c_2 = 1338,8 J/kgK, ρ_2 = 555,3876 kg/m^3, pure Al k_{Al} = 85% 104,675 w/mK, c_L = 1088,568 J/kgK, ρ_L = 2380 kg/m^3, λ_S = 209,2750 w/mK, c_S = 1130,436 J/kgK,/m^3, λ_L^C = 89,006 w/m K, c_L^C = 1217,5 J/kg K, ρ_L^C = 2106,3 kg/m^3, λ_S^C = 177,9 w/mK, c_S^C = 1253,1 J/kg K, ρ_S^C = 2242,31 kg/m^3, T_m = 660.1 ° C - same for pure Al and composite material, ΔT = 3,5 ° C, D = 1,51 ° C, Q_F = 401932.8 J/kg, = 730 ° C = 250 ° C, $T_{AR.M.}$ = 20 ° C, heat transfer coefficient at the working surface W_S up to the moment of application of pressure - α_{WS} = 3292,3 w/m^2 K, after applying pressure to the end of the hardening - α_{WS} = 29000 w/m^2 K and coefficient of the heat transfer on the outer surface Γ of the form - α_Γ = = 12 w/m^2 K. The numerical solution of the three-dimensional task is by the finite element method with a time step δτ = 0,001s.*

a) Closed unpressurized (i.e. pressure 1 atmosphere) mold with clear preform limit – Melt from pure Al at time point ***τ = 0,003s****, only in casting 720 ^{O} C and currently* ***τ = 0,034s*** *in the melt 700 ^{O} C, in the form 250C; b) pressure hardening at three different time points in the time interval* ***τ = 0,14÷2,5s****, where in the casting — — — the composite-pure Al, 700 ^{O} C-blue border, the hardening front is approximated to the temperature range $T_{LS}^+ = T_m + \Delta T$ and $T_{LS}^- = T_m - \Delta T$, in the form 255 ^{O} C – blue color, 262 ^{O} C – yellow color and 271 ^{O}C red color; c) – pressure hardening of a cast of pure Al currently τ = 0,14s.*

And important *Methodology for connection crystallization and quantum mechanics is* in the frame of [16] – work φ two charges q_1, q_2 should be kept at a minimum distance r (metal chemical connection MCC) only coulomb forces. According to a classical methodological principle, is only for ionic crystals [16]:

$\varphi = (q_1 q_2)/(4\pi\varepsilon_0 r)$. (MCC)

Work to bring one positive charge to the end of a chain of alternating (+) and (-) charges of equal distance r is the coming expression:

$\varphi_{K/2} \equiv (-e^2/4\pi\varepsilon_0 r)(-e/1 + e/2 - e/3 - \cdots) = (-e^2/4\pi\varepsilon_0 r) ln2$

or $\varphi_{1/2} \equiv \left(-e^2/4\pi\varepsilon_0 r\right) \Phi$, (MCC2, 3)

where Φ corresponds of *ln*2 ⇒ for work to build a grid of large numbers of particles N (or Energy of lattice) is

$E_{N\ particles} = \left(-e^2/4\pi\varepsilon_0 r\right)\Phi$ and for energy 3D lattice, $E_{N\ particles} \equiv \mathbf{E}_{\mathbf{Lattice}}$, and Φ is constant of Madelung [16, 3]. To describe the chemical bond, quantum mechanics must be used [3, 16, and 17]. In an electronic approach, the Vigner-Zeitz cell method is used for solution Schrödinger equation (SEQ) in character volume $\Delta\vartheta_{corr}$ and time eq.(6 and 7) are the connection Classical physic and Quantum mechanics.

$-\hbar^2\nabla^2\psi(r)/2m + V(r)\psi(r) = E\psi(r)$ and conditions of (SEQ1)

$\Psi_k(r) = \exp(ikr)u_k(r)$, (SEQ2)

$u_k(r) = u_k(r + T_n)$, (SEQ3)

where m is the electron mass; $\hbar$ – Planck constant; *V* is the periodic potential of the interaction electron/(all other electrons); ψ is a wave function, a solution to equation; $\boldsymbol{k}$ is a vector defined of the crystal Brave lattice $\mathbf{T}_{n_1n_2n_3} = n_1\mathbf{t}_1+n_2\mathbf{t}_2+n_3\mathbf{t}_3 \equiv \mathbf{T}_n$, n is numbers ($n_1$, n_2, n_3); u_k is a periodic function with the period of *V*.

Composite materials [5, 6 and 7] obtained by casting have great development potential. For example, heat-physical coefficients eq.(SS5). The machines and technologies created in our institute allow create of new composites.

The characteristic volume $\Delta\vartheta_{corr}$ and time eq.(6 and 7) is a model of consideration for mathematical and theoretical consideration of processes to create structures in phase transitions. This approach allows the conditions of structuring in foundry machines, technologies and new materials to be stored and used in new technological solutions. Works [11, 12, 13, 14 and 15] are the scientific approach to generalization on work-based science [11 and 12].

The well-known 3D printer technology allows additive engineering summation of ideas called "cross-pollination" in [20]. Additive manufacturing technologies [18, 19, 20 and 21] is a basic idea as a molecular science and technique or a multivariate summary. Technology based on quantum mechanics is evolving, constantly shifting and capturing new production areas. Additive Manufacturing [18÷21] are tied to a 3D printer. Important moment in additive manufacturing is combination between new [21] software and traditional production (for our institute foundry machines and technologies). In [21] is called „hybrid production“ and „hybrid machines“.

At work [23] it is emphasized the need to describe structures by quantum mechanics in a "small volume". For us, this is a clear emphasis on "knowledge transfer" or the most difficult work with "full knowledge" and "prognosis". Concentration of research is precisely the "drop" model chosen by us (Δϑcorr and time eq. (6 and 7)).

3. Conclusions

A characteristic volume on the consolidation front was obtained to calculate the microstructure using quantum mechanics software.

It is obtain the numerical result of solidification composite material at squeeze casting.

3D Printer is additive through its drop and the characteristic volume for storing the solidification conditions in foundry and creating hybrid technologies.

5. Reference

1. A. Balevski, Metal science, Technics, Sofia, 1962.

2. M. Flemings, Solidification processing, Peace, Moscow, 1977. (In Russian)

3. M. Borisov, K. Marinova, Science and Art, Sofia, 1977.

4. S. Vodenicharov, Dynamic destruction of metal structures, *Bulged Ltd.*, Sofia, 2011. ISBN 978-954-92552-3-2 (In Bulgarian)

5. R. E. Smallman, R. J. Bishop, Modern Physical Metallurgy and Materials Engineering, Butterworth-Heinemann, Oxford, 6E, 1999. ISBN 0 7506 4564 4

6. Marco van Oosten, Composite – Metal connections, Report ITD 9006-2A.01. Issue no.: 1, Issue date: 29-01-2015

7. W. D. Callister, Jr., D. G. Rethwisch, Materials Science and Engineering, John Wiley & Sons, Inc. 9 edition, 2014. Wiley ISBN: 978-1-118-47770-0, Printed in USA 10 9 8 7 6 5 4 3 2 1

8. S. M. Bushev, PhD Tesis, Technical University, Sofia, Bulgaria, 1995.

9. S. Bushev, G. Moumjian, A possibility to influence the dynamics of a phase transition of first order during casting in open thermodynamic system, Comptes rendes de l'Academie bulgare des Sciences, *Tome 46, № 7p 1993*.

10. G. Mumdgian, Automatic ruling and regulation of the heat processes, Technique, Sofia, 1980. (In Bulgarian)

11. G. Nicolis, I. Prigogine, Exploring complexity, Peace, Moscow, 1990. (In Russian)

12. A. Polikarov, Methodology of scientific knowledge, Science and Art, Sofia, printing house, Alexander Peshev, Pleven, 1972.

13. https://www.vocabulary.com/dictionary/synergistic

14. M. Bushev, *Synergetics: Chaos, Order, Self-Organization*. Singapore: World Scientific, 1994.

15. D. Cerra, R. Müller, P. Reinartz, A Classification Algorithm for Hyperspectral Images Based on Synergetics Theory, IEEE Transactions on Geoscience and Remote Sensing, p. 1-12, May 2013. DOI: 10.1109/TGRS.2012.2219059

16. G. Schulze, Metallphysik, Peace, Moscow, 1971. (In Russian)

17. J. S. Blakemore, Solid state physics, Metallurgy, Moscow, 1972. (In Russian)

18. I. Gibson, D. Rosen, B. Stucker, Additive manufacturing technologies, Springer Science+Business, Media New, York 2015,DOI 10.1007/978-1-4939-2113-3_2

19. J. Hart, An Introduction to Additive Manufacturing - MIT http://web.mit.edu/2.810/www/files/lectures/2015_lectures/lec9-additive-manuf-2015.pdf

20. B. Wu, C. Myant, S. Z. Weider, The value of additive manufacturing: future opportunities, Briefing Paper No 2 September , p.1÷13, 2017. *https://www.imperial.ac.uk/media/imperial-college/.../IMSE-Briefing-paper-2-AM.pdf*

21. N. Aschenbrenner, New Software Combines 3D Printing with Traditional Manufacturing

norbert.aschenbrenner@siemens.com
Adnew.siemens.com/additive/manufacturing, Siemens AG.

22. E. Fermi, Thermodynamics, Prentice-Hall, INC, New York, 1937, second stereotype edition, publishing house of Kharkov University, 1973. (In Russian)

23. F. Suzuki, PhD Tesis, Quantum mechanics of composite objects with international entanglement, University of British Columbia, Vancouver, 2012.

MATERIALS – ADDITIVE OF KNOWLEGE PROPERTIES AND TECHNOLOGIES

Ass. Prof. Eng. St. Bushev, PhD.
Bulgarian academy of sciences
Institute of Metal Science, Equipment and Technologies With Hydro- and
Aerodynamics Center „Acad. A. Balevski“
Sofia 1574, 67 „Shipchenski prohod“ blvd. Bulgaria
stbushev@abv.bg

Abstract: Two tasks are enumerated: a task of hardening spheres with a radius of 50 nm and a task of crystallization - the underlying kinetic equation of formation of new phases. These tasks are rational bridges for multi-scale approach.
There is an opportunity to create additive production with traditional machines and technologies in the field of anti-pressure casting
Keywords: ADDITIVE MANUFACTORING GAS COUNTER-PRESSURE, „CORRELATION VOLUME“, 3D PRINTING

1. Introduction

Definition of the thermodynamics: Thermodynamics (from Greece) [1] is called the general science of energy dealing with the relationship between heat and mechanical energy and heat transformations at work and vice versa. The purpose of the article in [1] is to show the application of the two general principles (1) the Joule's Law on Heat and Work Equivalence, and (2) the Carnot principle that the efficiency of a reversible engine depends only on the temperatures between which it does work;

The main content of thermodynamics - this is a description of the conversion of heat into work and, conversely, the conversion of mechanical work into heat [2]; Thermodynamics: the science that deals with heat and work, and those properties of matter that refer to heat and work [3]. Thermodynamics is a branch of physics that deals with heat and temperature and their relationship to energy, work, radiation, and the properties of the bodies of matter [5]. The main meaning in all definitions is preserved, which is an example of accurate knowledge.

The classical thermodynamics presented in the essay of Table 1:

Table 1: *Thermodynamics [1, 2, 4].*

1. LIQUIDUS IS HOMOGENEOUS OR HETEROGENEOUS OPEN THERMODYNAMICS SYSTEM; **2.** PARAMETERS: VOLUME **V** PRESSURE PARAMETERS **p** TEMPERATURE **T** AND AGREGATE STATE; **3.** FOR A SUBSTANCE VARIABLES **V**, **p** AND **T** ARE NOT INDEPENDENT BUT ARE CONNECTED IN **THE STATE EQYATION *f*(p, V, T) = 0** AND THE SOLUTION FOR EACH VARIABLE IS A FUNCTION OF THE OTHERS TWO; **4. EXTENSIVE QUANTITIES** ARE: VOLUME (v), MASS (m), ENERGY (U), ENTALPY (H), ENTROPY (s), BECAUSE THEY ARE PROPORTIONAL TO THE QUANTITY OF MATTER. **INTENSIVE QUANTITIES** ARE: DENSITY (ρ = m/V) AND TEMPERATURE T, WHICH DO NOT SATISFIES WITH THE CONDITION OF EXTENSIVE; **5. ANALYSIS APPROACH**: THE HETEROGENEOUS SYSTEM IS DISTRYBUTED AT THE END OR EXRTEME NUMBER OF HOMOGENEOUS VOLUMES (PARTS). **6. THE STATE OF THERMODYNAMICS EQUILIBRIUM** OF A SYSTEM IS SIMULTANEOUSLY THE THREE THERMAL, MECHANICAL AND CHEMICAL EQUILIBRIUM. **THE DYNAMICALLY-THERMODYNAMIC** STATE IS A COMBINATION OF DYNAMIC STATES THROUGH WHICH THE SYSTEM REPIDLY MIGRATES AS A RESULT OF MOLECULAR MOVEMENT; **7.** THE SYSTEM HAS A **STEADY EQUOLIBRIUM** WITH A MINIMUM OF FREE ENERGY; **8. THE CONVERSION OF THE SYSTEM STATUS** IS EXCHENGED UNDER AN INCORRECT RANGE OF INTERMEDIATE CONDITION. **THEREVERSIBLE TRANSFORMATION** IS WHEN THE ARRAY OF INTERMEDIATE STATES ARE INFINITELY CLOSE TO **THE EQUILIBRIUM**; **9. INTERNAL ENERGY (U)** IS THE SUM OF: THE TOTAL KINETIK ENERGY $\Sigma E_{Cinetic}$ OF THE MOVMENT OF MOLECULES AND THE FULL POTENTIAL ENERGY $\Sigma E_{potential}$ OF ELECTROMAGNETIC INTERACTION KEEPS THE ELECTRONS IN THE ATOMS AND CONNECTS THE ATOMS IN MOLECULES AND CRYSTALS $U = \Sigma E_{Cinetic} + \Sigma E_{Potential}$;

10. LAWS OF THERMODYNAMICS: ZERO LAW: IF THRMODYNAMICS SYSTEM **A** IS IN THERMODYNAMIC EQUILIBRIUM WITH SYSTEM **B** AND IN TURN SYSTEM **B** IS IN THERMODYNAMIC EQUILIBRIUM WITH SYSTEM **C**, THEN **A** AND **C** ARE ALSO IN THERMODYNAMIC EQUILIBRIUM. PHYSICAL PRINCIPLE EXPRESSING THE TRANSITIVITY OF THERMODYNAMIC EQUILIBRIUM AND DEFINING TEMPERATURE; **FIRST LAW:** THE CHANGE IN THE INTERNAL EMERGY **U** OF A THERMODYNAMIC SYSTEM IN AN RABITRARY THYERMODYNAMIC PROCESS WITH INITIAL AND FINAL STATE IS EQUAL TO THE QUANTITY OF HEAT **Q** INPUT OR OUTPUT FROM THE SYSTEM AND THE OPERATION **W** PERFORMED ON THE SYSTEM **ΔU = Q + W** or **ΔQ = dU + pdV**; ***CHANGE*** **BETWEEN TWO EQUILIBRIUM STATEES:** CLOSED SYSTEM $\Delta E = \Delta E_{C(macro)} + \Delta E_{P(macro)} + \Delta U$; AND **OPEN SYSTEM** $\Delta E = \Delta E_{C(macro)} + \Delta E_{P(macro)} + \Delta U + m(u)_{Inlet} - m(u)_{Outlet}$, WHERE MASS $m(u)_{OUTLE(INLET)}$ ARE MASS FLOW ENTERING AND LIVING THE SYSTEM; **10.1** THERMODYNAMIC FUNCTIONS: ***EMTALPY*** **H = U + pV**; ***ENTROPY*** **(S) dS = dQ/T** or $S(A) = \int_0^A dQ/T$. ***10.2 THE SECOND LOW:*** IT IS NOT A POTENTIAL PROCESS IN WHICH THE ONLY ULTIMATE RESULT IS TO SWICH TO THE HEAT OF A HEAT REMOVED FROM A SOURCE THAT ALWAYS HAS A SINGLE TEMPERATURE (KELVIN POSTULATE); IT IS NOT AN INHERENT PROCESS IN WHICH THE ONLY ULTIMATE RESULT IS A HEAT TRANSFER FROM A BODY HAVING A GIVEN TEMPERATURE TO A BODY WITH A HIGHER TEMPERATURE (CLAUSIUS POSTULATE) IF THE HEAT REMAINS FROM THE BODY **A** AND ANAOTHER **B**, THIS IS NOT A POSSIBLE PROCESS TO WHICH THE ONLY END RESULT IS TO BE TRANSFERRED TO THE HEAT FROM **B** TO **A** (OTHER CLAUSIUS POSTULATE); ***SECOND LOW:*** THE ENTROPY OF A CLOSED SYSTEM THAT IS NOT IN EQUILIBRIUM INCREASES WITH TIME REACHING ITS MAXIMUM VALUE WHEN EQUILIBRIUM **ΔQ ≤ TS**; **10.3 THERMODYNAMICAL POTENTIALS OF THE SYSTEM:** INTERNAL EMERGY **dU = TdS - PdV**, IN VARRIABLES **S**, **P**, **V**, **T**; POTENTIAL ENTROPY **H = U + PV** OR **dH = d (U + PV) = dU + PdV + VdP = TdS + VdP** IN VARIABLES **S**, **P**, **V**, **T**; HELMHOLTZ'S FREE ENERGY **F = U-TS (dF = - SdT - PdV)** IN VARIABLES **T** AND **V**; POTENTIAL OF GIBBS **G = U + PV - TS ≡ H - TS** IN VARIABLES **T** AND **P**; OFEN G IS CALLED FREE ENTALPY; THE RANDOME CHOICE OF THE INITIAL STATE *O* INTRODUCES INTO THE ENTROPY **S** AN UNDETERMINED ADDITIVE CONSTANT. **10.4 THE THIRD LAW OF THERMODYNAMICS OR THEOREM OF NERNST:** THE ENTROPY OF ANY SYSTEM AT ABSOLUTE ZERO CAN ALWAYS BE ASSUMED TO BE ZERO. **11. ASSESSMENT OF THERMODYNAMICS:** FROM ALL POSSIBLE STATE, WHICH OF THEM IS EQUILIBRIUM. MAKE THE RELATIONSHIP BETWEEN I-st LOW AND II-nd THE THERMODYNAMICS LAW OF THE TIPE **dU + pdV = ΔQ ≤ TdS** at **dp = dT = 0 ⇒ dG ≤ 0**. i.e. **G → min**. ANALOGGUE WHEN SET **V** AND **T**, **dV = dT = 0 ⇒ dF = dU - TdS - SdT ≤ - PdV - SdT** and from **dV = dT = 0 ⇒ F → min**. IN FUTURE AMENDMENS WITH FAST FREQUENCY CONFLICTS FREEFIELD PHRASES **dF = dU - TdS - SdT = - PdV - SdT** AND GIBBS POTENTIAL **dU = pdV = ΔQ = TdS** WE HAVE AN EQUALITY WE HAVE EQUALITY MARK. HERE ARE FOLLOWING RELATIONS: AT **F → min** $(\partial F/\partial V)_{T,N_k} = -P\,(\partial F/\partial T)_{V,N_k} = -S$; AT **G → min** $(\partial G/\partial p)_{T,N_k} = V$, $(\partial G/\partial T)_{p,N_k} = -S$.

THE CHEMICAL COMPOSITION DETERMINES THE AMOUNT OF $\mathbf{N_k}$ OF EACH COMPONENTS **k** IN EACH PHASE φ I.E. **KΦ** ARE QUANTITIES WHERE **K** – THE NUMBER OF COMPONENTS AND **Φ** – THE NUMBER OF PHASES. THE MAGNITUDE $\mathbf{N_{kφ}}$ DENOTES THE CHEMICAL COMPOSITION WHICH FOR EACH PHASES. THE MAGNITUDE $\mathbf{N_{kφ}}$ IS UNICUELY CHARACTERIZED BY **K – 1** PARTS: $x_{k\varphi} = N_{k\varphi} / \sum_{i=1}^{K} N_{i\varphi}$, BUT ALSOW THE TOTAL QUANTITY OF SUBSTANCE AS THE AMOUNT OF SUBSTANCE ∀ PHASE **φ** IS EQUAL TO $x_{k\varphi} = \sum_{i=1}^{K} N_{i\varphi}$. EXTENSIVE **Ψ** FOR HETEROGENEOUS MIXTURE IS OBTAINED BY SUMMING (ADDITIVE RULE) $\Psi = \Sigma\Psi_i$; THE RELATION $\Psi(\alpha N_1, \alpha N_2, ..., \alpha N_K) = \alpha\Psi(N_1, N_2, ..., N_K)$ IS TRUE; MATHEMATICAL REPRESENTATION OF THE EXTENSIVE DIMENSIONS ARE HOMOGENEOUS FUNCTIONS OF THE 1-ST DEGREE AND IS TRUE EULER'S THEOREM $\Psi=\Sigma_i(\partial\Psi/\partial N_i)N_i$, WHILE FOR ANY FUNCTIONS **Ξ** IT IS ONLY THE CORRESPONDING DIFFERENTIAL RATIO TRUE $d\Xi = \Sigma_i(\partial\Xi/\partial N_i)dN_i$.

The basic processes of material science, casting and heating flow in open thermodynamic systems [2, 3, 4, 5 ana 6]. The two processes are irreversible phase transitions of the first and second order. The classical thermodynamics Table 1, [2, 3 and 4] is used to describe the casting process that is basically considered. Mathematics is presented alongside the laws of thermodynamics, showing in depth the historical development. We also use the synergistic approach [18, 19, 20, 21 and 22]. The overall dynamic state of the system in the synergistic approach [18, 19, 20, 21 and

22]. is the extended form of I. Prigogine's second law of thermodynamics [18] in the view:

$$\left[\frac{Entropy\ of\ OTS}{Time}\right] = \left[\left(\frac{Internally\ entropy\ production\ of\ irreversible\ processes\ (crystallization)\ in\ OTS}{Time}\right)\right] + \left[\left(\frac{Externally\ entropy\ flow\ by\ interaction\ OTS\ with\ environment}{Time}\right)\right]$$

or $\frac{dS}{d\tau} = \frac{dS_I}{d\tau} + \frac{dS_{EX}}{d\tau}$. (1)

The thermodynamic driving force $\Delta\mu > 0$ of the phase transition of first order and at crystallization of melts [15, 16, and 17]

$$\Delta\mu = \Delta S_m(T_m - T), \quad (2)$$

Where T_m – the temperature of phase transition. Temperature of undercooling is defined from Stefan's problem. The work W_n for the formation of n-atoms complex in the system ΔV under the influence of the case eq, (2) we have

$$W_n(\Delta\mu) = -n\Delta\mu + F_n(\Delta). \quad (3)$$

For description the nucleation and growth we use fundamental kinetic equation phase transition of Kashchiev [30]. It expresses a balance between the distribution function $Z_n(t)$ of new phase complex of n-atoms and its total change $dZ_n(t)/dt$

$$\frac{dZ_n(t)}{dt} = \sum_{m=1}^{N}\left[f_{mn}(t)Z_m(t) - f_{nm}(t)Z_{n(t)}\right] + K_n(t) - L_n(t) \ at\ t \in [0, t_F] \quad . (4)$$

With a suitable definition of the transition frequencies $f_{nm}(t)$ the equation (4) is valid not only for the initial stage of nucleation, but also for coagulation from unified point of view. The general number N(T) of the over-nuclei complex in the subsystem ΔV is obtained. So as the rate of nucleation J(t)

$$N(t) = f|Z_n|, J(t) = \frac{dN(t)}{dt}\ t \in [0, t_f]. \quad (5)$$

The equations (2÷5) introduce the phase transition of first order of the three levels [31]. The local function

$$\sigma_S = F[N(t), J(t)] \ at\ t\epsilon[0, t_f]. \quad (6)$$

We separate the volume of the open thermodynamic system in macroscopic cells ΔV_i, i =1, …, N and the phase transition of first order is

$$\sigma_S = \sum_i \sigma_S^i \quad \text{for time:} \quad t = \sum_i t_f^i \quad . \quad (7)$$

Thus with eq.(7) a generalized model of phase transition of first order in the complex casting process is present.

In order to have a technology we can reproduced in every local volume ΔV_i degradation of energy and condition.

$$\sigma_S^i \le J_i(t) \ at\ t \in [0, t_f^i].$$

The functional relation between kinetic motion and velocity of crystallization v_{crys} is driving force of crystallization ΔT_k at three growth mechanisms: 1. 2D nucleus formation $V_{crys} \sim \Delta T_k$; 2. through screw dislocation $V_{crys} \sim \Delta T_k^2$; 3. Continuous growth $V_{crys} \sim \Delta T_k$. Character macro- and micro-scales on the base of [11] in [8 and 9] is obtained: $\Delta v_{corr} = l_{corr}^d \tau_{ch}^{-1} = D\Delta v^{-2/d} \quad d = 1, 2, 3$ (8)

where Δv_{corr}, l_{corr}^d are correlations scales and local characteristics volume and time τ_{ch} d is growth directions; and from [2] we accept

$$\tau_{ch} = t_f \Leftrightarrow \Delta\vartheta^{2/d}/D = \Delta\mu/\Delta T_f V_f, \quad (9)$$

where D, ΔT_f, V_f are coefficient of diffusion, locals temperature gradient and velocity of solidification. On Fig.1 present gas counter-pressure technology

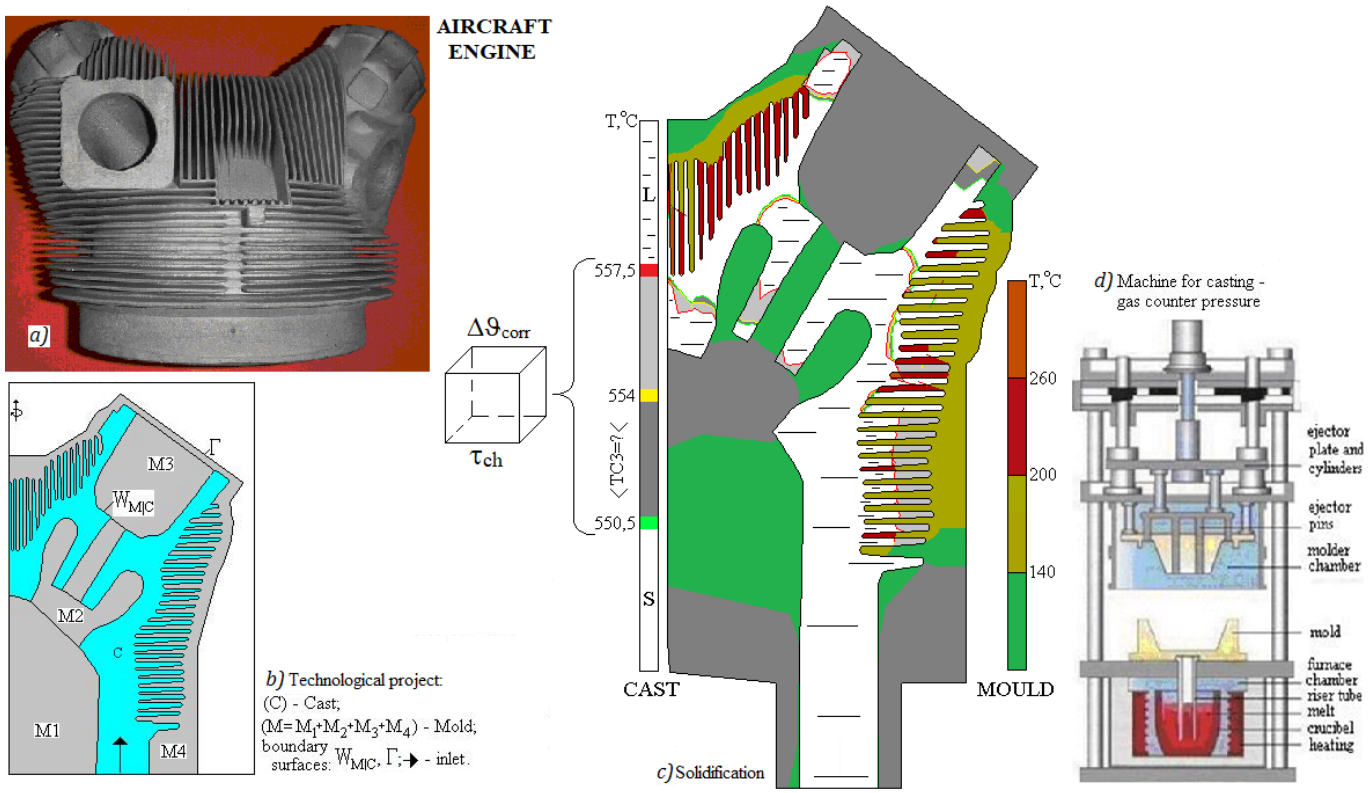

Fig.1 Integration *of casting technology to produce an article whose material has a particular structure and working properties for the longest possible life of the product.* ***Integration of Foundry Technologies we consider as hybrid technology - a combination of foundry machines and 3D printers [25, 26, 27 and 28]. We wanted correlation volume eq. (8) and (9) with condition of solidification. The idea is produce cast with simple geometry and finish with 3D printer***

2. Materials science in foundry – sciences and technologies

Bridge to unite science and technology in materials science is the basic process - the phase transition of the first order is the fundamental task at foundry Stefan-Schwarz problem (St-Sch) Fig. 2 and 3 are shown the choice of $\Delta\vartheta_{corr}$ and τ_{ch} two bridge tasks: solidification of spheres with radius 50 nm and solution of eq.(4)

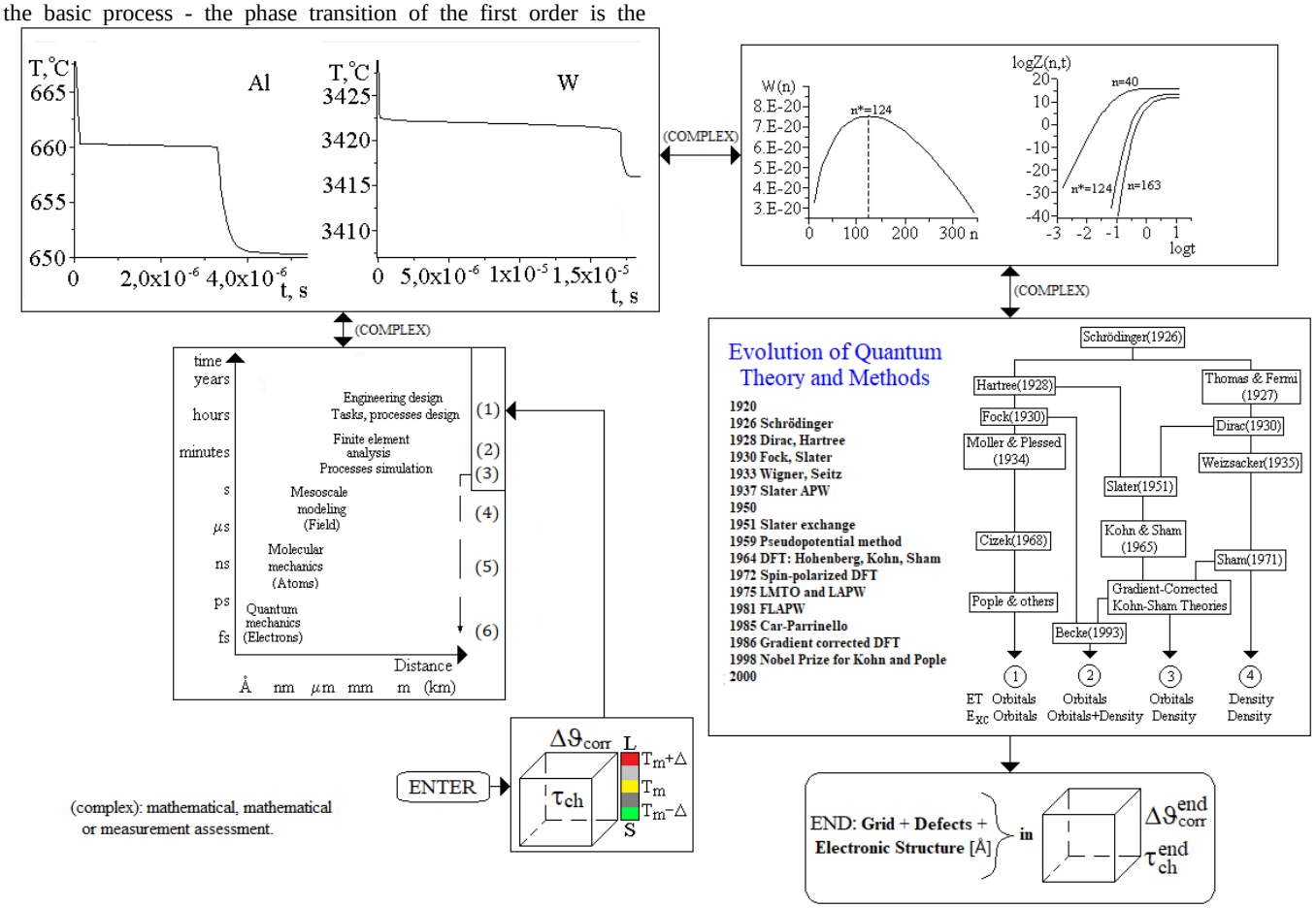

***Fig.2**. Determination of correlation volume$\Delta\vartheta_{corr}$ and characteristic phase transition timeτ_{ch} of first order. We use a multi-scales approach.*

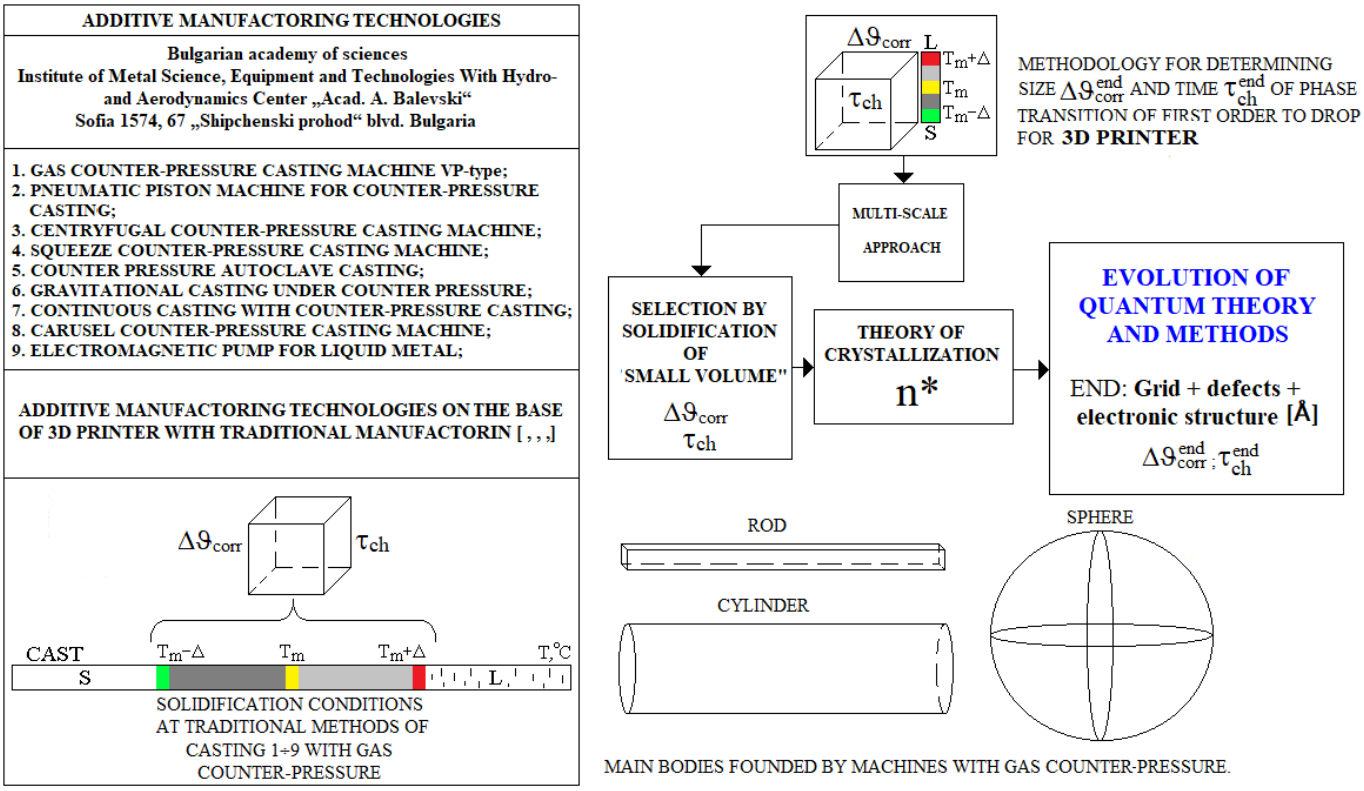

***Fig. 3**. Additive manufacturing gas counter-pressure casting machines: Castings with simple geometry and final operation with 3D printer.*

From Fig. 1, 2 and 3, the correlated volume and the characteristic phase transition time $\Delta\vartheta_{corr}^{end}$ and τ_{ch}^{end} we take for a drop size of a 3D printer. This way we can preserve the capabilities of the machines, technologies and materials of our institute. Tasks for solidification of spheres with a radius of 50 nm are key, and the solution of eq.(4) represents the number of nuclei-forming particles. This information is very close to the actual structure of the material. Using quantum mechanics allows you to get complete information about the real structure i.e. the properties of the material.

The multi-scales approach by the bridge tasks of solidification and crystallization are shown interacts with thermodynamics [1, 2, 3, 4, 5, 6]; material science [12, 13, 14]; synergy and methodology of science [18, 19, 20, 21, 22]; metal science [8, 9, 11]; metallography [23]; solid state physics and quantum physics [7, 10, 24, 29]. By choosing a correlation volume, phase transition conditions [25, 26, 27, and 28] allow to transfer through a 3D printer

3. Conclusions

Bridged tasks such as solidification a sphere with a radius of 50 nm and a crystallization task are selected.

Nano-scale and number of nuclei-forming particles are robust scientific and technological tools in multi-scale approach and additive production.

An additive manufacturing methodology is created by choosing a drop size for a 3D printer.

5. Reference

1. The Encyclopedia Britannica, Eleventh Edition, and Cambrige, England: at the University Press, 1911.

2. E. Fermi, Thermodynamics, Prentice-Hall, INC, New York, 1937, second stereotype edition, publishing house of Kharkov University, 1973. (In Russian)

3. J. M. Powers, Lecture notes on thermodynamics, Department of Aerospace and Mechanical Engineering, University of Notre Dame, July 2018, Indiana 46556-5637, USA.

4. D. Arovas, Lecture Notes on Thermodynamics and Statistical Mechanics, University of California, San Diego, November 14, 2013.

5. *https://en.wikipedia.org/wiki/Thermodynamics*

6. R. Fitzpatrick, Thermodynamics & Statistical Mechanics, University of Texas at Austin,

https://farside.ph.utexas.edu/teaching/sm1/Thermal.pdf

7. R. Fitzpatrick, Quantum Mechanics, the University of Texas at Austin Contents. 1 Introduction. 5. 1.1. Intended audience.

farside.ph.utexas.edu/teaching/qmech/qmech.pdf

8. A. Balevski, Metal science, Technics, Sofia, 1962.

9. M. Flemings, Solidification processing, Peace, Moscow, 1977. (In Russian)

10. M. Borisov, K. Marinova, Science and Art, Sofia, 1977.

11. S. Vodenicharov, Dynamic destruction of metal structures, *Bulged Ltd.*, Sofia, 2011. ISBN 978-954-92552-3-2 (In Bulgarian)

12. R. E. Smallman, R. J. Bishop, Modern Physical Metallurgy and Materials Engineering, Butterworth-Heinemann, Oxford, 6E, 1999. ISBN 0 7506 4564 4

13. Marco van Oosten, Composite – Metal connections, Report ITD 9006-2A.01. Issue no.: 1, Issue date: 29-01-2015

14. W. D. Callister, Jr., D. G. Rethwisch, Materials Science and Engineering, John Wiley & Sons, Inc. 9 edition, 2014. Wiley ISBN: 978-1-118-47770-0, Printed in USA 10 9 8 7 6 5 4 3 2 1

15. S. M. Bushev, PhD Thesis, Controllability problems of crystallization process in casting, Technical University, Sofia, Bulgaria, 1995.

16. S. Bushev, G. Moumjian, A possibility to influence the dynamics of a phase transition of first order during casting in open thermodynamic system, Comptes rendes de l'Academie bulgare des Sciences, *Tome 46, № 7p 1993*.

17. G. Mumdgian, Automatic ruling and regulation of the heat processes, Technique, Sofia, 1980. (In Bulgarian)

18. G. Nicolis, I. Prigogine, Exploring complexity, Peace, Moscow, 1990. (In Russian)

19. A. Polikarov, Methodology of scientific knowledge, Science and Art, Sofia, printing house, Alexander Peshev, Pleven, 1972.

20. https://www.vocabulary.com/dictionary/synergistic

21. M. Bushev, *Synergetics: Chaos, Order, Self-Organization*. Singapore: World Scientific, 1994.

22. D. Cerra, R. Müller, P. Reinartz, A Classification Algorithm for Hyperspectral Images Based on Synergetics Theory, IEEE Transactions on Geoscience and Remote Sensing, p. 1-12, May 2013. DOI: 10.1109/TGRS.2012.2219059

23. G. Schulze, Metallphysik, Peace, Moscow, 1971. (In Russian)

24. J. S. Blakemore, Solid state physics, Metallurgy, Moscow, 1972. (In Russian)

25. I. Gibson, D. Rosen, B. Stucker, Additive manufacturing technologies, Springer Science+Business, Media New, York 2015,DOI 10.1007/978-1-4939-2113-3_2

26. J. Hart, An Introduction to Additive Manufacturing - MIT http://web.mit.edu/2.810/www/files/lectures/2015_lectures/lec9-additive-manuf-2015.pdf

27. B. Wu, C. Myant, S. Z. Weider, The value of additive manufacturing: future opportunities, Briefing Paper No 2 September , p.1÷13, 2017. *https://www.imperial.ac.uk/media/imperial-college/.../IMSE-Briefing-paper-2-AM.pdf*

28. N. Aschenbrenner, New Software Combines 3D Printing with Traditional Manufacturing

norbert.aschenbrenner@siemens.com
Adnew.siemens.com/additive/manufacturing, Siemens AG.

29. L. Litov, Lectures on quantum physics, *atomic.phys.uni-sofia.bg/elektronna.../lekcii-po-kvantova-fizika*

30. D. Kashchiev, Nucleation, Basic Theory with Application, Butterworth Heinemann, Oxford, 2000. ISBN 0 75064682 9